



AD-A219 548

RESEARCH AND DEVELOPMENT TECHNICAL REPORT  
SLCET-TR-90-1

TEMPERATURE AND COUPLING BEHAVIOR OF RESONATORS  
AND TRANSDUCERS OF LITHIUM TETRABORATE DRIVEN BY  
LATERAL AND THICKNESS FIELDS

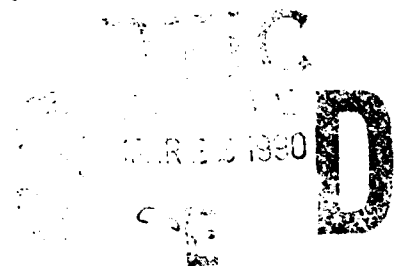
ARTHUR BALLATO, JOHN KOSINSKI, MUHAMMAD MIZAN,  
AND THEODORE LUKASZEK

ELECTRONICS TECHNOLOGY AND DEVICES LABORATORY

JANUARY 1990

DISTRIBUTION STATEMENT

Approved for public release;  
distribution is unlimited.



US ARMY  
LABORATORY COMMAND  
FORT MONMOUTH, NEW JERSEY 07703-5000

90 03 22 003

## NOTICES

### Disclaimers

The findings in this report are not to be construed as an official Department of the Army position, unless so designated by other authorized documents.

The citation of trade names and names of manufacturers in this report is not to be construed as official Government indorsement or approval of commercial products or services referenced herein.

UNCLASSIFIED

SECURITY CLASSIFICATION OF THIS PAGE

## REPORT DOCUMENTATION PAGE

Form Approved  
OMB No. 0704-0188

1a. REPORT SECURITY CLASSIFICATION Unclassified			1b. RESTRICTIVE MARKINGS										
2a. SECURITY CLASSIFICATION AUTHORITY			3. DISTRIBUTION / AVAILABILITY OF REPORT Approved for public release; distribution is unlimited.										
2b. DECLASSIFICATION/DOWNGRADING SCHEDULE			5. MONITORING ORGANIZATION REPORT NUMBER(S)										
4. PERFORMING ORGANIZATION REPORT NUMBER(S) SLCET-TR-90-1			7a. NAME OF MONITORING ORGANIZATION										
6a. NAME OF PERFORMING ORGANIZATION US Army Laboratory Command Electronics Tech & Devices Lab		6b. OFFICE SYMBOL (If applicable) SLCET-MA-A	7b. ADDRESS (City, State, and ZIP Code)										
6c. ADDRESS (City, State, and ZIP Code) Electronics Technology and Devices Laboratory ATTN: SLCET-MA-A Fort Monmouth, NJ 07703-5000			9. PROCUREMENT INSTRUMENT IDENTIFICATION NUMBER										
8a. NAME OF FUNDING/SPONSORING ORGANIZATION		8b. OFFICE SYMBOL (If applicable)	10. SOURCE OF FUNDING NUMBERS										
8c. ADDRESS (City, State, and ZIP Code)		<table border="1"> <tr> <td>PROGRAM ELEMENT NO.</td> <td>PROJECT NO.</td> <td>TASK NO.</td> <td>WORK UNIT ACCESSION NO.</td> </tr> <tr> <td>1L162705H</td> <td>H94</td> <td>K9</td> <td>DA303394</td> </tr> </table>				PROGRAM ELEMENT NO.	PROJECT NO.	TASK NO.	WORK UNIT ACCESSION NO.	1L162705H	H94	K9	DA303394
PROGRAM ELEMENT NO.	PROJECT NO.	TASK NO.	WORK UNIT ACCESSION NO.										
1L162705H	H94	K9	DA303394										
11. TITLE (Include Security Classification) TEMPERATURE AND COUPLING BEHAVIOR OF RESONATORS AND TRANSDUCERS OF LITHIUM TETRABORATE DRIVEN BY LATERAL AND THICKNESS FIELDS (U)													
12. PERSONAL AUTHOR(S) Arthur Ballato, John Kosinski, Muhammad Mizan, and Theodore Lukaszek													
13a. TYPE OF REPORT Technical Report		13b. TIME COVERED FROM Jun 88 to Jun 89		14. DATE OF REPORT (Year, Month, Day) 1990 January									
15. PAGE COUNT 88													
16. SUPPLEMENTARY NOTATION													
17. COSATI CODES			18. SUBJECT TERMS (Continue on reverse if necessary and identify by block number)										
FIELD	GROUP	SUB-GROUP	Piezoelectric resonators; piezoelectric transducers; lithium tetraborate; acousto-optics										
09	01												
17	02												
19. ABSTRACT (Continue on reverse if necessary and identify by block number)													
<p>→ Lithium tetraborate is a tetragonal material of considerable promise for signal processing, transducer, and frequency control applications. It exhibits piezoelectric coupling values that fall between those of lithium niobate and quartz, but possesses orientations for which the temperature coefficient of frequency or delay time is zero for both bulk and surface acoustic waves.</p> <p>→ Calculations have previously been made for rotated y-cut, bulk wave plates, including the regions where the quasi-extensional and quasi-shear thickness modes have zero temperature coefficients of frequency. In this report we extend the calculations to doubly rotated bulk wave resonators, and compute the coupling factors for the three simple thickness modes driven by [TE] and lateral [LE] quasistatic electric fields as a function of the orientation angles phi and theta, and the direction of the applied lateral field psi. Because of the temperature coefficients of the piezoelectric coupling factors, the temperature coefficient</p> <p style="text-align: right;">(contd)</p>													
20. DISTRIBUTION / AVAILABILITY OF ABSTRACT <input checked="" type="checkbox"/> UNCLASSIFIED/UNLIMITED <input type="checkbox"/> SAME AS RPT <input type="checkbox"/> DTIC USERS			21. ABSTRACT SECURITY CLASSIFICATION Unclassified										
22a. NAME OF RESPONSIBLE INDIVIDUAL Dr. Arthur Ballato			22b. TELEPHONE (Include Area Code) (201) 544-2773		22c. OFFICE SYMBOL SLCET-MA-A								

UNCLASSIFIED

SECURITY CLASSIFICATION OF THIS PAGE

19. ABSTRACT (contd)

of a resonator will depend not only upon orientation, but also upon harmonic number and location of the resonator operating point on the immittance circle.

It is found that two unique orientations exist in lithium tetraborate for which plate resonators have zero temperature coefficients of frequency of both first- and second-order with high values of piezo coupling factor. One cut has this favorable behavior in its thickness-stretch mode, while the other possesses it for its slow thickness-shear mode.

For	
A	
Distribution/	
Availability Code	
Dist and/or	
Dist	Special
A-1	



UNCLASSIFIED

SECURITY CLASSIFICATION OF THIS PAGE

## CONTENTS

	Page
INTRODUCTION . . . . .	1
DETERMINATION OF CONSTANTS . . . . .	1
COMPUTATIONAL SCHEME . . . . .	2
FREQUENCY CONSTANTS AND COUPLING FACTORS . . . . .	2
TEMPERATURE COEFFICIENTS . . . . .	3
COMPENSATED, DOUBLY ROTATED CUTS . . . . .	3
REFERENCES . . . . .	4

## FIGURES

Figure	Page
1. Frequency constant, $N_m$ , for $(yxwl)\phi=0^\circ/\theta$ cuts . . .	7
2. Piezocoupling, $k_m$ , for $(yxwl)\phi=0^\circ/\theta$ cuts . . .	8
3. Piezocoupling, $\underline{k}_m$ , for $(yxwl)\phi=0^\circ/\theta$ , $\psi=0^\circ$ cuts . . .	9
4. Piezocoupling, $\underline{k}_m$ , for $(yxwl)\phi=0^\circ/\theta$ , $\psi=30^\circ$ cuts . . .	10
5. Piezocoupling, $\underline{k}_m$ , for $(yxwl)\phi=0^\circ/\theta$ , $\psi=60^\circ$ cuts . . .	11
6. Piezocoupling, $\underline{k}_m$ , for $(yxwl)\phi=0^\circ/\theta$ , $\psi=90^\circ$ cuts . . .	12
7. Frequency constant, $N_m$ , for $(yxwl)\phi=15^\circ/\theta$ cuts . . .	13
8. Piezocoupling, $k_m$ , for $(yxwl)\phi=15^\circ/\theta$ cuts . . .	14
9. Piezocoupling, $\underline{k}_m$ , for $(yxwl)\phi=15^\circ/\theta$ , $\psi=0^\circ$ cuts . . .	15
10. Piezocoupling, $\underline{k}_m$ , for $(yxwl)\phi=15^\circ/\theta$ , $\psi=30^\circ$ cuts . . .	16
11. Piezocoupling, $\underline{k}_m$ , for $(yxwl)\phi=15^\circ/\theta$ , $\psi=60^\circ$ cuts . . .	17
12. Piezocoupling, $\underline{k}_m$ , for $(yxwl)\phi=15^\circ/\theta$ , $\psi=90^\circ$ cuts . . .	18
13. Frequency constant, $N_m$ , for $(yxwl)\phi=30^\circ/\theta$ cuts . . .	19
14. Piezocoupling, $k_m$ , for $(yxwl)\phi=30^\circ/\theta$ cuts . . .	20

15. Piezocoupling, $k_m$ , for $(yxwl)\phi=30^\circ/\theta$ , $\psi=0^\circ$ cuts .	21
16. Piezocoupling, $k_m$ , for $(yxwl)\phi=30^\circ/\theta$ , $\psi=30^\circ$ cuts .	22
17. Piezocoupling, $k_m$ , for $(yxwl)\phi=30^\circ/\theta$ , $\psi=60^\circ$ cuts .	23
18. Piezocoupling, $k_m$ , for $(yxwl)\phi=30^\circ/\theta$ , $\psi=90^\circ$ cuts .	24
19. Frequency constant, $N_m$ , for $(yxwl)\phi=45^\circ/\theta$ cuts .	25
20. Piezocoupling, $k_m$ , for $(yxwl)\phi=45^\circ/\theta$ cuts . . .	26
21. Piezocoupling, $k_m$ , for $(yxwl)\phi=45^\circ/\theta$ , $\psi=0^\circ$ cuts .	27
22. Piezocoupling, $k_m$ , for $(yxwl)\phi=45^\circ/\theta$ , $\psi=30^\circ$ cuts .	28
23. Piezocoupling, $k_m$ , for $(yxwl)\phi=45^\circ/\theta$ , $\psi=60^\circ$ cuts .	29
24. Piezocoupling, $k_m$ , for $(yxwl)\phi=45^\circ/\theta$ , $\psi=90^\circ$ cuts .	30
25. TC(1) for $(yxwl)\phi=0^\circ/\theta$ cuts; $M = 1, 3, \infty$ ; mode "a"; [TE] . . . . .	31
26. TC(2) for $(yxwl)\phi=0^\circ/\theta$ cuts; $M = 1, 3, \infty$ ; mode "a"; [TE] . . . . .	32
27. Locus of TC(1)=0 for $(yxwl)\phi/\theta$ cuts; $M = 1, 3, \infty$ ; mode "a"; [TE] . . . . .	33
28. Locus of TC(2)=0 for $(yxwl)\phi/\theta$ cuts; $M = 1, 3, \infty$ ; mode "a"; [TE] . . . . .	34
29. TC(1) for $(yxwl)\phi=0^\circ/\theta$ cuts; $M = 1, 3, \infty$ ; mode "b"; [TE] . . . . .	35
30. TC(2) for $(yxwl)\phi=0^\circ/\theta$ cuts; $M = 1, 3, \infty$ ; mode "b"; [TE] . . . . .	36
31. Locus of TC(1)=0 for $(yxwl)\phi/\theta$ cuts; $M = 1, 3, \infty$ ; mode "b"; [TE] . . . . .	37
32. Locus of TC(2)=0 for $(yxwl)\phi/\theta$ cuts; $M = 1, 3, \infty$ ; mode "b"; [TE] . . . . .	38
33. TC(1) for $(yxwl)\phi=0^\circ/\theta$ cuts; $M = 1, 3, \infty$ ; mode "c"; [TE] . . . . .	39
34. TC(2) for $(yxwl)\phi=0^\circ/\theta$ cuts; $M = 1, 3, \infty$ ; mode "c"; [TE] . . . . .	40
35. Locus of TC(1)=0 for $(yxwl)\phi/\theta$ cuts; $M = 1, 3, \infty$ ; mode "c"; [TE] . . . . .	41
36. Locus of TC(2)=0 for $(yxwl)\phi/\theta$ cuts; $M = 1, 3, \infty$ ; mode "c"; [TE] . . . . .	42

37.	TC(1) for $(yxwl)\phi=0^\circ/\theta$ cuts; $M = 1$ ; mode "a"; $\psi=0^\circ(30^\circ)90^\circ$ ; [LE]	43
38.	TC(2) for $(yxwl)\phi=0^\circ/\theta$ cuts; $M = 1$ ; mode "a"; $\psi=0^\circ(30^\circ)90^\circ$ ; [LE]	44
39.	Locus of TC(1)=0 for $(yxwl)\phi/\theta$ cuts; $M = 1$ ; mode "a"; $\psi=0^\circ(30^\circ)90^\circ$ ; [LE]	45
40.	Locus of TC(2)=0 for $(yxwl)\phi/\theta$ cuts; $M = 1$ ; mode "a"; $\psi=0^\circ(30^\circ)90^\circ$ ; [LE]	46
41.	TC(1) for $(yxwl)\phi=0^\circ/\theta$ cuts; $M = 3$ ; mode "a"; $\psi=0^\circ(30^\circ)90^\circ$ ; [LE]	47
42.	TC(2) for $(yxwl)\phi=0^\circ/\theta$ cuts; $M = 3$ ; mode "a"; $\psi=0^\circ(30^\circ)90^\circ$ ; [LE]	48
43.	Locus of TC(1)=0 for $(yxwl)\phi/\theta$ cuts; $M = 3$ ; mode "a"; $\psi=0^\circ(30^\circ)90^\circ$ ; [LE]	49
44.	Locus of TC(2)=0 for $(yxwl)\phi/\theta$ cuts; $M = 3$ ; mode "a"; $\psi=0^\circ(30^\circ)90^\circ$ ; [LE]	50
45.	TC(1) for $(yxwl)\phi=0^\circ/\theta$ cuts; $M = \infty$ ; mode "a"; $\psi=0^\circ(30^\circ)90^\circ$ ; [LE]	51
46.	TC(2) for $(yxwl)\phi=0^\circ/\theta$ cuts; $M = \infty$ ; mode "a"; $\psi=0^\circ(30^\circ)90^\circ$ ; [LE]	52
47.	Locus of TC(1)=0 for $(yxwl)\phi/\theta$ cuts; $M = \infty$ ; mode "a"; $\psi=0^\circ(30^\circ)90^\circ$ ; [LE]	53
48.	Locus of TC(2)=0 for $(yxwl)\phi/\theta$ cuts; $M = \infty$ ; mode "a"; $\psi=0^\circ(30^\circ)90^\circ$ ; [LE]	54
49.	TC(1) for $(yxwl)\phi=0^\circ/\theta$ cuts; $M = 1$ ; mode "b"; $\psi=0^\circ(30^\circ)90^\circ$ ; [LE]	55
50.	TC(2) for $(yxwl)\phi=0^\circ/\theta$ cuts; $M = 1$ ; mode "b"; $\psi=0^\circ(30^\circ)90^\circ$ ; [LE]	56
51.	Locus of TC(1)=0 for $(yxwl)\phi/\theta$ cuts; $M = 1$ ; mode "b"; $\psi=0^\circ(30^\circ)90^\circ$ ; [LE]	57
52.	Locus of TC(2)=0 for $(yxwl)\phi/\theta$ cuts; $M = 1$ ; mode "b"; $\psi=0^\circ(30^\circ)90^\circ$ ; [LE]	58
53.	TC(1) for $(yxwl)\phi=0^\circ/\theta$ cuts; $M = 3$ ; mode "b"; $\psi=0^\circ(30^\circ)90^\circ$ ; [LE]	59
54.	TC(2) for $(yxwl)\phi=0^\circ/\theta$ cuts; $M = 3$ ; mode "b"; $\psi=0^\circ(30^\circ)90^\circ$ ; [LE]	60

55.	Locus of $TC(1)=0$ for $(yxwl)\Phi/\theta$ cuts; $M = 3$ ; mode "b"; $\psi=0^\circ(30^\circ)90^\circ$ ; [LE]	61
56.	Locus of $TC(2)=0$ for $(yxwl)\Phi/\theta$ cuts; $M = 3$ ; mode "b"; $\psi=0^\circ(30^\circ)90^\circ$ ; [LE]	62
57.	$TC(1)$ for $(yxwl)\Phi=0^\circ/\theta$ cuts; $M = \infty$ ; mode "b"; $\psi=0^\circ(30^\circ)90^\circ$ ; [LE]	63
58.	$TC(2)$ for $(yxwl)\Phi=0^\circ/\theta$ cuts; $M = \infty$ ; mode "b"; $\psi=0^\circ(30^\circ)90^\circ$ ; [LE]	64
59.	Locus of $TC(1)=0$ for $(yxwl)\Phi/\theta$ cuts; $M = \infty$ ; mode "b"; $\psi=0^\circ(30^\circ)90^\circ$ ; [LE]	65
60.	Locus of $TC(2)=0$ for $(yxwl)\Phi/\theta$ cuts; $M = \infty$ ; mode "b"; $\psi=0^\circ(30^\circ)90^\circ$ ; [LE]	66
61.	$TC(1)$ for $(yxwl)\Phi=0^\circ/\theta$ cuts; $M = 1$ ; mode "c"; $\psi=0^\circ(30^\circ)90^\circ$ ; [LE]	67
62.	$TC(2)$ for $(yxwl)\Phi=0^\circ/\theta$ cuts; $M = 1$ ; mode "c"; $\psi=0^\circ(30^\circ)90^\circ$ ; [LE]	68
63.	Locus of $TC(1)=0$ for $(yxwl)\Phi/\theta$ cuts; $M = 1$ ; mode "c"; $\psi=0^\circ(30^\circ)90^\circ$ ; [LE]	69
64.	Locus of $TC(2)=0$ for $(yxwl)\Phi/\theta$ cuts; $M = 1$ ; mode "c"; $\psi=0^\circ(30^\circ)90^\circ$ ; [LE]	70
65.	$TC(1)$ for $(yxwl)\Phi=0^\circ/\theta$ cuts; $M = 3$ ; mode "c"; $\psi=0^\circ(30^\circ)90^\circ$ ; [LE]	71
66.	$TC(2)$ for $(yxwl)\Phi=0^\circ/\theta$ cuts; $M = 3$ ; mode "c"; $\psi=0^\circ(30^\circ)90^\circ$ ; [LE]	72
67.	Locus of $TC(1)=0$ for $(yxwl)\Phi/\theta$ cuts; $M = 3$ ; mode "c"; $\psi=0^\circ(30^\circ)90^\circ$ ; [LE]	73
68.	Locus of $TC(2)=0$ for $(yxwl)\Phi/\theta$ cuts; $M = 3$ ; mode "c"; $\psi=0^\circ(30^\circ)90^\circ$ ; [LE]	74
69.	$TC(1)$ for $(yxwl)\Phi=0^\circ/\theta$ cuts; $M = \infty$ ; mode "c"; $\psi=0^\circ(30^\circ)90^\circ$ ; [LE]	75
70.	$TC(2)$ for $(yxwl)\Phi=0^\circ/\theta$ cuts; $M = \infty$ ; mode "c"; $\psi=0^\circ(30^\circ)90^\circ$ ; [LE]	76
71.	Locus of $TC(1)=0$ for $(yxwl)\Phi/\theta$ cuts; $M = \infty$ ; mode "c"; $\psi=0^\circ(30^\circ)90^\circ$ ; [LE]	77
72.	Locus of $TC(2)=0$ for $(yxwl)\Phi/\theta$ cuts; $M = \infty$ ; mode "c"; $\psi=0^\circ(30^\circ)90^\circ$ ; [LE]	78

## INTRODUCTION

Lithium tetraborate (LBO) is a tetragonal material in crystal class  $4mm$  ( $C_{4v}$ ). As such it possesses a single 4-fold polar axis, and four symmetry planes containing the 4-fold axis; consequently, there are 6 independent linear elastic constants, three independent linear piezoelectric constants, and two independent linear dielectric constants.

The primitive region is 1/8th of a hemisphere, which we comprise as the angle ranges  $(\gamma x w l)\phi/\theta$ , with  $0 \leq \phi \leq \pi/4$  and  $0 \leq \theta \leq \pi/2$ . As a consequence of its symmetry, LBO is

- ▲ Pyroelectric
- ▲ Optically uniaxial (LBO is negative)
- ▲ Piezoelectric
- ▲ Not enantiomorphic (no twinning)
- ▲ Nonferroelectric (poling not required)

Particularizing to the substance lithium tetraborate (LBO), we find from the literature [1]-[26], [30]-[32], the following specific properties and virtues:

### Properties of $Li_2B_4O_7 = Li_2O \cdot 2B_2O_3$

- ▼ Congruently melting phase in the lithium oxide-boron oxide system; transparent and colorless.
- ▼ Low melting point:  $917^\circ C$ .
- ▼ Czochralski growth, Pt crucibles, diameters  $> 50$  mm along  $[100]$ ,  $[001]$ , or  $[110]$ ; sensitive to thermal shock (cooling).
- ▼ Lattice spacings:  $a = b = 9.479 \text{ \AA}$ ,  $c = 10.280 \text{ \AA}$ .
- ▼ Mohs hardness = 6 (between  $LiTaO_3$  and quartz = 7).
- ▼ Low density =  $2451 \text{ kg/m}^3$ , but acoustic velocities only slightly greater than those in  $LiNbO_3$  and  $LiTaO_3$ .
- ▼ Solubility: 1) dissolves rapidly in acids, slowly in bases. 2) hot water used as etchant. 3) insolvent in organic "solvents."
- ▼ Relatively high piezocoupling  $k$  and  $k$  values.
- ▼ Surface acoustic wave (SAW) reflectivity per stripe  $> 5$  times that for  $LiNbO_3$ ,  $LiAlO_3$ , and quartz, leading to miniaturization.
- ▼ Zero temperature coefficients of frequency and time delay for BAW and SAW.

## DETERMINATION OF CONSTANTS

The elastic, piezoelectric, and dielectric constants of  $4mm$  crystals may be determined from the simple thickness modes of thin plates driven by thickness excitation [TE] and lateral excitation [LE].

Orientation ( $\gamma x$ ); Y-cut = X-cut

[TE]: pure shear along  $X_3$   
 $c_{44}^E, e_{15}, \epsilon_{11}^S$

[LE]: pure stretch along  $X_2$ , driven by  $X_3$   
 field  
 $c_{11}^E, e_{31}$

Orientation (zx); Z-cut

[TE]: pure stretch along  $X_3$   
 $c_{33}^E, e_{33}, \epsilon_{33}^S$

Orientation (yxl) $\theta$ ; rotated Y-cut

[TE]: coupled shear-stretch  
 $c_{13}^E$

[LE]: pure shear along  $X_1$ , driven by  $X_1$   
 field  
 $c_{66}^E$

Orientation (yxw) $\phi$

[LE]: coupled shear-stretch, field along  
 $X_3$ ;  $X_1, X_2$  motion  
 $c_{12}^E$

#### COMPUTATIONAL SCHEME

Input data are taken from Ref. [19], and used as follows:

- $s^E, d, \epsilon^T$  are converted to  $c^E, e, \epsilon^S$ .
- $c^E, e, \epsilon^S$ , density, and thickness are given at reference temperature  $T_0 = 25^\circ\text{C}$ .
- First- and second-order temperature coefficients  $TC(1)$  and  $TC(2)$  are used to compute  $c^E$ , etc., at two other temperatures,  $T_c$  and  $T_h$ .
- For assumed angles  $\phi, \theta$ , and  $\psi$ , the conventional eigenvalue problem is solved to yield  $N_m, k_m, k_m(\psi)$ , etc., for each temperature,  $T_c, T_0$ , and  $T_h$ .
- $TC(1)$  and  $TC(2)$  of  $f_R, f_A$ , etc., are computed for each mode, harmonic, and excitation type; for further details, see Refs. [27]-[29].

#### FREQUENCY CONSTANTS AND COUPLING FACTORS

The frequency constants,  $N_m$ , [TE] coupling factors,  $k$ , and [LE] coupling factors,  $k(\psi)$ , for (yxwl) $\phi=0^\circ(15^\circ)45^\circ/\theta$  cuts having applied field direction  $\psi = 0^\circ(30^\circ)90^\circ$ , are given in Figs. 1 to 24, respectively.

## TEMPERATURE COEFFICIENTS

The first- and second-order temperature coefficients of frequency,  $TC(1)$  and  $TC(2)$ , and the loci of  $TC(1)=0$  and  $TC(2)=0$ , for  $M = 1, 3$ , and  $\infty$ , for [TE]  $(yxw1)\phi=0^\circ/\theta$  plates are given, respectively, for the "a" mode in Figs. 25 to 28, for the "b" mode in Figs. 29 to 32, and for the "c" mode in Figs. 33 to 36.

The first- and second-order temperature coefficients of frequency,  $TC(1)$  and  $TC(2)$ , and the loci of  $TC(1)=0$  and  $TC(2)=0$ , for mode "a",  $\psi=0^\circ(30^\circ)90^\circ$ , for [LE]  $(yxw1)\phi=0^\circ/\theta$  plates are given, respectively, for  $M=1$  in Figs. 37 to 40, for  $M=3$  in Figs. 41 to 44, and for  $M=\infty$  in Figs. 45 to 48.

The first- and second-order temperature coefficients of frequency,  $TC(1)$  and  $TC(2)$ , and the loci of  $TC(1)=0$  and  $TC(2)=0$ , for mode "b",  $\psi=0^\circ(30^\circ)90^\circ$ , for [LE]  $(yxw1)\phi=0^\circ/\theta$  plates are given, respectively, for  $M=1$  in Figs. 49 to 52, for  $M=3$  in Figs. 53 to 56, and for  $M=\infty$  in Figs. 57 to 60.

The first- and second-order temperature coefficients of frequency,  $TC(1)$  and  $TC(2)$ , and the loci of  $TC(1)=0$  and  $TC(2)=0$ , for mode "c",  $\psi=0^\circ(30^\circ)90^\circ$ , for [LE]  $(yxw1)\phi=0^\circ/\theta$  plates are given, respectively, for  $M=1$  in Figs. 61 to 64, for  $M=3$  in Figs. 65 to 68, and for  $M=\infty$  in Figs. 69 to 72.

## COMPENSATED, DOUBLY ROTATED CUTS

Superposition of Figs. 27 and 28 discloses that a unique doubly rotated "a" mode orientation in LBO exists for which  $TC(1) = TC(2) = 0$ . It occurs for  $\phi/\theta \approx 40^\circ/33^\circ$  at the fundamental harmonic, driven in [TE]. In a plate resonator or transducer cut at this orientation, both  $TC(1)$  and  $TC(2)$  are zero. This means that the first surviving temperature coefficient will be  $TC(3)$ ; i.e., the frequency-temperature curve will be cubic in nature, like that of the AT and SC cuts of quartz, and the overall excursions in frequency over a wide temperature range will be small. The corresponding  $N_a$  and  $k_a$  values may be read approximately from the graphs in Figs. 19 and 20, respectively. The frequency constant  $N_a$  is nearly a maximum when  $\theta \approx 33^\circ$ , and the piezocoupling factor  $k_a$  is approximately 20%.

Superposition of Figs. 35 and 36 discloses that a unique doubly rotated "c" mode orientation in LBO also exists for which  $TC(1) = TC(2) = 0$ . It occurs for  $\phi/\theta \approx 19^\circ/56^\circ$  at the fundamental harmonic, driven in [TE]. In a plate resonator or transducer cut at this orientation, both  $TC(1)$  and  $TC(2)$  are likewise zero. This again means that the first surviving temperature coefficient will be  $TC(3)$ ; i.e., the frequency-temperature curve will be cubic in nature, like that of the AT and SC cuts of quartz, and the overall excursions in frequency over a wide temperature range will be small. The corresponding  $N_a$  and  $k_a$  values may be read approximately from the graphs in Figs. 7 and 8, respectively. The frequency constant  $N_a$  is nearly a minimum when  $\theta \approx 56^\circ$ , and the piezocoupling factor  $k_a$  is approximately 27%.

## REFERENCES

- [01] G. S. Smith and G. E. Rindone, "High-Temperature Energy Relations in the Alkali Borates: Binary Alkali Borate Compounds and Their Glasses," J. Am. Ceram. Soc., Vol. 44, No. 2, 1961, pp. 72-78.
- [02] J. Krogh-Moe, "The Crystal Structure of Lithium Diborate,  $\text{Li}_2\text{O} \cdot 2\text{B}_2\text{O}_3$ ," Acta Cryst., Vol. 15, 1962, pp. 190-193.
- [03] J. Krogh-Moe, "Refinement of the Crystal Structure of Lithium Diborate,  $\text{Li}_2\text{O} \cdot 2\text{B}_2\text{O}_3$ ," Acta Cryst., Vol. B24, Pt.2, 1968, pp. 179-181.
- [04] S. R. Nagel, L. W. Herron, and C. G. Bergeron, "Crystal Growth of  $\text{Li}_2\text{B}_4\text{O}_7$ ," J. Am. Ceram. Soc., Vol. 60, No. 3-4, March-April 1977, pp. 172-173.
- [05] J. D. Garrett, M. N. Iyer, and J. E. Greedan, "The Czochralski Growth of  $\text{LiBO}_2$  and  $\text{Li}_2\text{B}_4\text{O}_7$ ," J. Cryst. Growth, Vol. 41, 1977, pp. 225-227.
- [06] R. W. Whatmore, N. M. Shorrocks, C. O'Hara, F. W. Ainger, and I. M. Young, "Lithium Tetraborate: A New Temperature-Compensated SAW Substrate Material," Elx. Lett., Vol. 17, No. 1, 8th January 1981, pp. 11-12.
- [07] N. M. Shorrocks, R. W. Whatmore, F. W. Ainger, and I. M. Young, "Lithium Tetraborate: A New Temperature Compensated Piezoelectric Substrate Material for Surface Acoustic Wave Devices," IEEE Ultrasonics Symp. Proc., 1981, pp. 337-340.
- [08] B. Lewis, N. M. Shorrocks, and R. W. Whatmore, "An Assessment of Lithium Tetraborate for SAW Applications," IEEE Ultrasonics Symp. Proc., 1982, pp. 389-393.
- [09] D. S. Robertson and I. M. Young, "The Growth and Growth Mechanism of Lithium Tetraborate," J. Mater. Sci., Vol. 17, 1982, pp. 1729-1738.
- [10] Y. Ebata, H. Suzuki, S. Matsumura, and K. Fukuta, "SAW Propagation Characteristics on  $\text{Li}_2\text{B}_4\text{O}_7$ ," Proc. 3rd Symp. Ultrasonic Elx., Tokyo, 1982; Jpn. J. Appl. Phys., Vol. 22, 1983, Suppl. 22-3, pp. 160-162.
- [11] C. D. J. Emin and J. F. Werner, "The Bulk Acoustic Wave Properties of Lithium Tetraborate," Proc. 37th Annual Frequency Control Symp., June 1983, pp. 136-143.
- [12] R. C. Peach, C. D. J. Emin, J. F. Werner, and S. P. Doherty, "High Coupling Piezoelectric Resonators Using Lithium Tetraborate," IEEE Ultrasonics Symp. Proc., 1983, pp. 521-526.

- [13] K. Fukuta, J. Ushizawa, H. Suzuki, Y. Ebata, and S. Matsumura, "Growth and Properties of  $\text{Li}_2\text{B}_4\text{O}_7$  Single Crystal for SAW Device Applications," Proc. 4th Meeting on Ferroelectric Materials and Their Applications, Kyoto, 1983; Jpn. J. Appl. Phys., Vol. 22, 1983, Suppl. 22-2, pp. 140-142.
- [14] T. Shiosaki, M. Adachi, H. Kobayashi, K. Araki, and A. Kawabata, "Elastic, Piezoelectric, Acousto-Optic and Electro-Optic Properties of  $\text{Li}_2\text{B}_4\text{O}_7$ ," Proc. 5th Symp. Ultrasonic Elx., Tokyo, 1984, pp. 5-8; Jpn. J. Appl. Phys., Vol. 24, 1985, Suppl. 24-1, pp. 25-27.
- [15] M. Adachi, T. Shiosaki, and A. Kawabata, "Crystal Growth of Lithium Tetraborate ( $\text{Li}_2\text{B}_4\text{O}_7$ )," Proc. 5th Meeting on Ferroelectric Materials and Their Applications, Kyoto, 1985; Jpn. J. Appl. Phys., Vol. 24, 1985, Suppl. 24-3, pp. 72-75.
- [16] Y. Fujiwara, M. Ono, M. Sakai, and N. Wakatsuki, "Strip Type Resonator of Lithium Tetraborate," Proc. 39th Annual Frequency Control Symp., May 1985, pp. 351-355.
- [17] M. Adachi, T. Shiosaki, H. Kobayashi, O. Ohnishi, and A. Kawabata, "Temperature Compensated Piezoelectric Lithium Tetraborate Crystal for High Frequency Surface Acoustic Wave and Bulk Wave Device Applications," IEEE Ultrasonics Symp. Proc., 1985, pp. 228-232.
- [18] A. S. Bhalla, L. E. Cross, and R. W. Whatmore, "Pyroelectric and Piezoelectric Properties of Lithium Tetraborate Single Crystal," Jpn. J. Appl. Phys., Vol. 24, 1985, Suppl. 24-2, pp. 727-729.
- [19] T. Shiosaki, M. Adachi, and A. Kawabata, "Growth and Properties of Piezoelectric Lithium Tetraborate Crystal for BAW and SAW Devices," IEEE Intl. Symp. Applications Ferroelectrics (ISAF) Proc., Lehigh University, Bethlehem, PA, June 1986, pp. 455-464.
- [20] A. Ballato, E. R. Hatch, T. Lukaszek, and M. Mizan, "Lateral-Field Coupling of Rotated BAW Plates with 3m, 4mm, & 4 bar 3m Symmetries," IEEE Ultrasonics Symp. Proc., 1986, pp. 339-342.
- [21] H. Suzuki, Y. Ebata, S. Matsumura, and J. Ushizawa, "Surface Acoustic Wave Device," U.S. Patent 4,672,255, issued June 9, 1987.
- [22] Y. Ebata and M. Koshino, "SAW Resonator and Resonator Filter on  $\text{Li}_2\text{B}_4\text{O}_7$  Substrate," Jpn. J. Appl. Phys., Vol. 26, 1987, Suppl. 26-1, pp. 123-125.
- [23] H. Abe, H. Saitou, M. Ohmura, T. Yamada, and K. Miwa, "Lithium Tetraborate ( $\text{Li}_2\text{B}_4\text{O}_7$ ) SAW Resonators," IEEE Ultrasonics Symp. Proc. 1987, pp. 91-94.

- [24] W. S. Ishak, C. A. Flory, and B. A. Auld, "Acoustic Modes in Lithium Tetraborate," IEEE Ultrasonics Symp. Proc., 1987, pp. 241-245.
- [25] S. Matsumura, T. Omi, N. Yamaji, and Y. Ebata, "A 45° X Cut  $\text{Li}_2\text{B}_4\text{O}_7$  Single Crystal Substrate for SAW Resonators," IEEE Ultrasonics Symp. Proc., 1987, pp. 247-250.
- [26] M. Murota and Y. Shimizu, "Characteristics of Leaky Surface Waves Propagating on  $\text{Li}_2\text{B}_4\text{O}_7$ ," IEEE Ultrasonics Symposium Proc., Montréal, PQ, Canada, October 1989, in press.
- [27] M. Onoe, "Relationship between Temperature Behavior of Resonant and Antiresonant Frequencies and Electromechanical Coupling Factors of Piezoelectric Resonators," Proc. IEEE, Vol. 57, No. 4, April 1969, pp. 702-703.
- [28] T. Yamada and N. Niizeki, "Admittance of Piezoelectric Plates Vibrating under the Perpendicular Field Excitation," Proc. IEEE, Vol. 58, No. 6, June 1970, pp. 941-942; "Formulation of Admittance for Parallel Field Excitation of Piezoelectric Plates," J. Appl. Phys., Vol. 41, No. 9, August 1970, pp. 3604-3609; "A New Formulation of Piezoelectric Plate Thickness Vibration," Rev. Elec. Comm. Lab. NTT (Tokyo), Vol. 19, Nos. 5-6, May-June 1971, pp. 705-713.
- [29] A. Ballato and T. Lukaszek, "Frequency-Temperature Coefficients of Mass-Loaded Plate Vibrators," Technical Report ECOM-4356, US Army Electronics Command, Fort Monmouth, NJ 07703, September 1975, 49pp.
- [30] A. Ballato, "Polarization Matrices of Lithium Tetraborate," Technical Report SLCET-TR-89-3, US Army Laboratory Command, Fort Monmouth, NJ 07703, June 1989, 29pp.
- [31] A. Ballato, J. Kosinski, M. Mizan, and T. Lukaszek, "Lateral- and Thickness-Field Coupling in Lithium Tetraborate," Proc. 43rd Annual Frequency Control Symp., May-June 1989, in press.
- [32] A. Ballato, J. Kosinski, and T. Lukaszek, "Lateral-Field Temperature Behavior of Lithium Tetraborate," IEEE Ultrasonics Symposium Proc., Montréal, PQ, Canada, October 1989, in press.

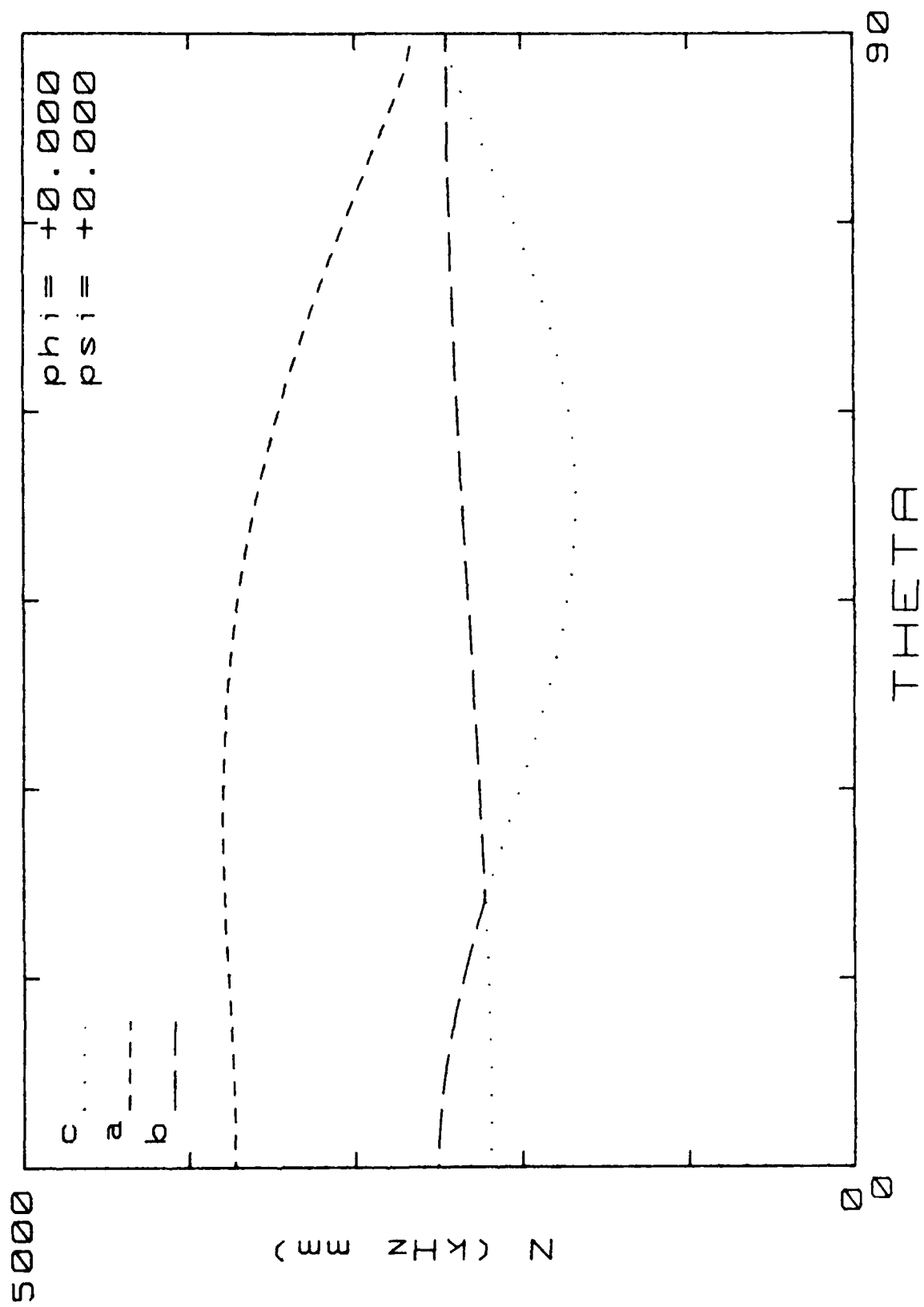


Figure 1. Frequency constant,  $N_m$ , for  $(yxw1)\phi = 0^\circ/\theta$  cuts.

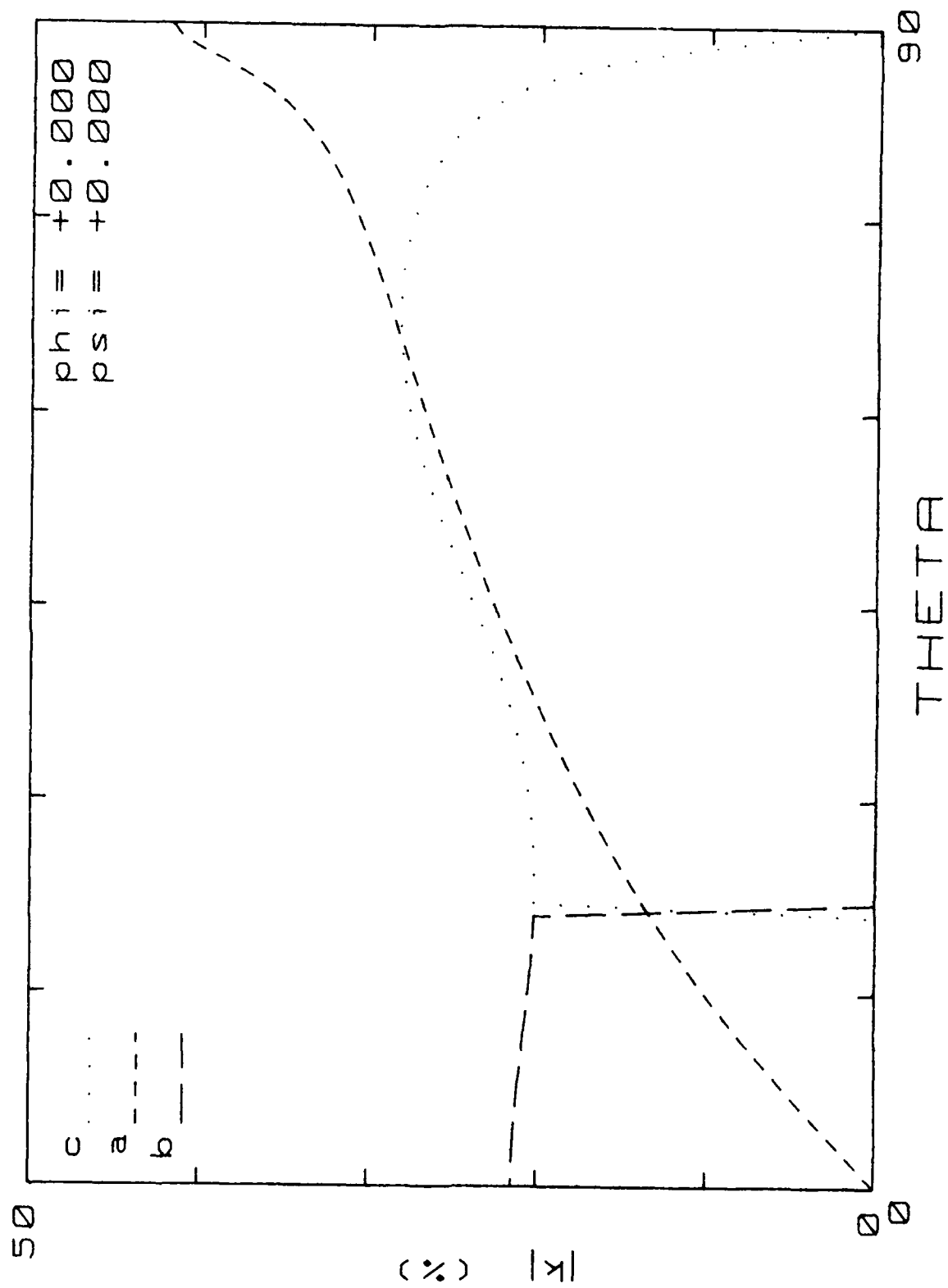


Figure 2. Piezocoupling,  $K_m$ , for  $(yxw1)\phi = 0^\circ/\theta$  cuts.

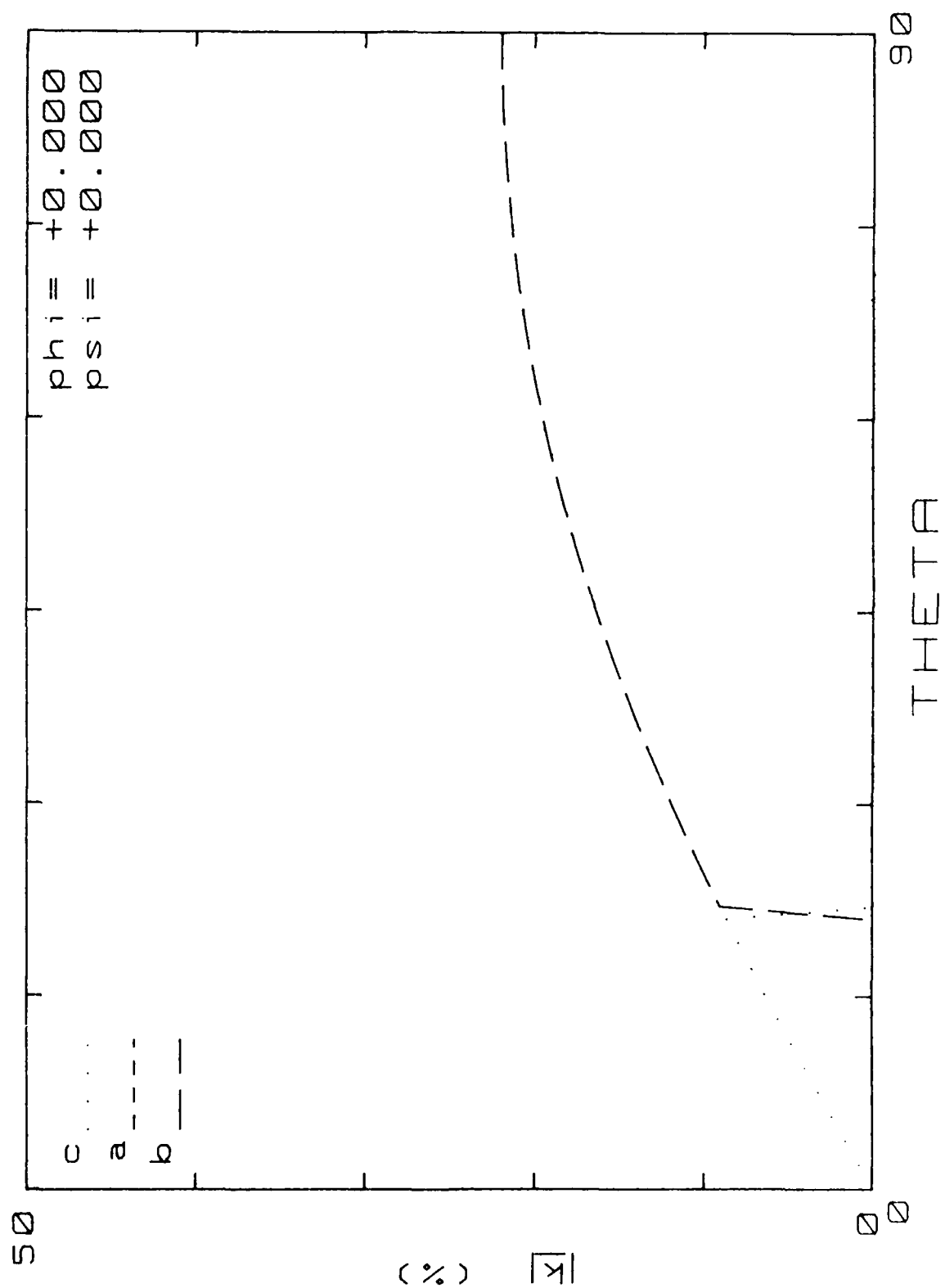


Figure 3. Piezocoupling,  $k_m$ , for  $(yxw)\phi = 0^\circ/\theta$ ,  $\psi = 0^\circ$  cuts.

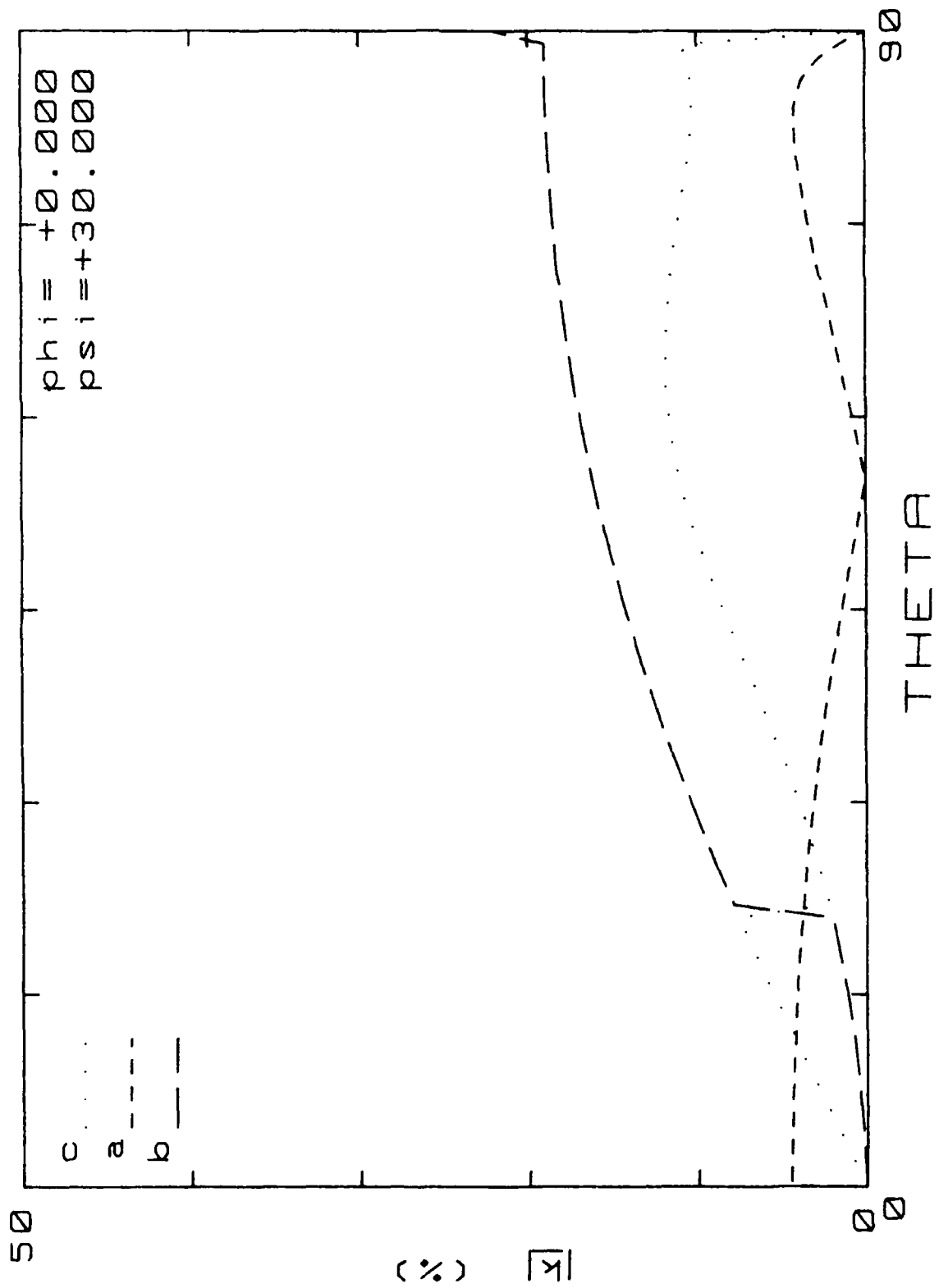


Figure 4. Piezocoupling,  $k_m$ , for  $(yxw)\phi = 0^\circ/\theta$ ,  $\psi = 30^\circ$  cuts.

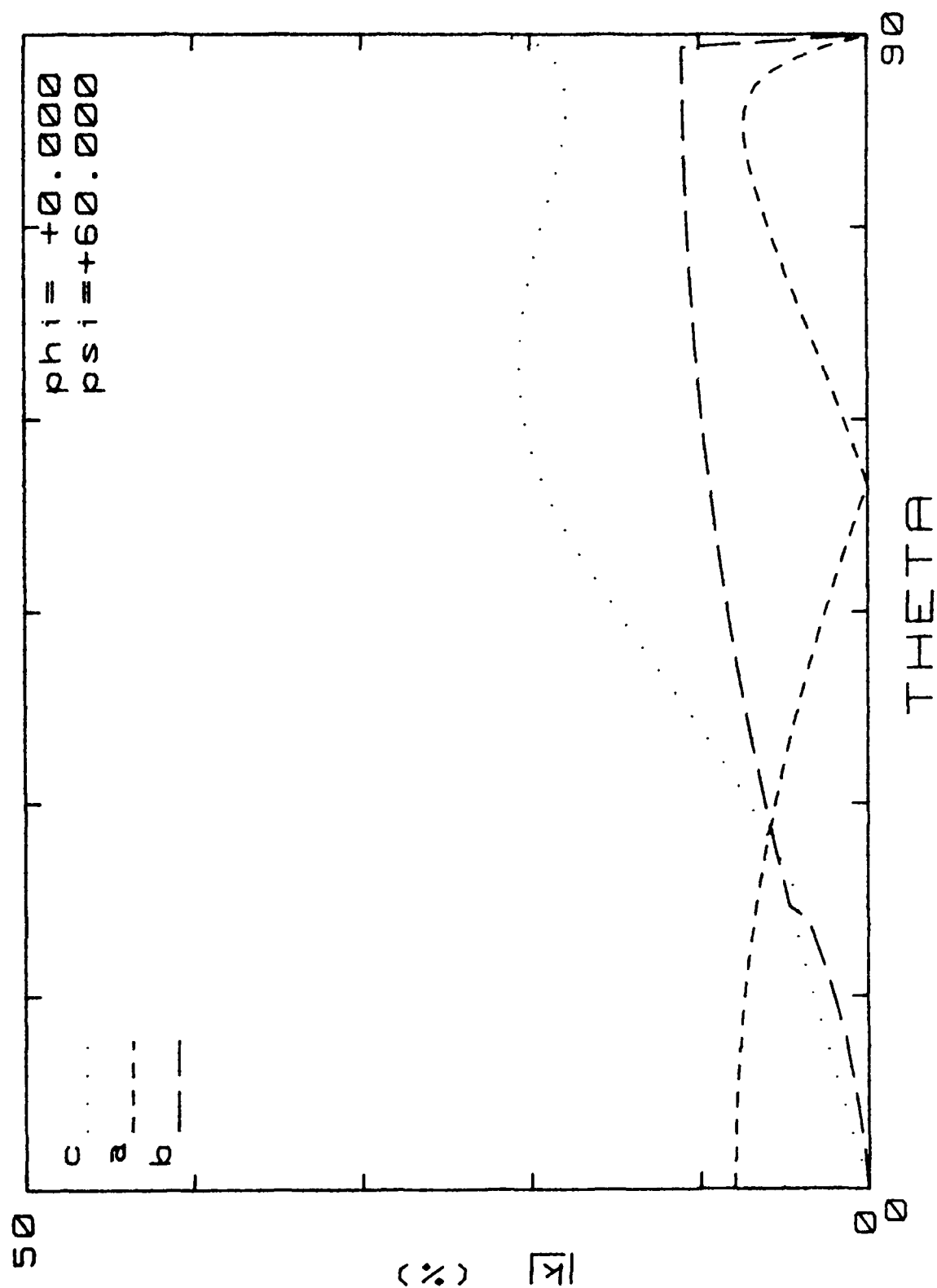


Figure 3. Piezocoupling,  $k_m$ , for  $(y_{xw1})\phi = 0^\circ/\theta$ ,  $\psi = 60^\circ$  cuts.

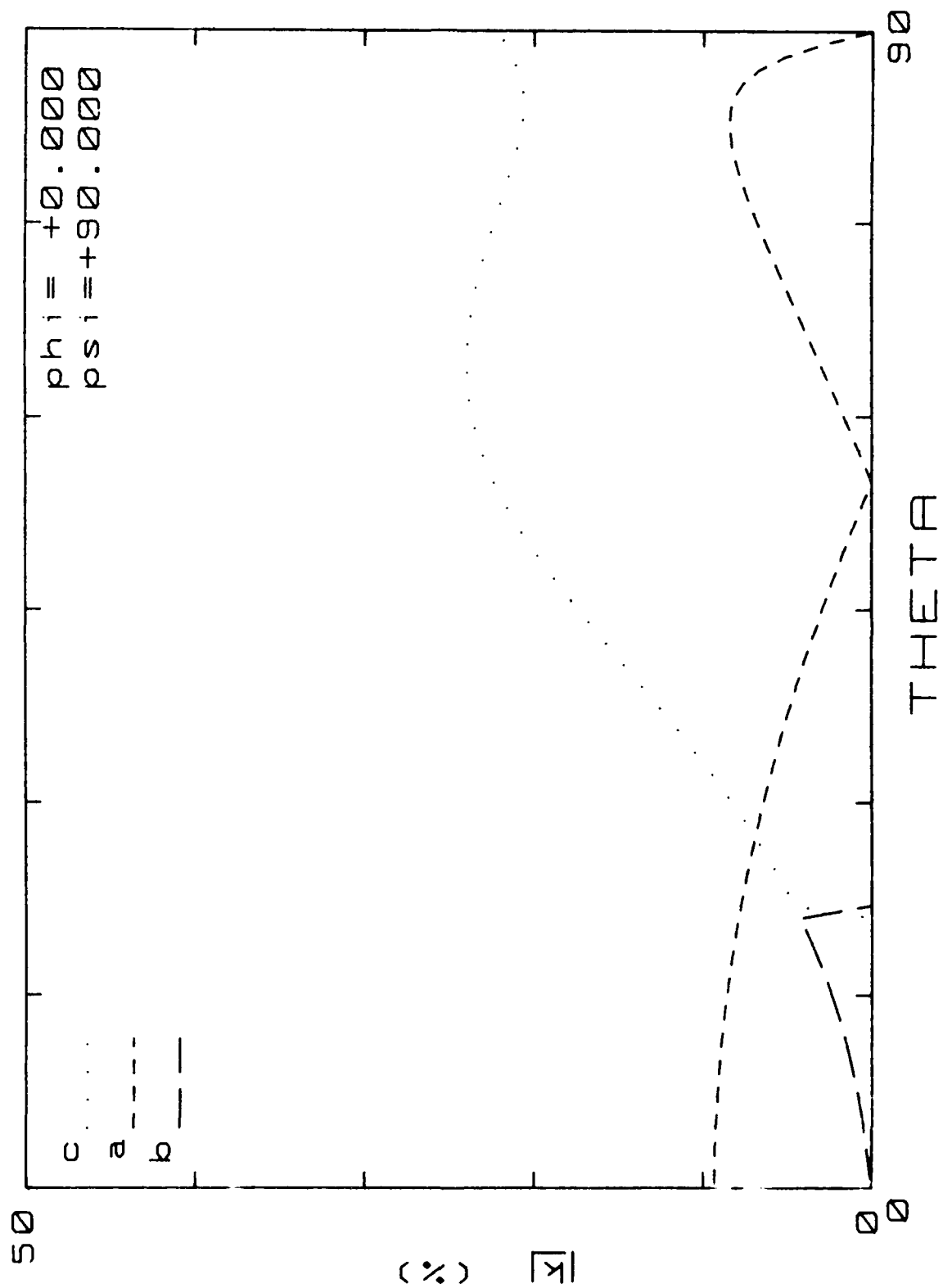


Figure 6. Piezocoupling,  $K_m$ , for  $(yxw1)\phi=0^\circ/\theta$ ,  $\psi=90^\circ$  clts.

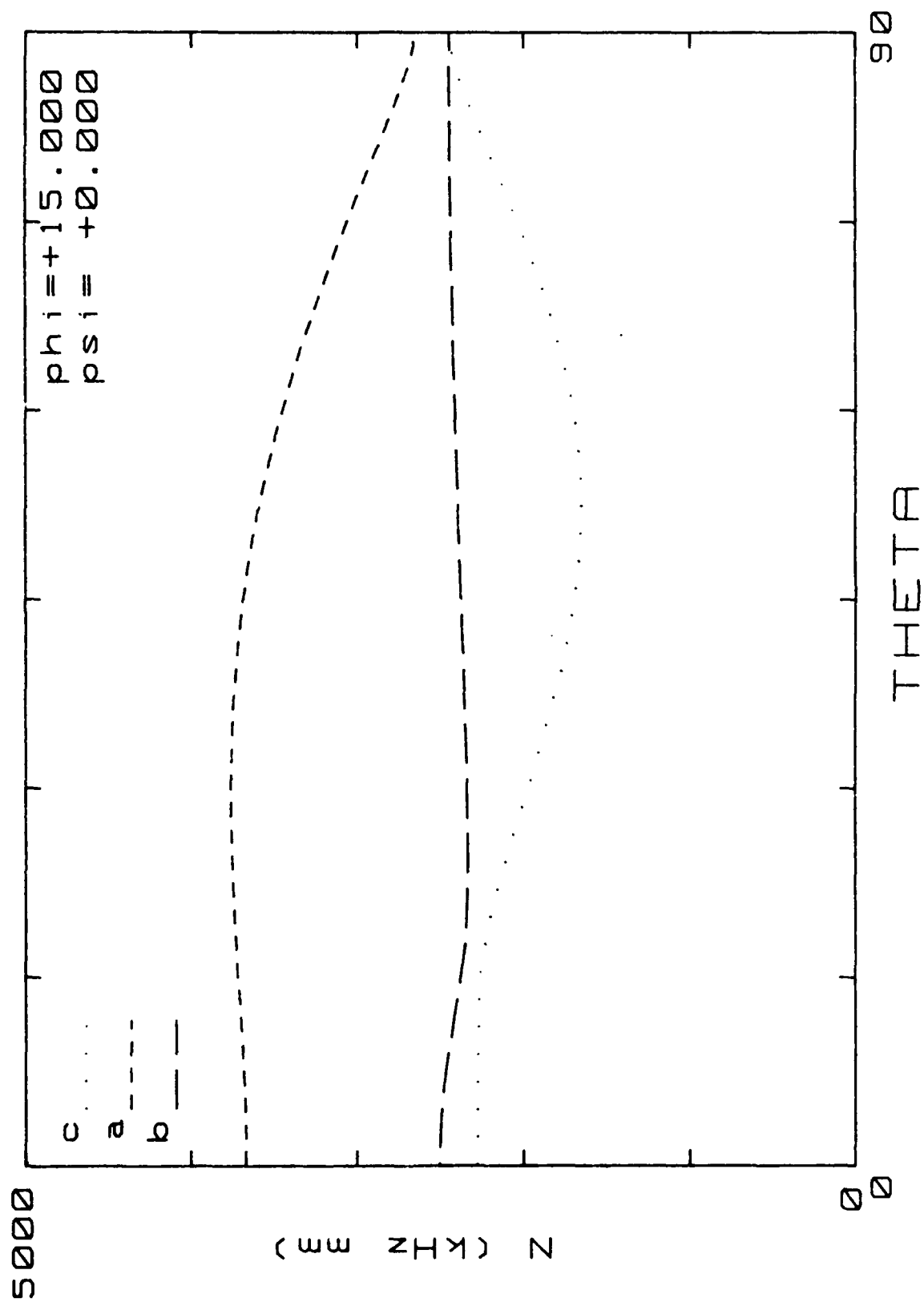


Figure 7. Frequency constant,  $N_m$ , for  $(yxw1) \phi = 15^\circ / \theta$  cuts.

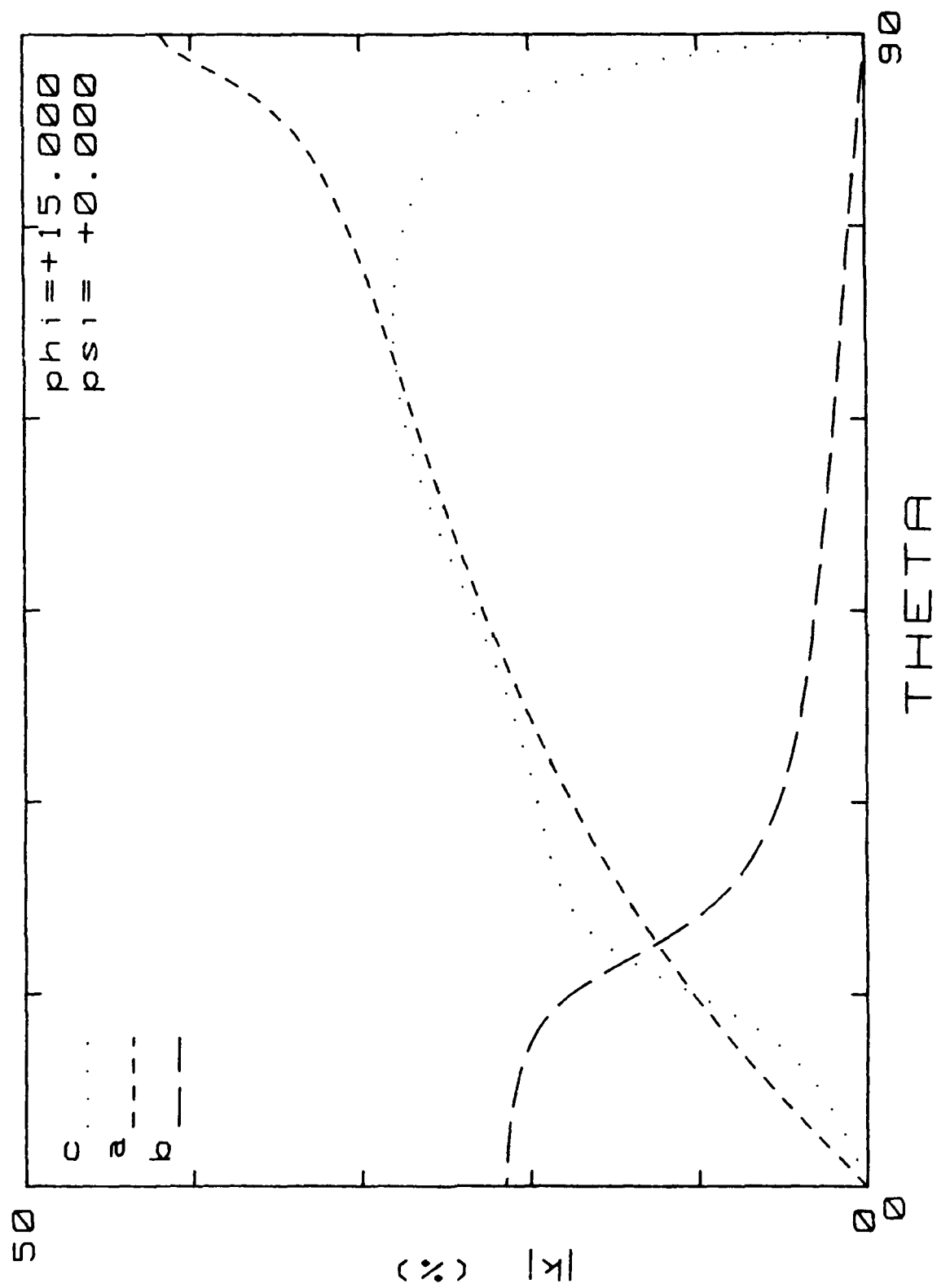


Figure 8. Piezocoupling,  $k_m$ , for  $(yxw)\phi = 15^\circ/\theta$  cuts.

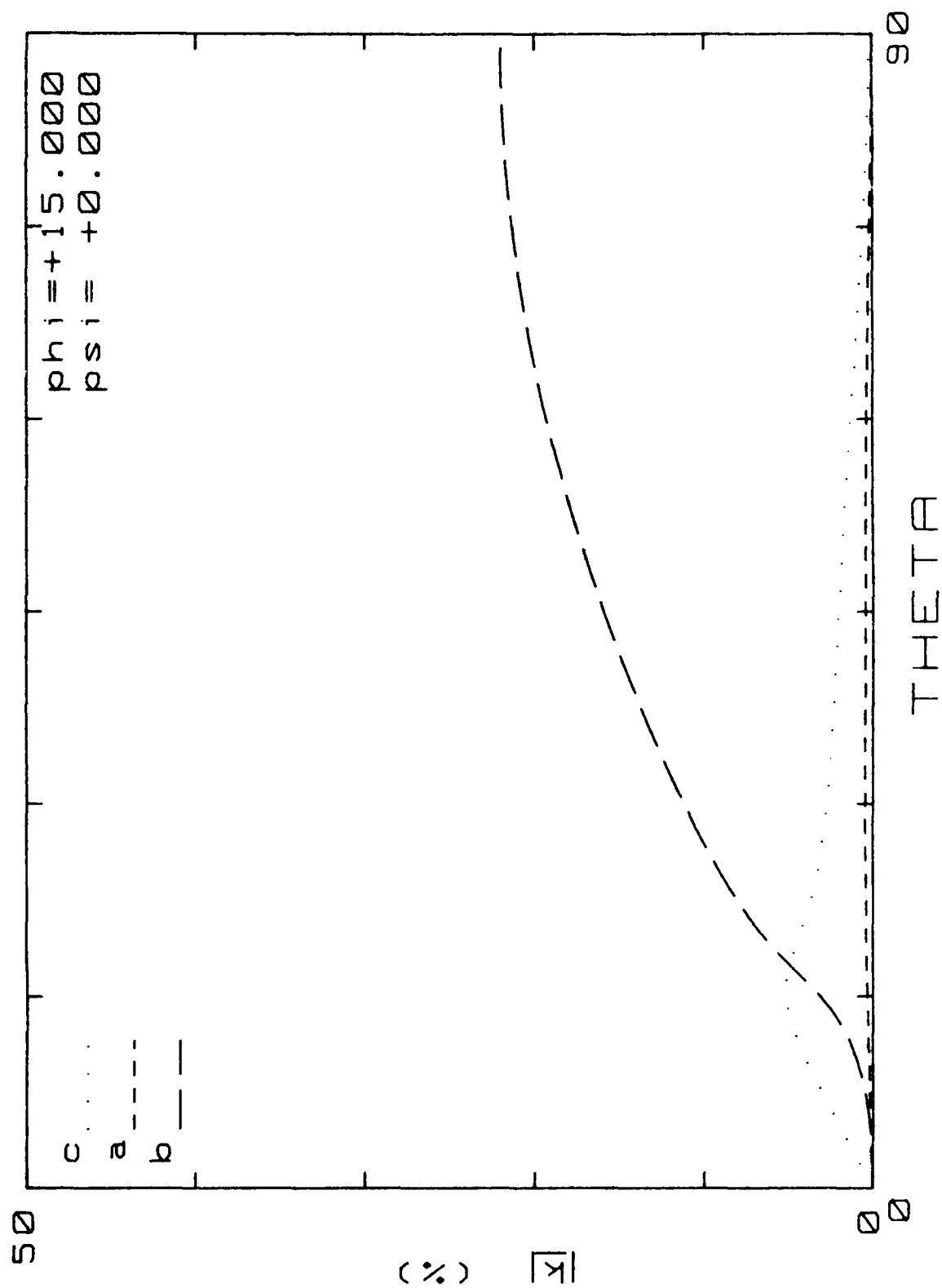


Figure 9. Piezocoupling,  $k_m$ , for  $(yxw)\phi = 15^\circ/\theta$ ,  $\psi_i = 0^\circ$  cuts.

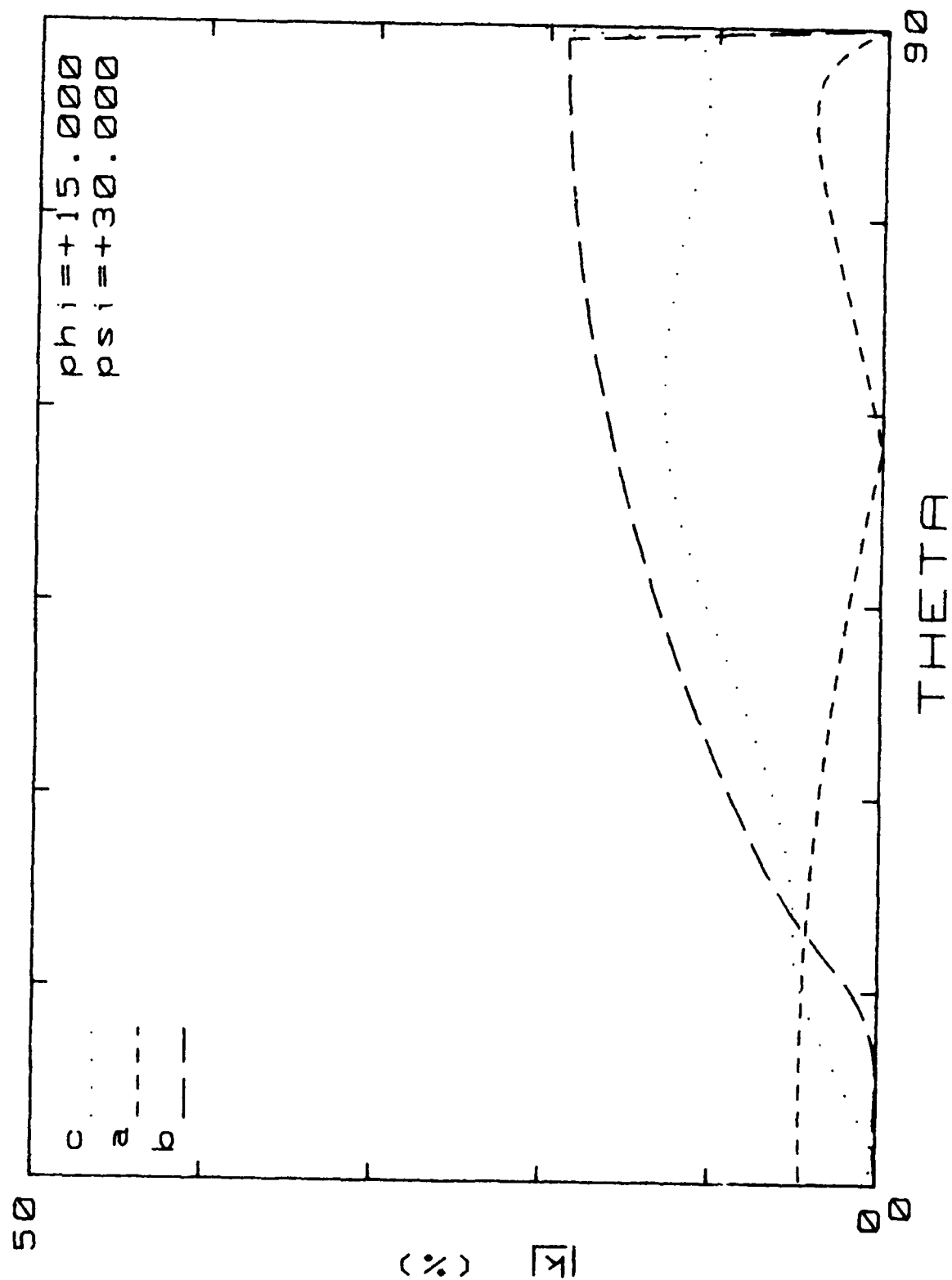


Figure 10. Piezocoupling,  $k_m$ , for  $(yxw)\phi = 15^\circ/\theta$ ,  $\psi = 30^\circ$  cuts.

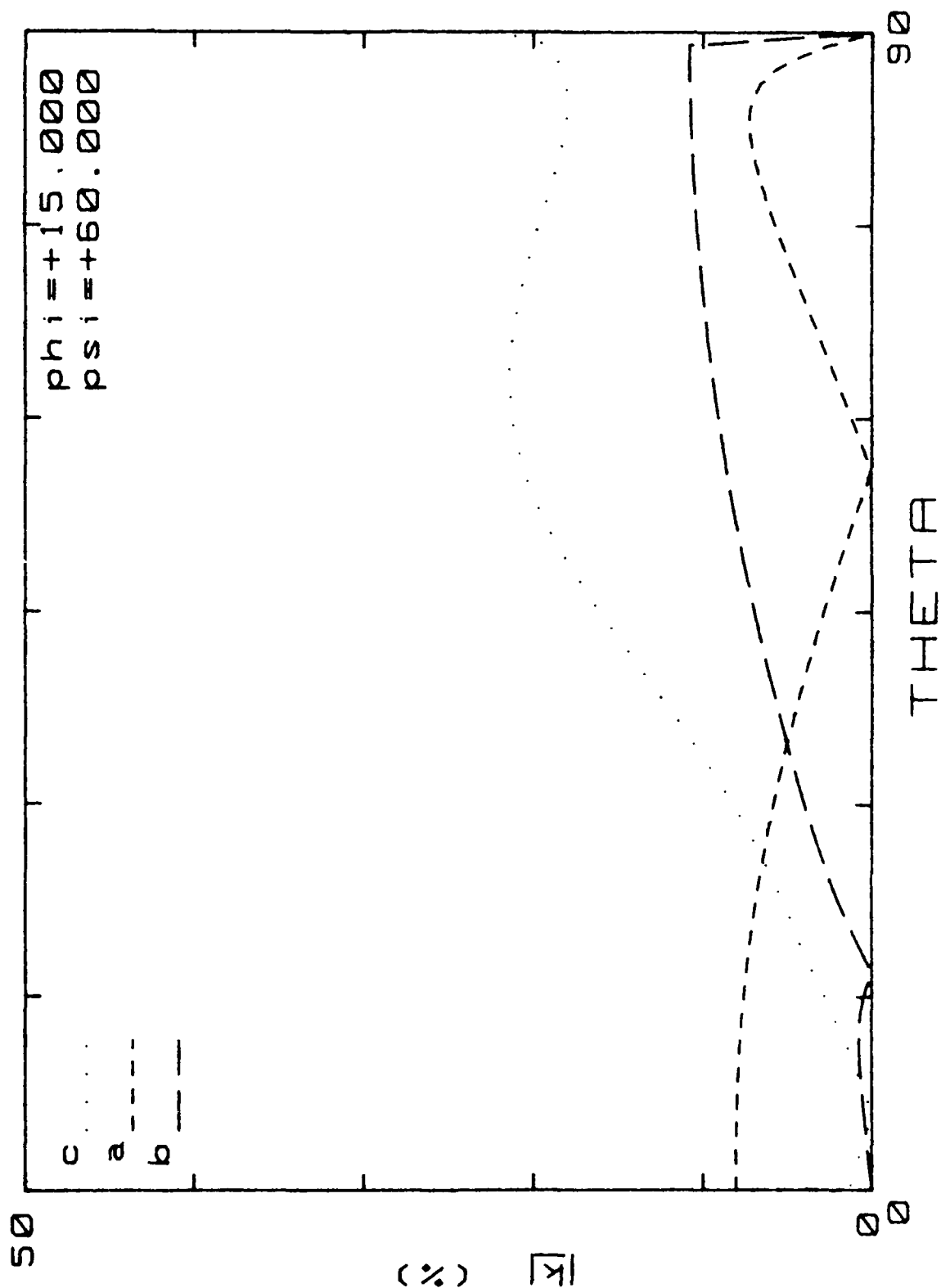


Figure 11. Piezocoupling,  $k_m$ , for  $(yxw1)\phi = 15^\circ/\theta$ ,  $\psi = 60^\circ$  cuts.

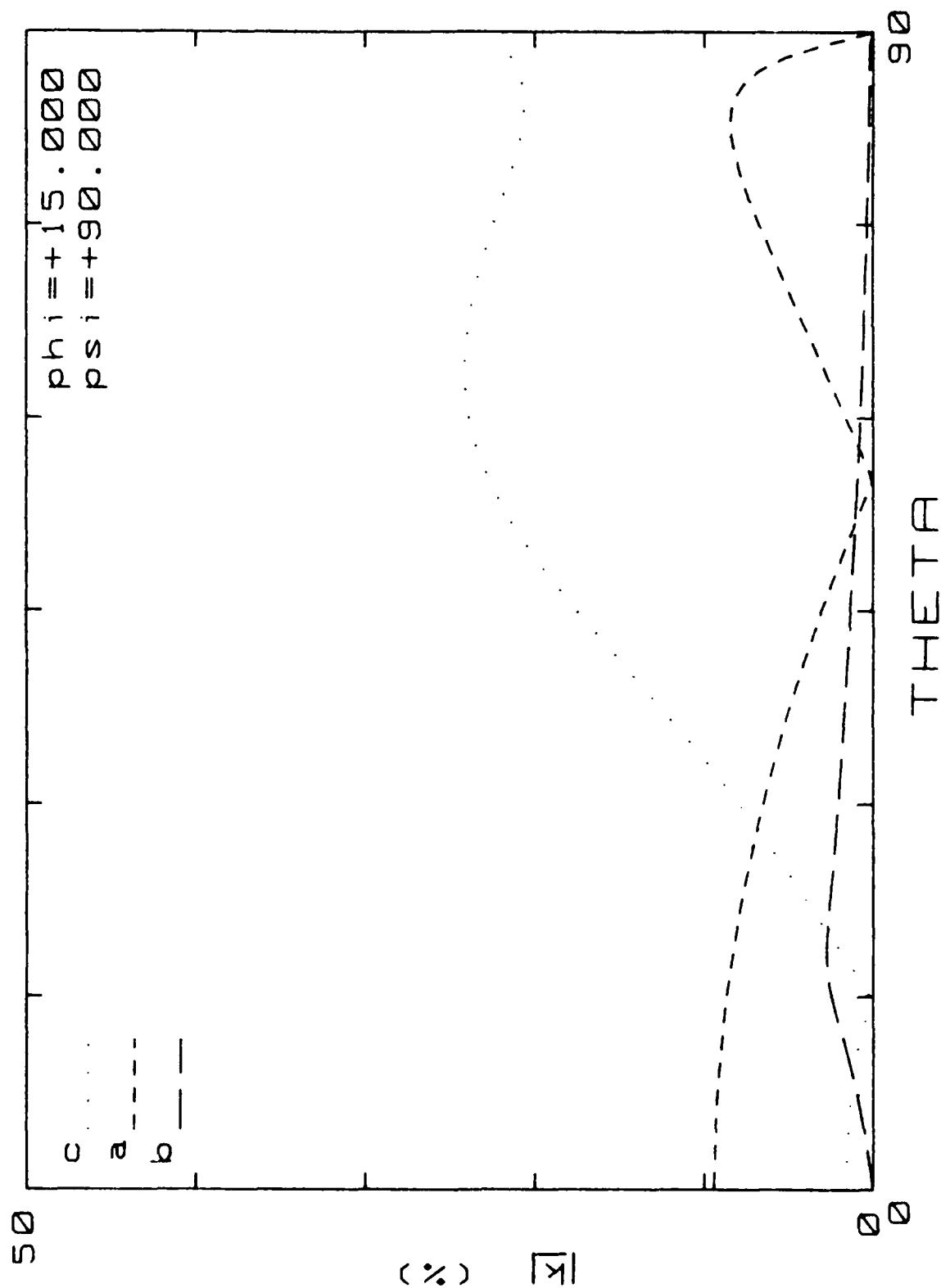


Figure 12. Piezocoupling,  $k_m$ , for  $(y \times w)\phi = 15^\circ/\theta$ ,  $\psi = 90^\circ$  cuts.

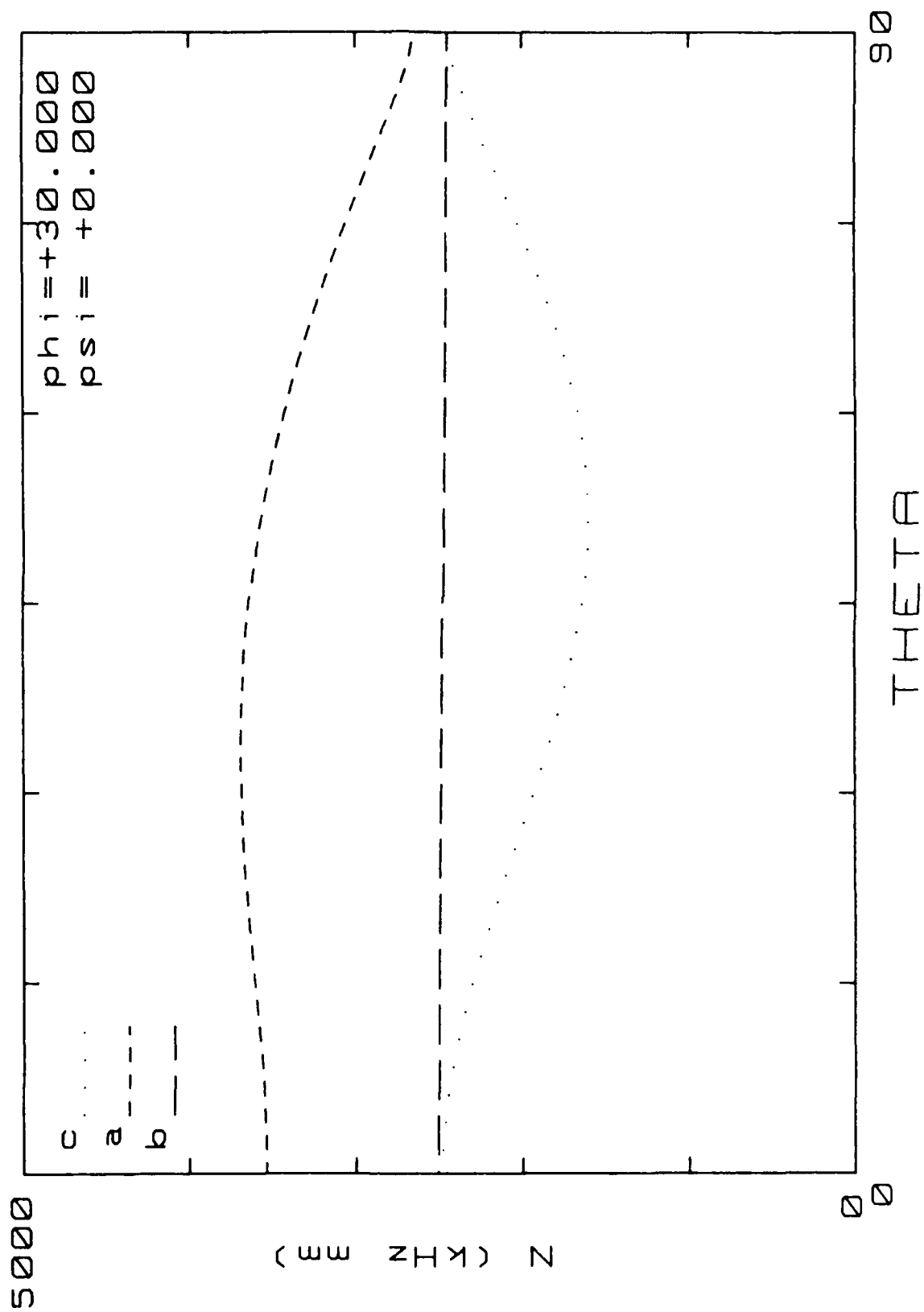


Figure 13. Frequency constant,  $N_m$ , for  $(y_{xw1})\phi = 30^\circ/\theta$  cuts.

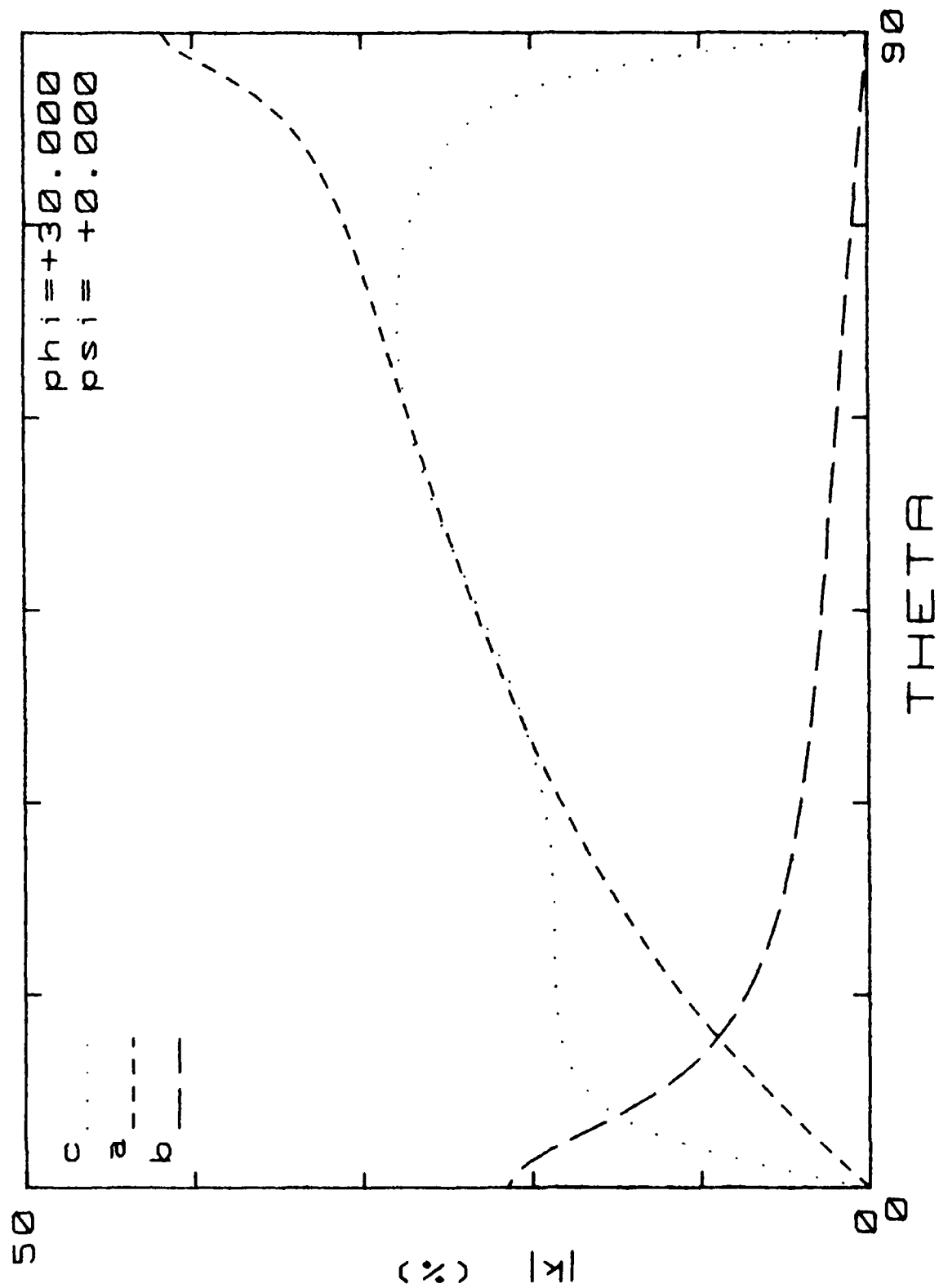


Figure 14. Piezocoupling,  $k_m$ , for  $(yxw1)\phi = 30^\circ/\theta$  cuts.

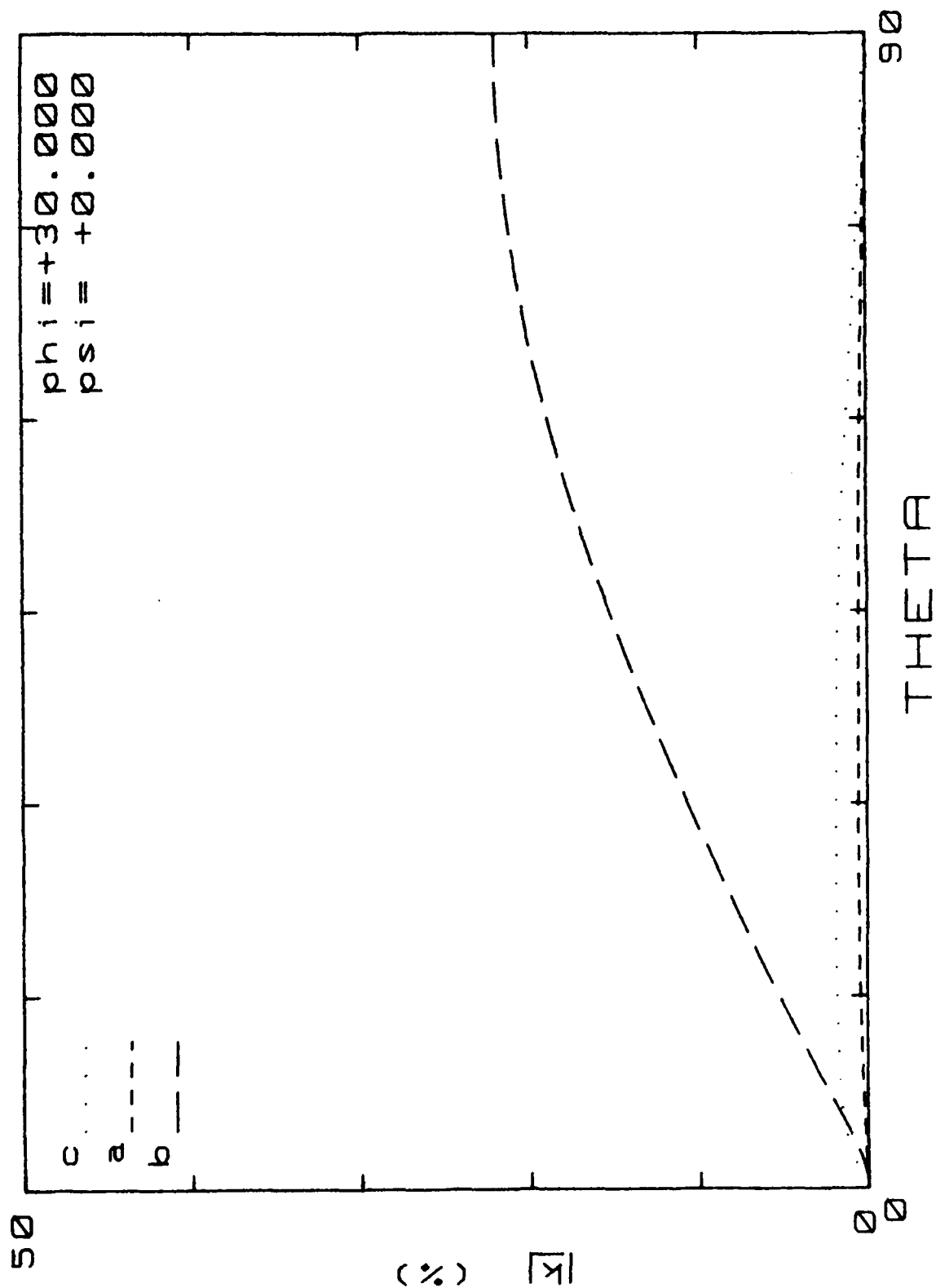


Figure 15. Piezocoupling,  $k_m$ , for  $(yxw)\phi = 30^\circ/\theta$ ,  $\psi_i = 0^\circ$  cuts.

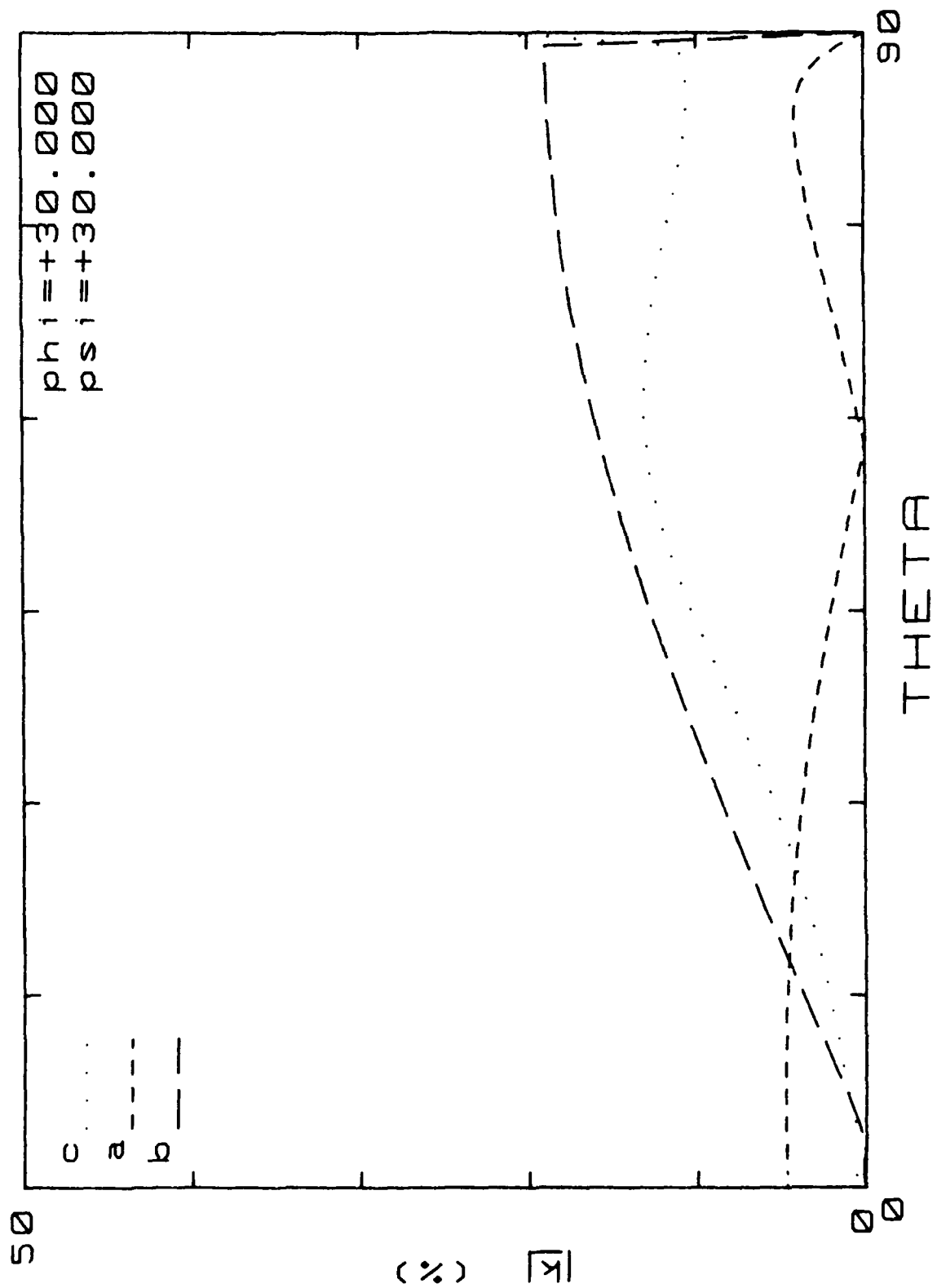


Figure 1b. Piezocoupling,  $k_m$ , for  $(y_{xw1})\phi = 30^\circ/\theta$ ,  $\psi = 30^\circ$  cuts.

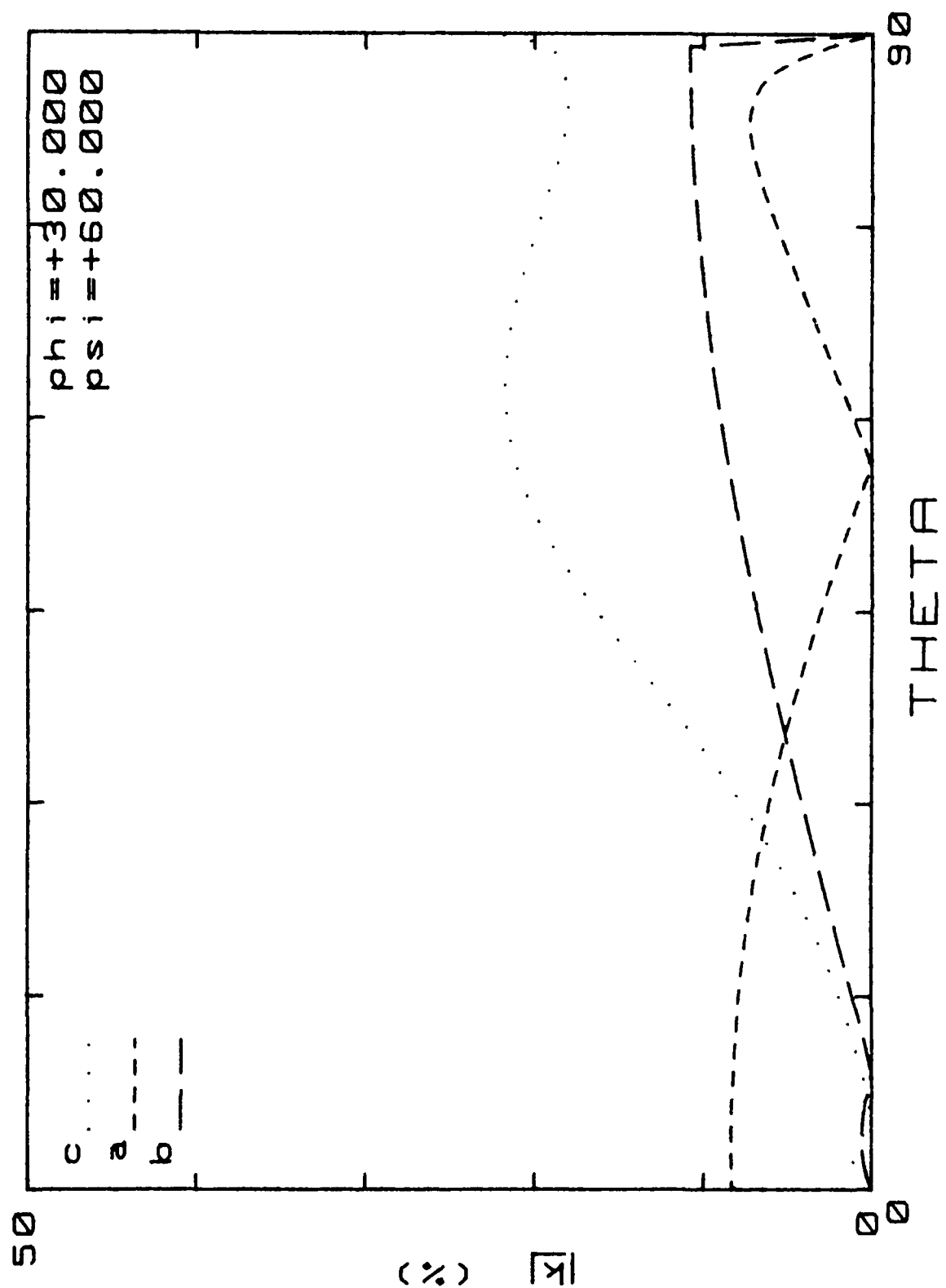


Figure 17. Piezocoupling,  $k_m$ , for  $(y_{xw1})\phi = 30^\circ/\theta$ ,  $\psi = 60^\circ$  cuts.

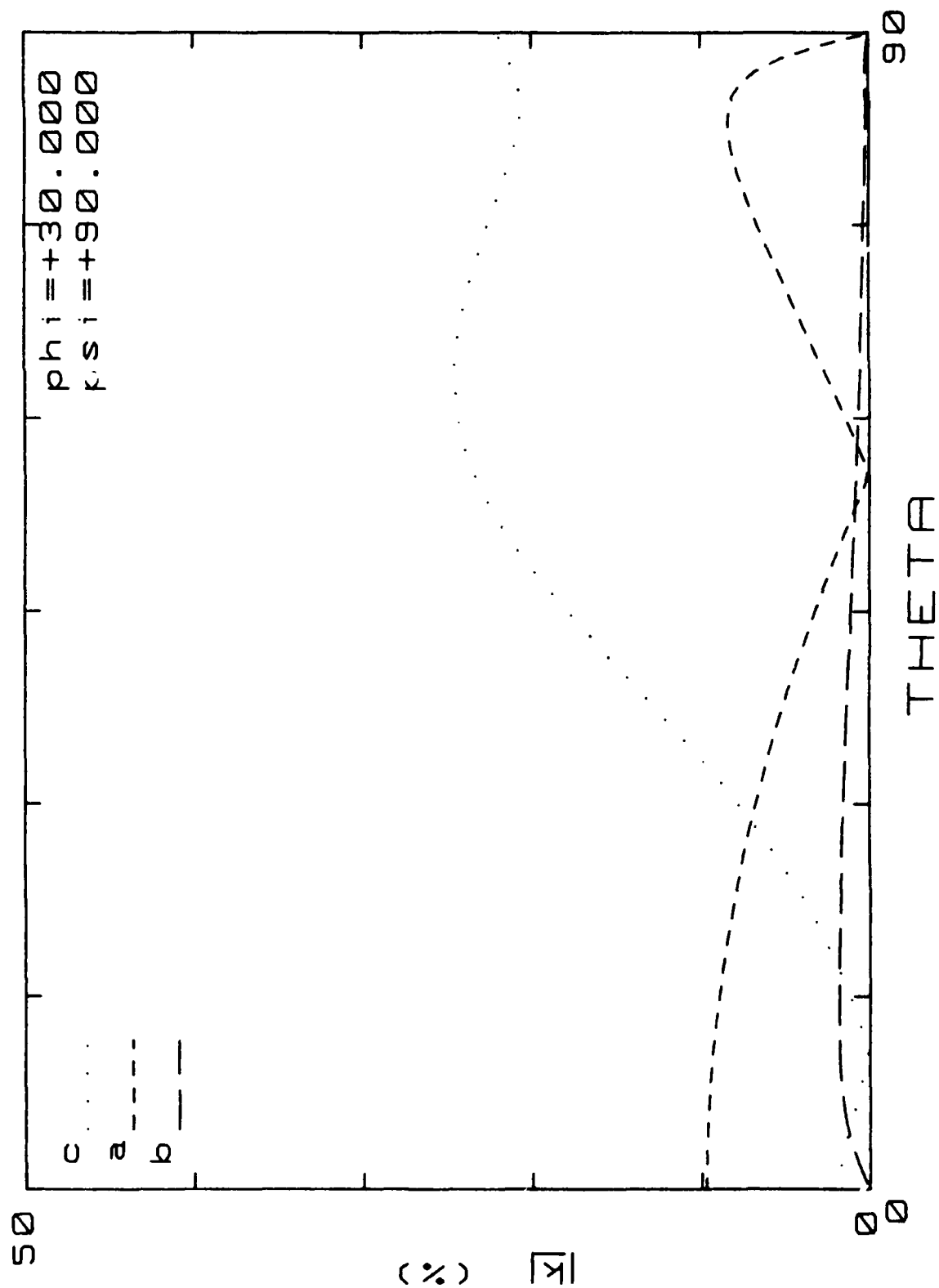


Figure 18. Piezocoupling,  $k_m$ , for  $(y_{xw1})\phi = 30^\circ/\theta$ ,  $\psi = 90^\circ$  cuts.

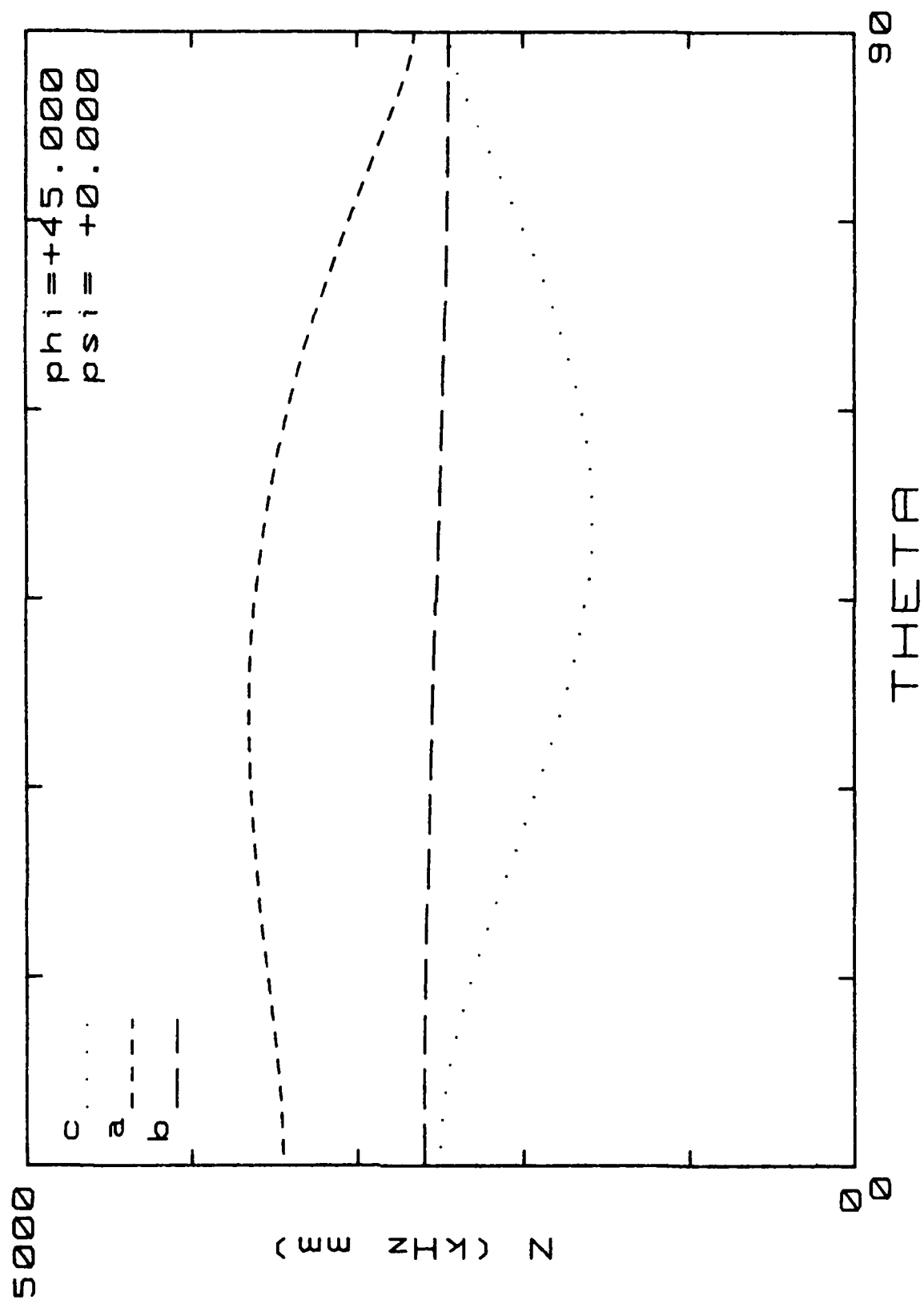


Figure 19. Frequency constant,  $N_m$ , for  $(yxw)\phi = 45^\circ/\theta_{cuts}$ .

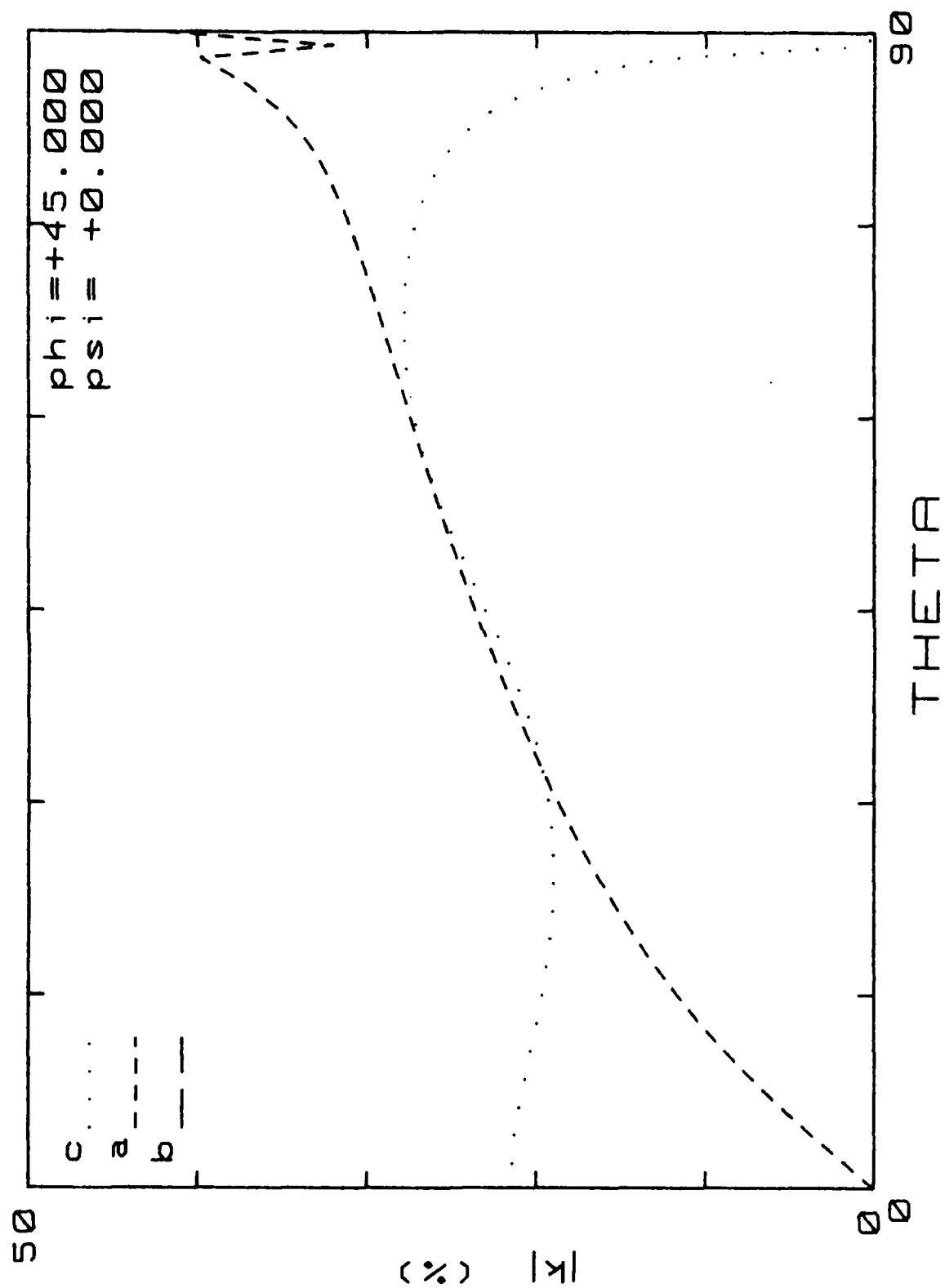


Figure 20. Piezocoupling,  $k_m$ , for  $(yxwl)\phi = 45^\circ/\theta$  cuts.

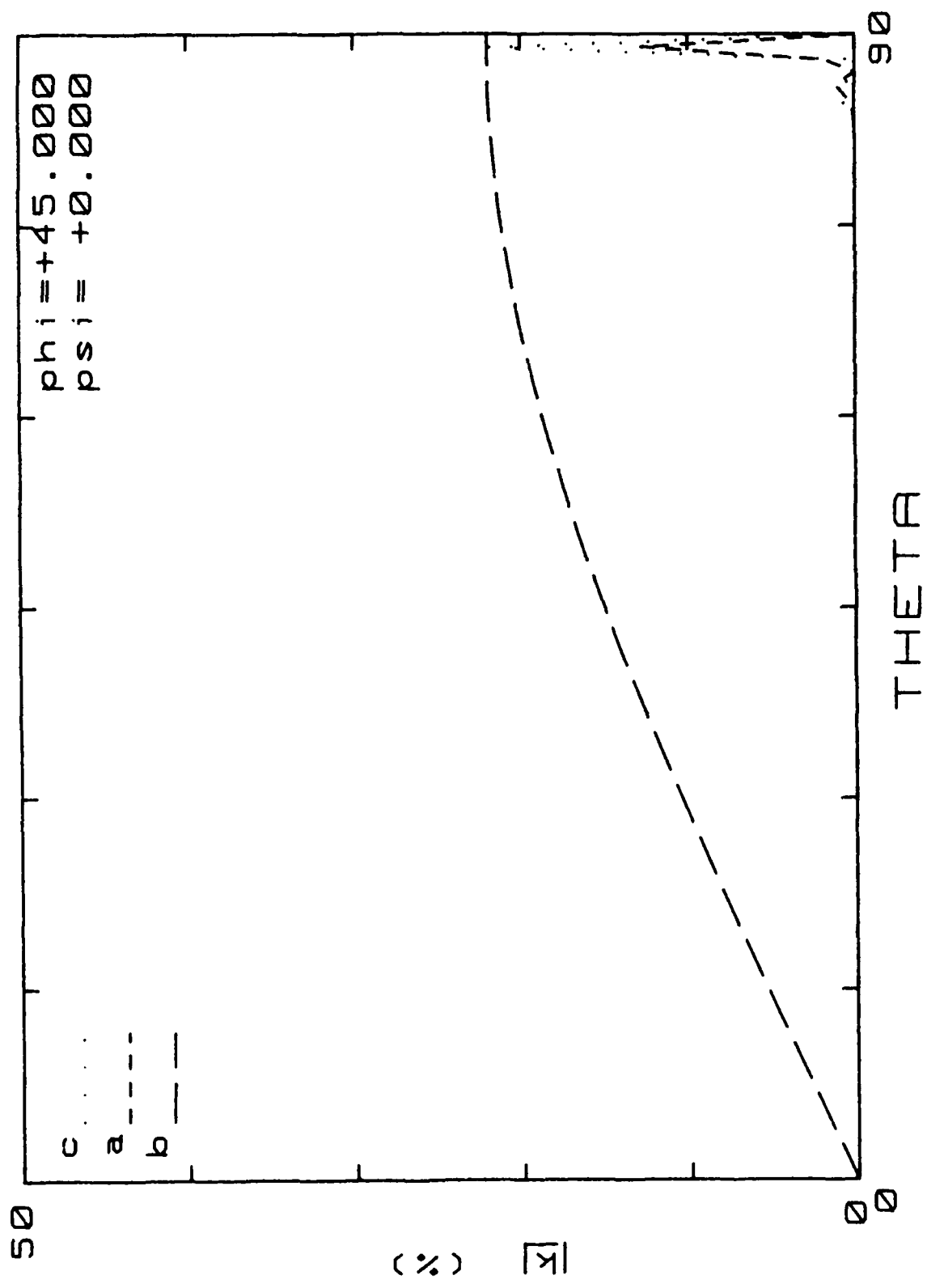


Figure 21. Piezocoupling,  $k_m$ , for  $(yxwl)\phi = 45^\circ/\theta$ ,  $\psi = 0^\circ$  cuts.

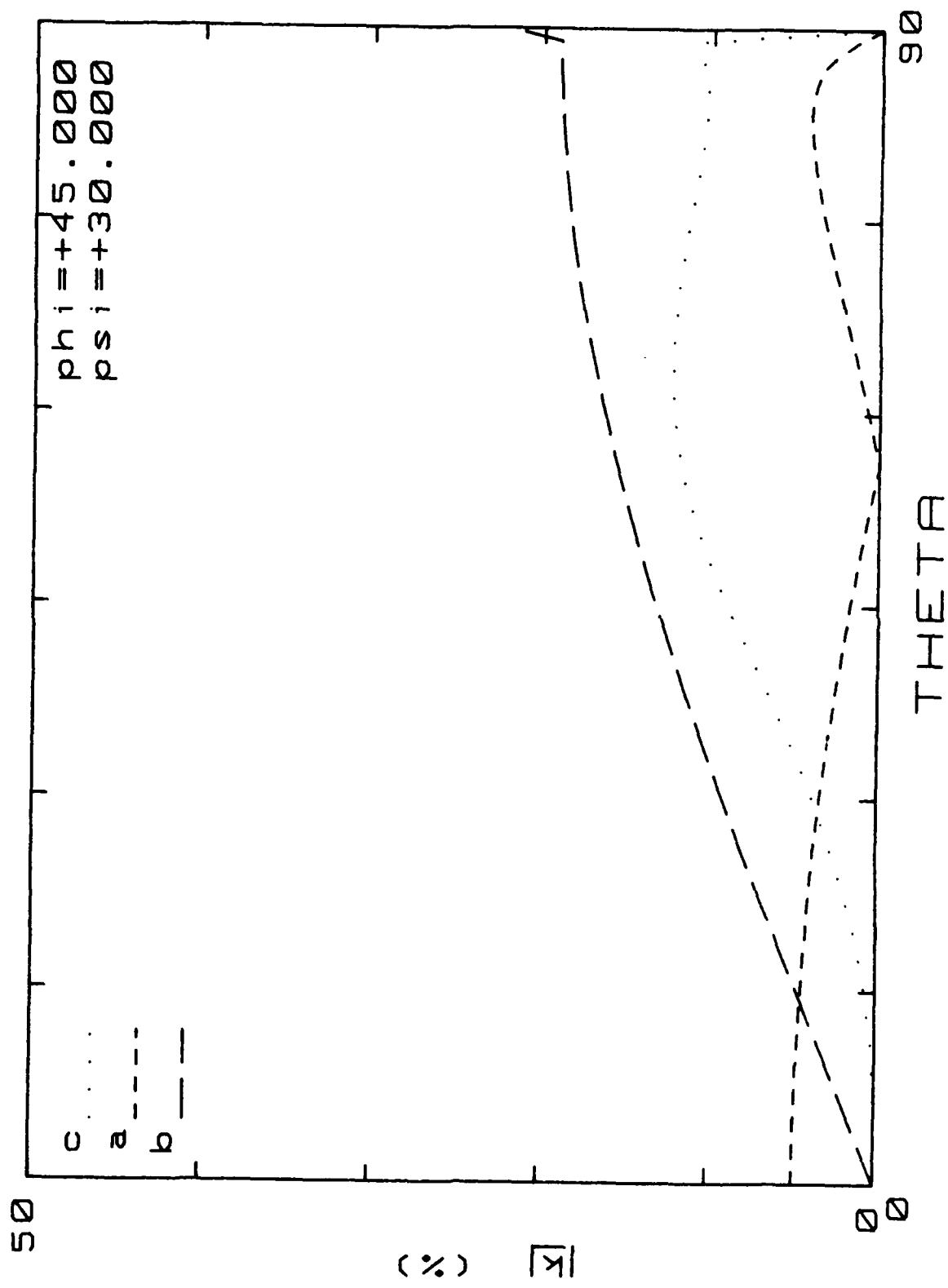


Figure 22. Piezocoupling,  $k_m$ , for  $(yxw)\phi = 45^\circ/\theta$ ,  $\psi = 30^\circ$  cuts.

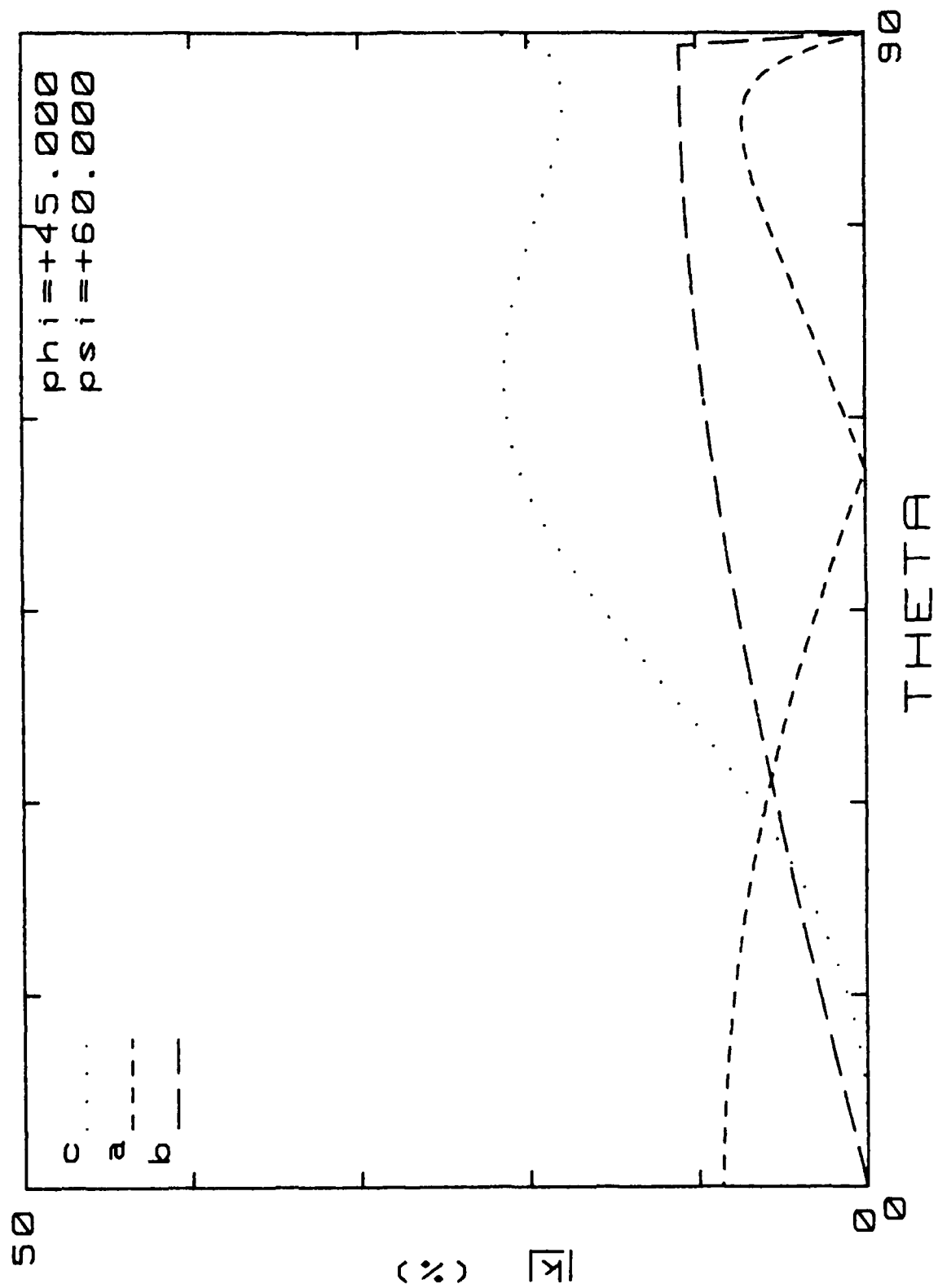


Figure 23. Piezocoupling,  $k_m$ , for  $(y_{xw1})\phi = 45^\circ/\theta$ ,  $\psi = 60^\circ$  cuts.

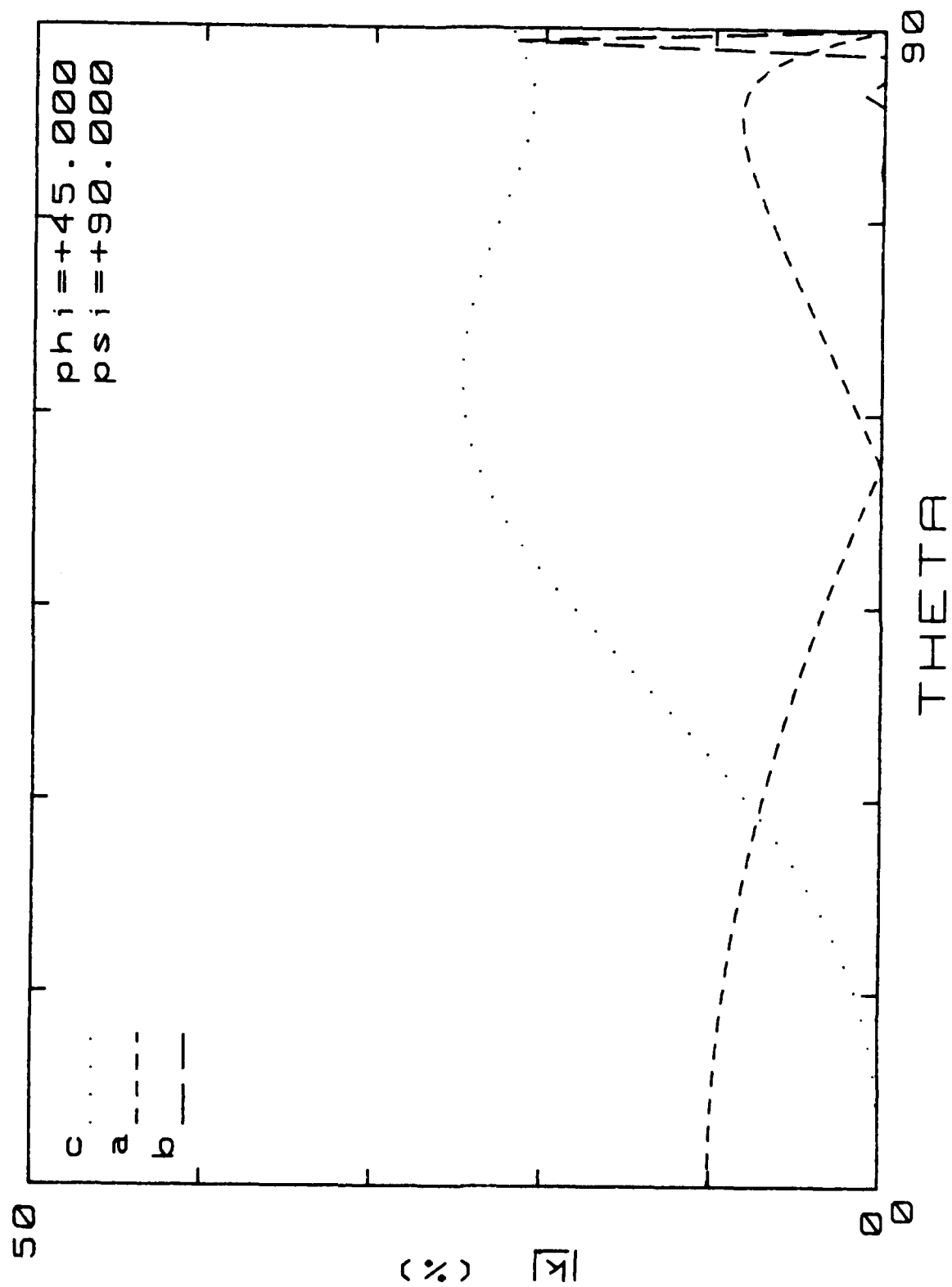


Figure 24. Piezocoupling,  $k_m$ , for  $(y_{xw1})\phi = 45^\circ/\theta$ ,  $\psi = 90^\circ$  cuts.

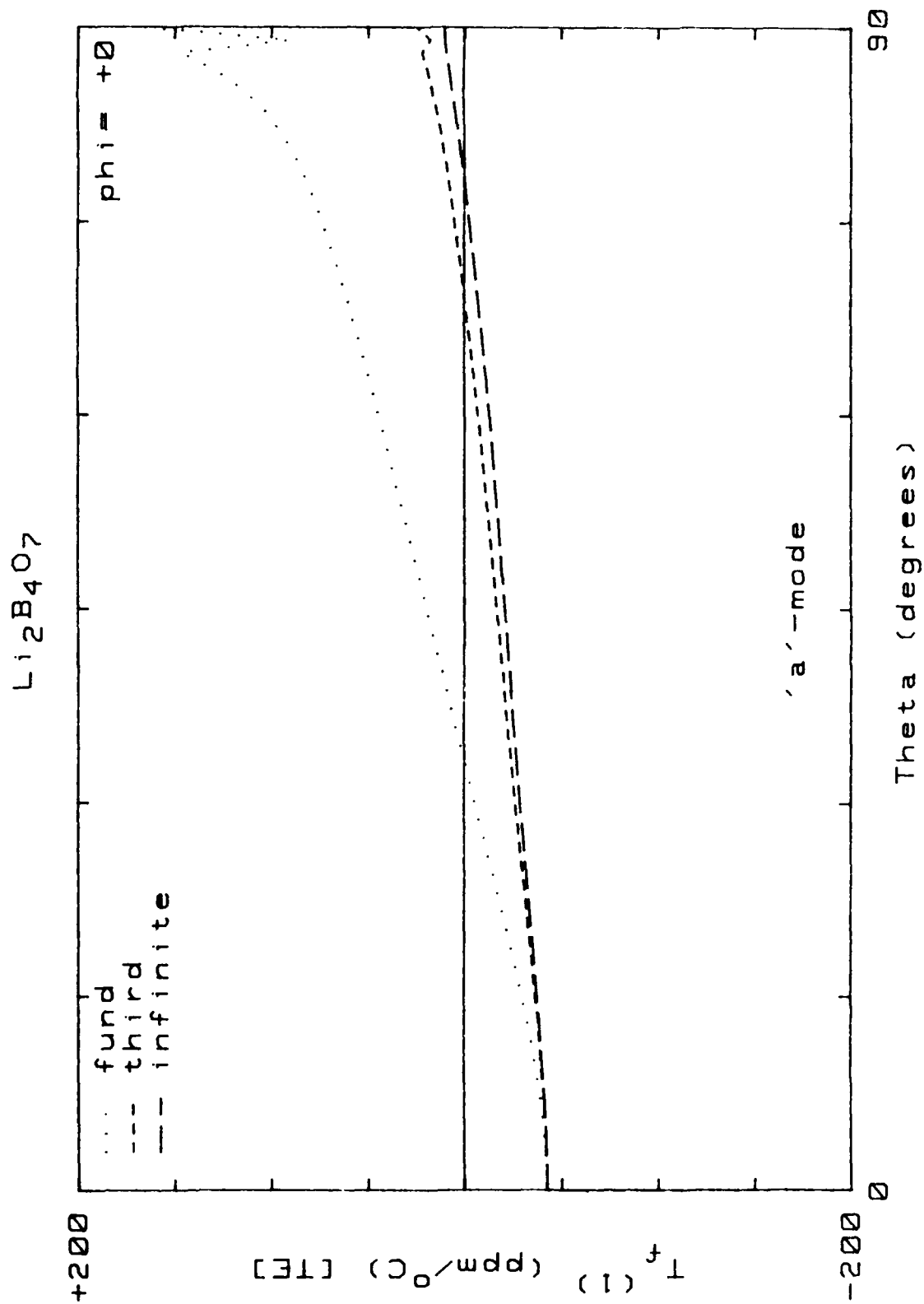


Figure 25.  $TC(1)$  for  $(yxw1)\phi = 0^\circ/\theta$  cuts;  $N = 1, 3, \infty$ ; mode "a"; [TE].

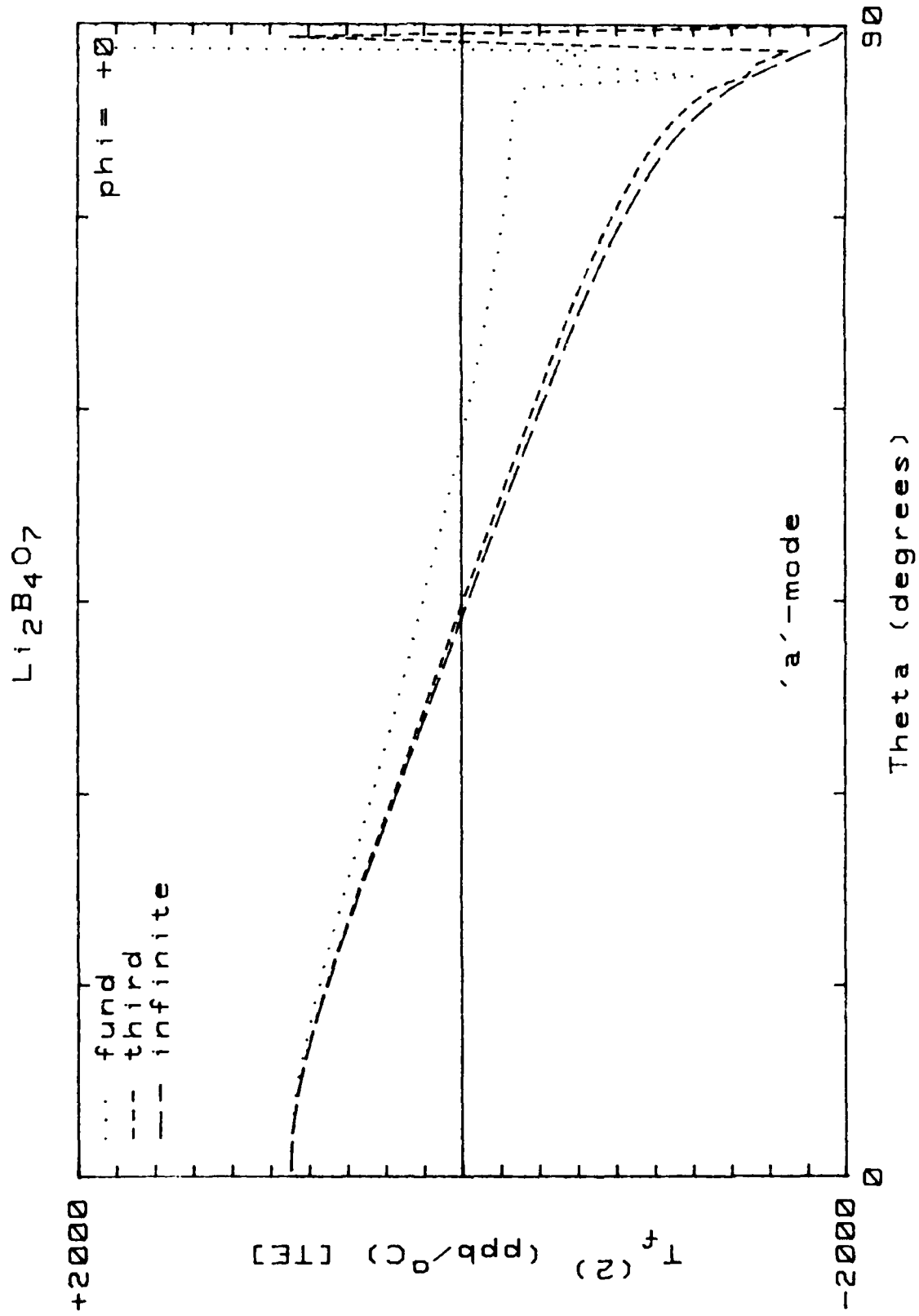


Figure 26. TC(2) for (yxw)  $\phi = 0^\circ/\theta$  cuts;  $M = 1, 3, \infty$ ; mode "a"; [TE].

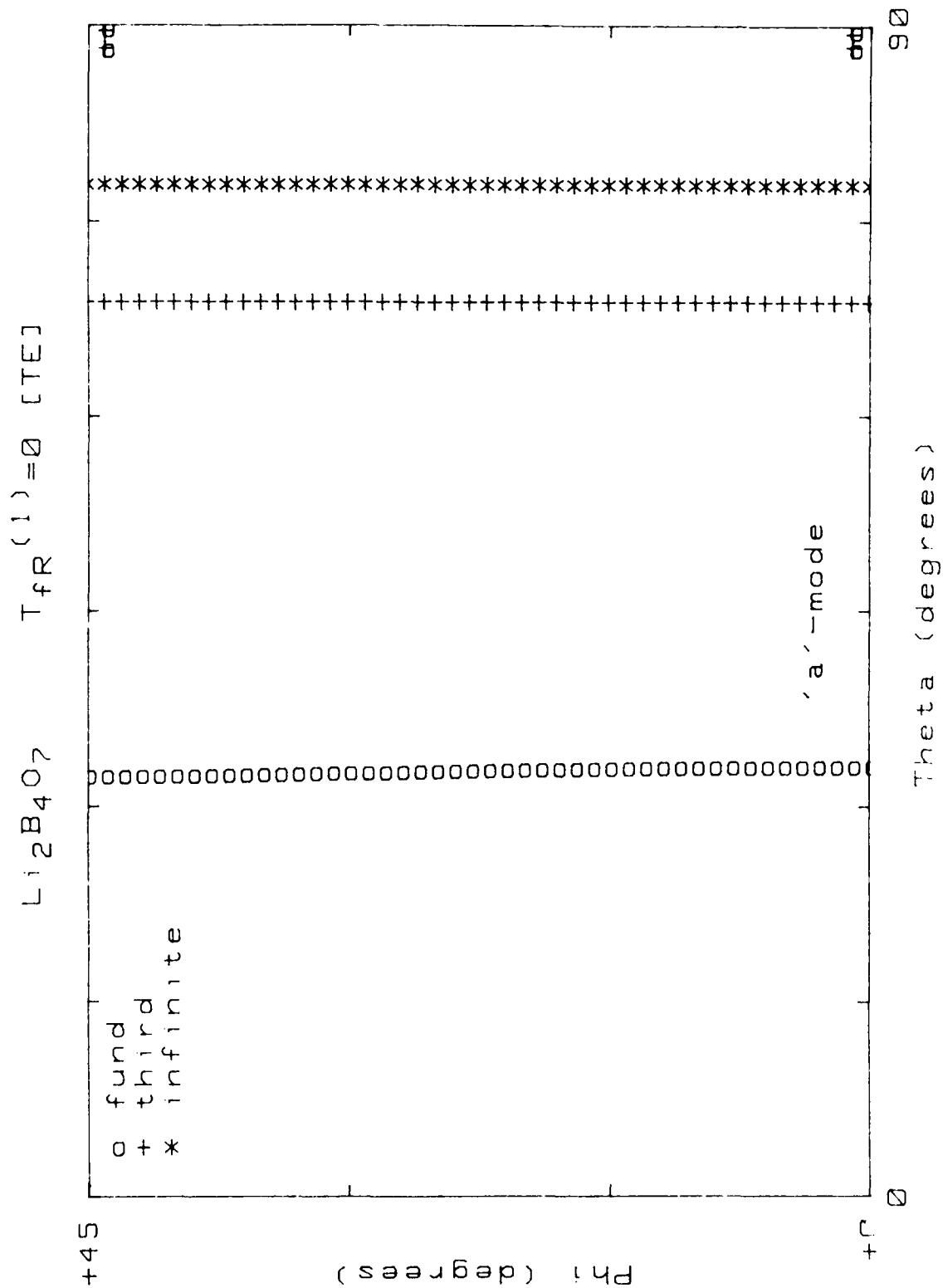


Figure 27. Locus of  $TC(1)=0$  for  $(yxw)\phi/\theta$ cuts;  $M = 1, 3, \infty$ ; mode "a"; [TE].

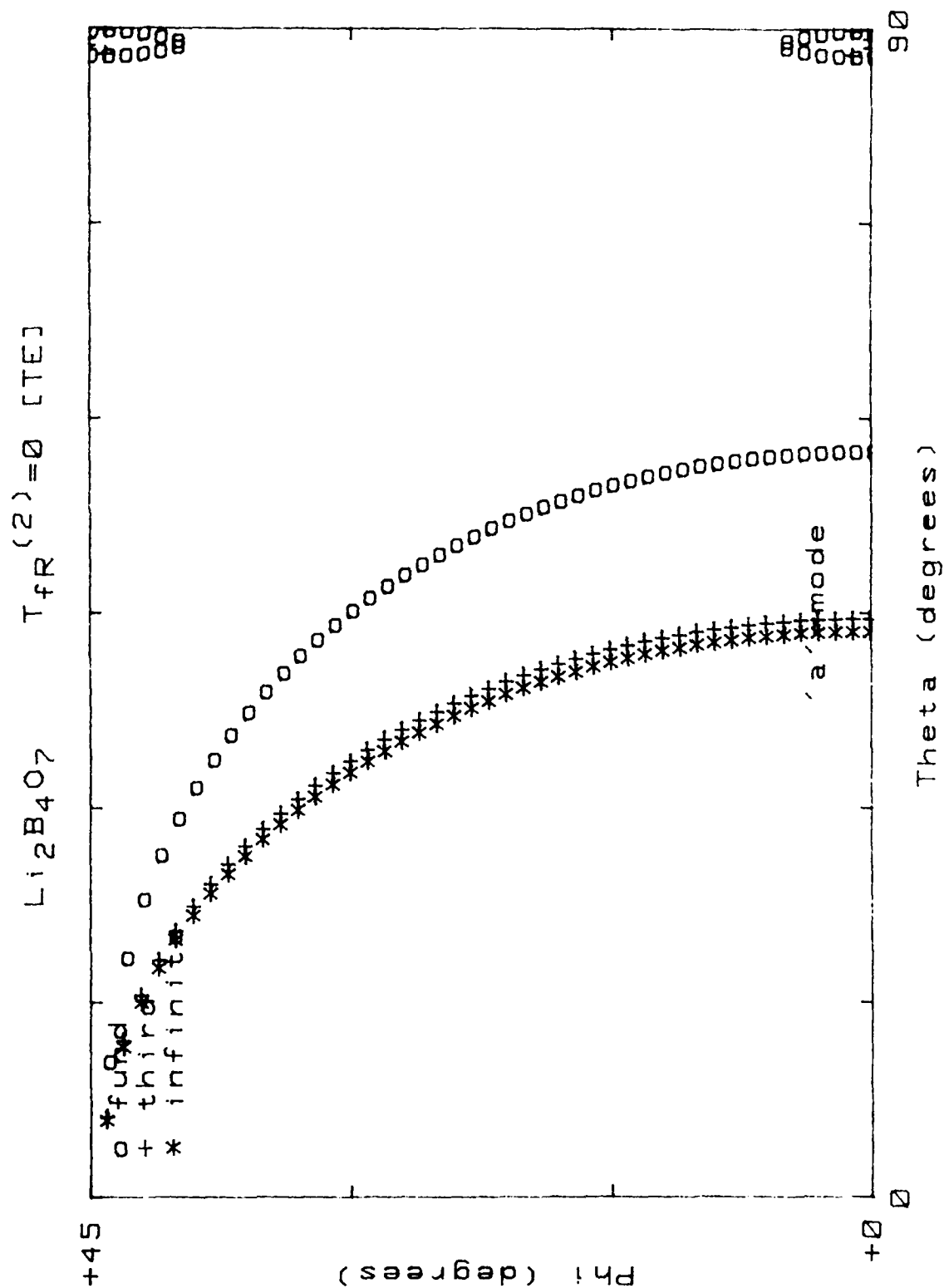


Figure 28. Locus of  $TC(2)=0$  for  $(yxw)\phi/\theta$ cuts;  $M = 1, 3, \infty$ ; mode "a"; [TE].

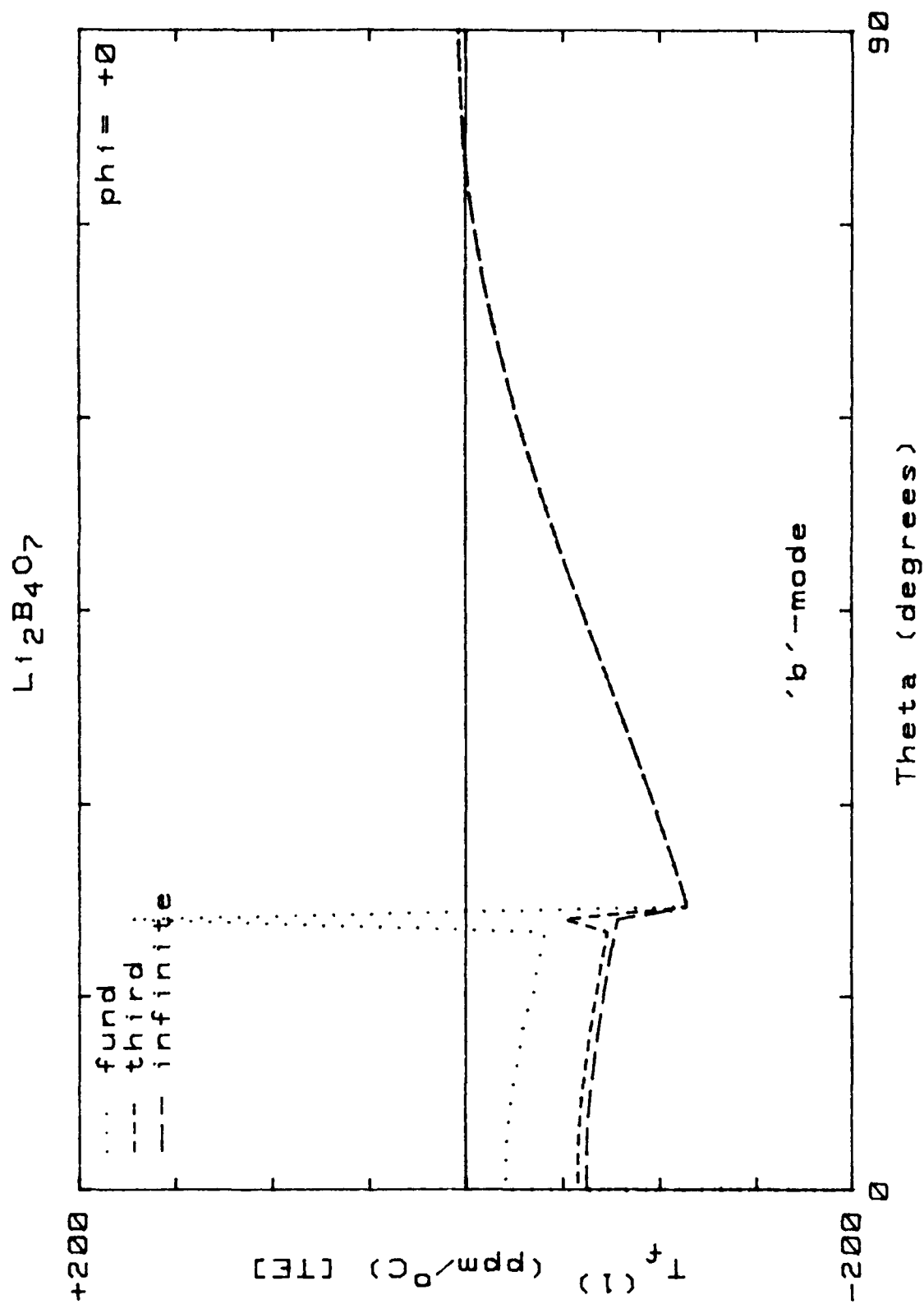


Figure 29.  $\text{TC}(1)$  for  $(\text{yxw})\phi = 0^\circ/\theta$  cuts;  $M = 1, 3, \infty$ ; mode "b"; [TE].

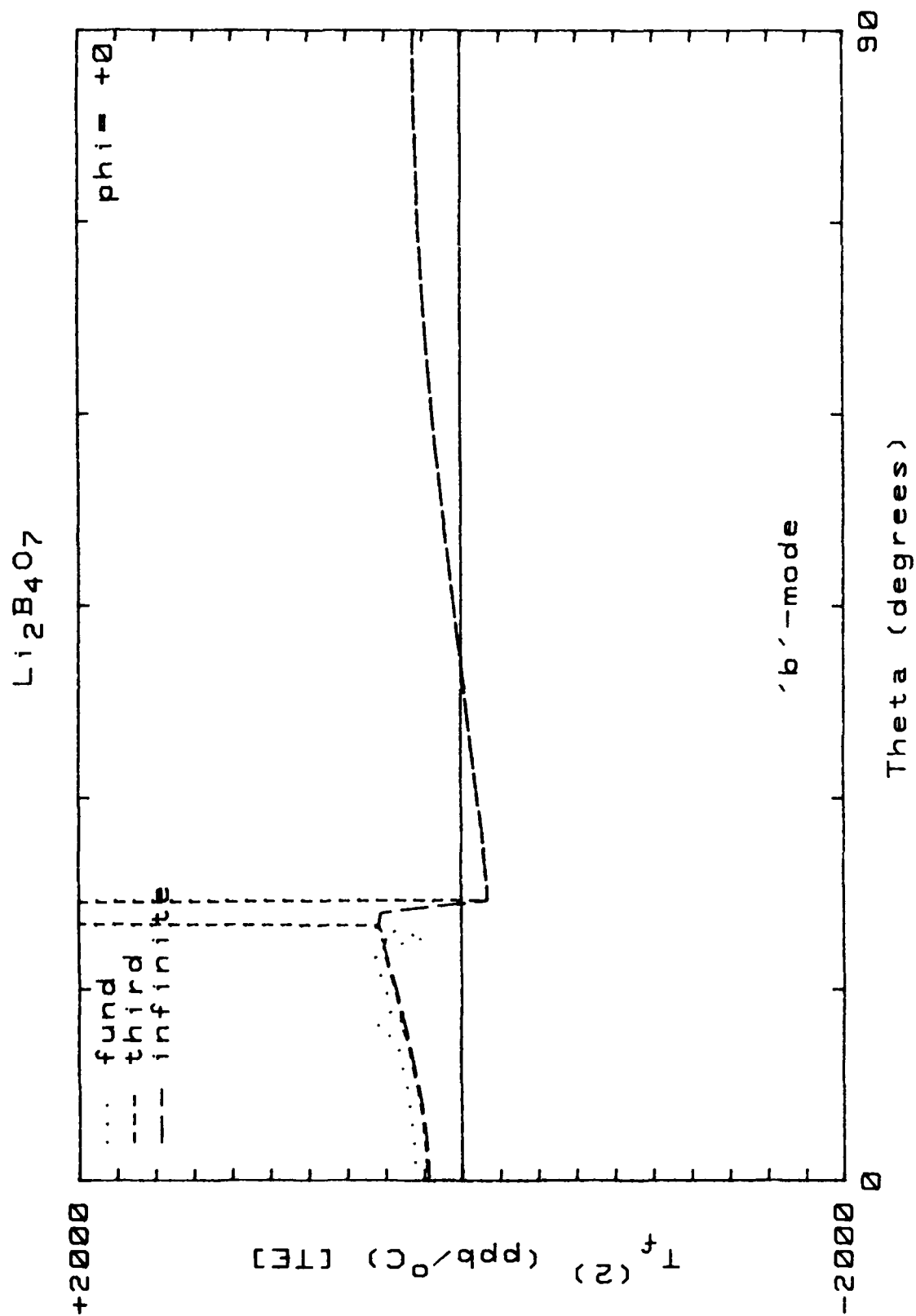


Figure 30.  $\text{TC}(2)$  for  $(\text{yxwl})\phi = 0^\circ/\theta$  cuts;  $M = 1, 3, \infty$ ; mode "b"; [TE].

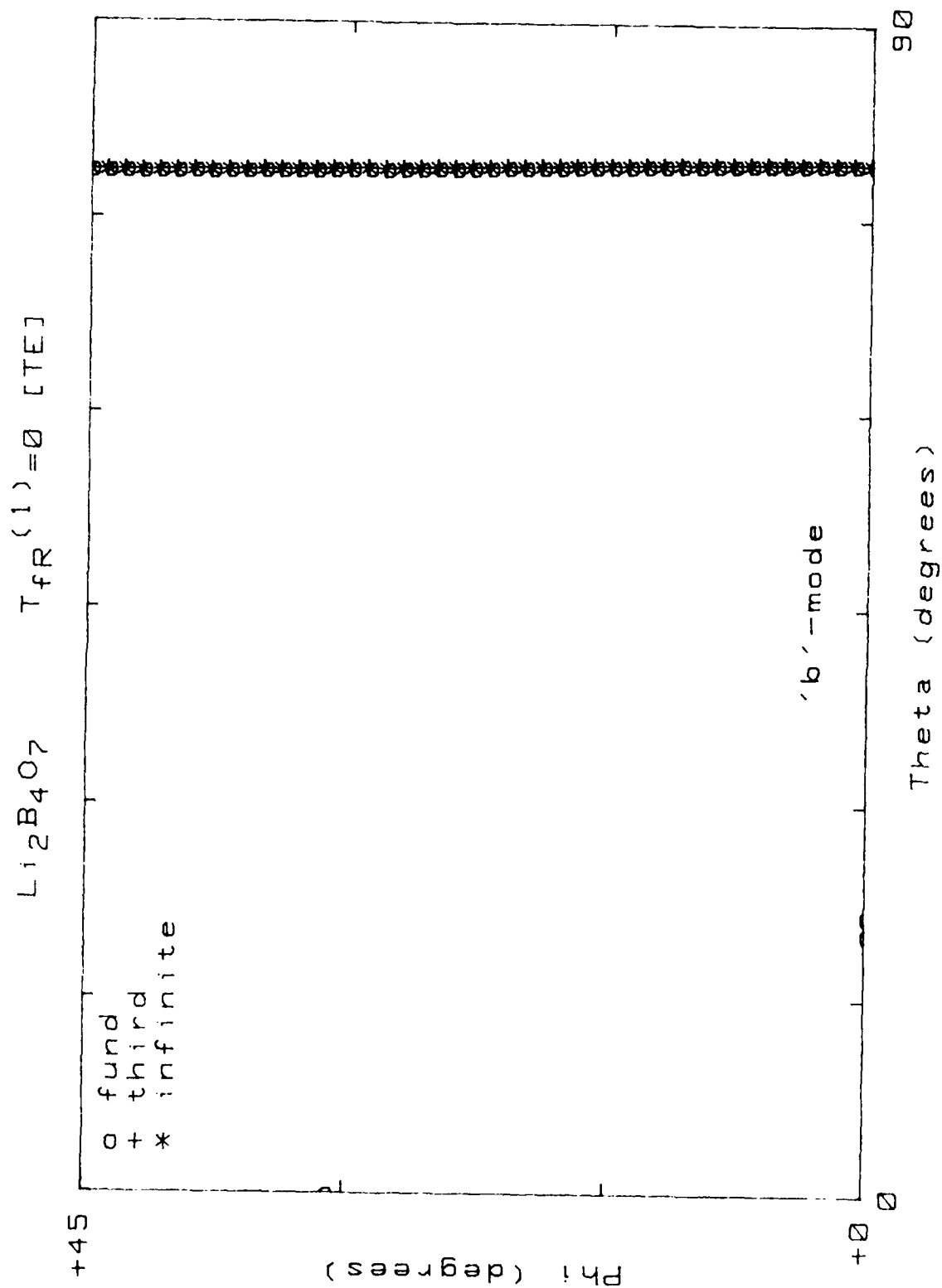


Figure 31 Locus of  $TC(1) = 0$  for  $(v_{xw}) \phi / \theta$  cuts;  $M = 1, 3, \infty$ ; mode "b"; [TE].

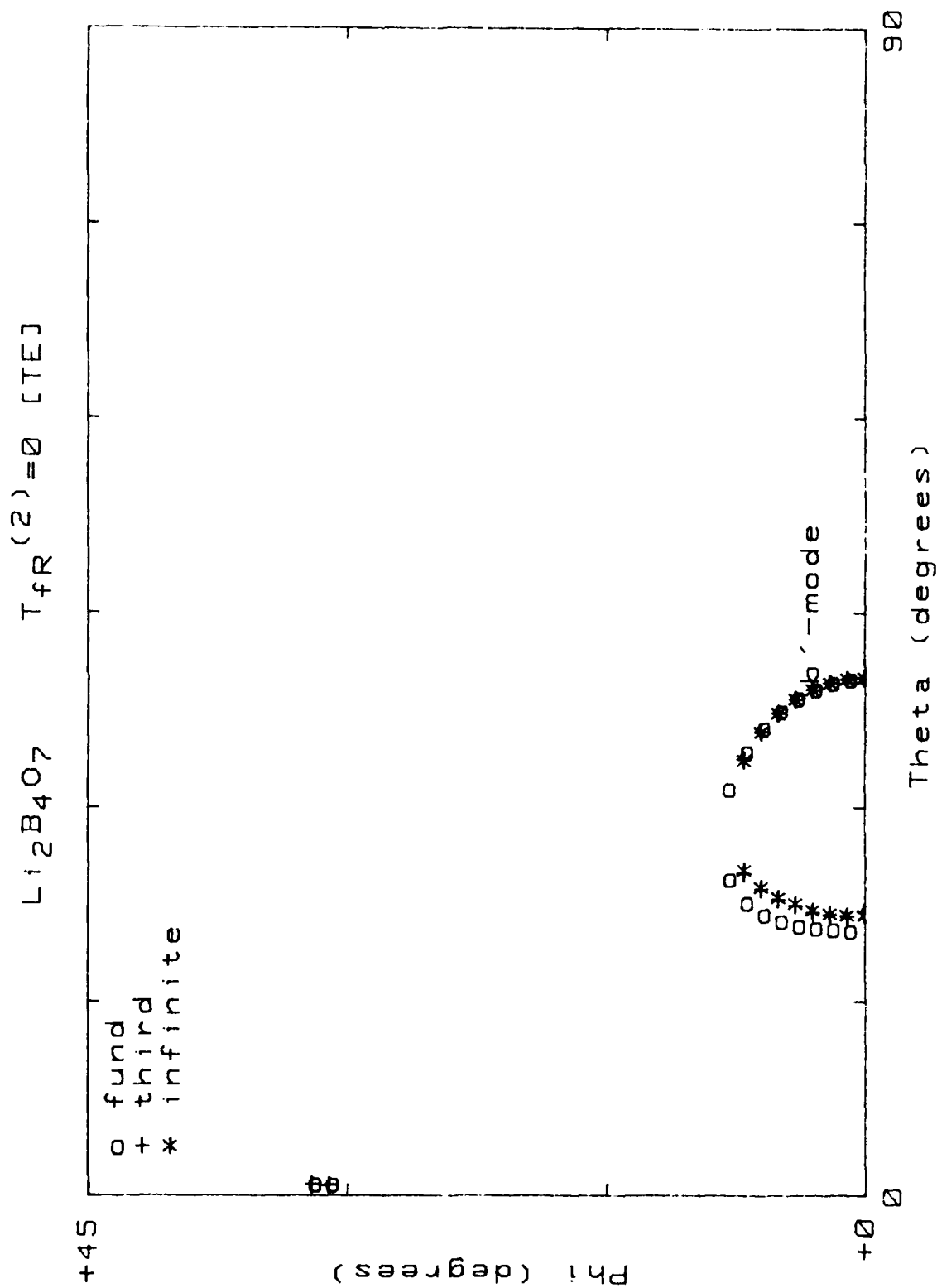


Figure 32. Locus of  $TC(2)=0$  for  $(yxw1)\phi/\theta$  cuts;  $M = 1, 3, \infty$ ; mode "b"; [TE].

$\text{Li}_2\text{B}_4\text{O}_7$

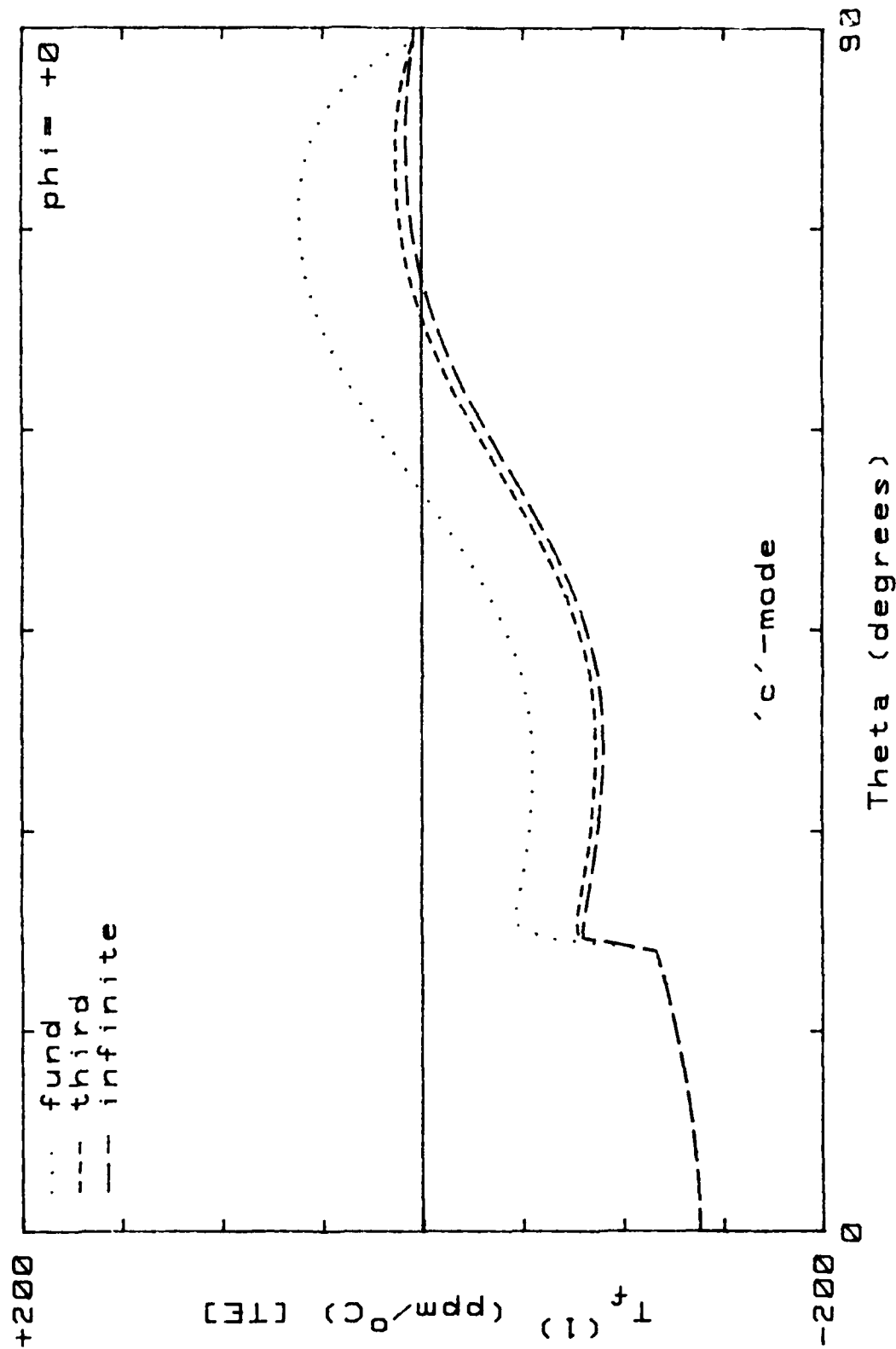


Figure 33.  $\text{TC}(1)$  for  $(yxw1)\phi=0^\circ/\theta$  cuts;  $M = 1, 3, \infty$ ; mode "c"; [TE].

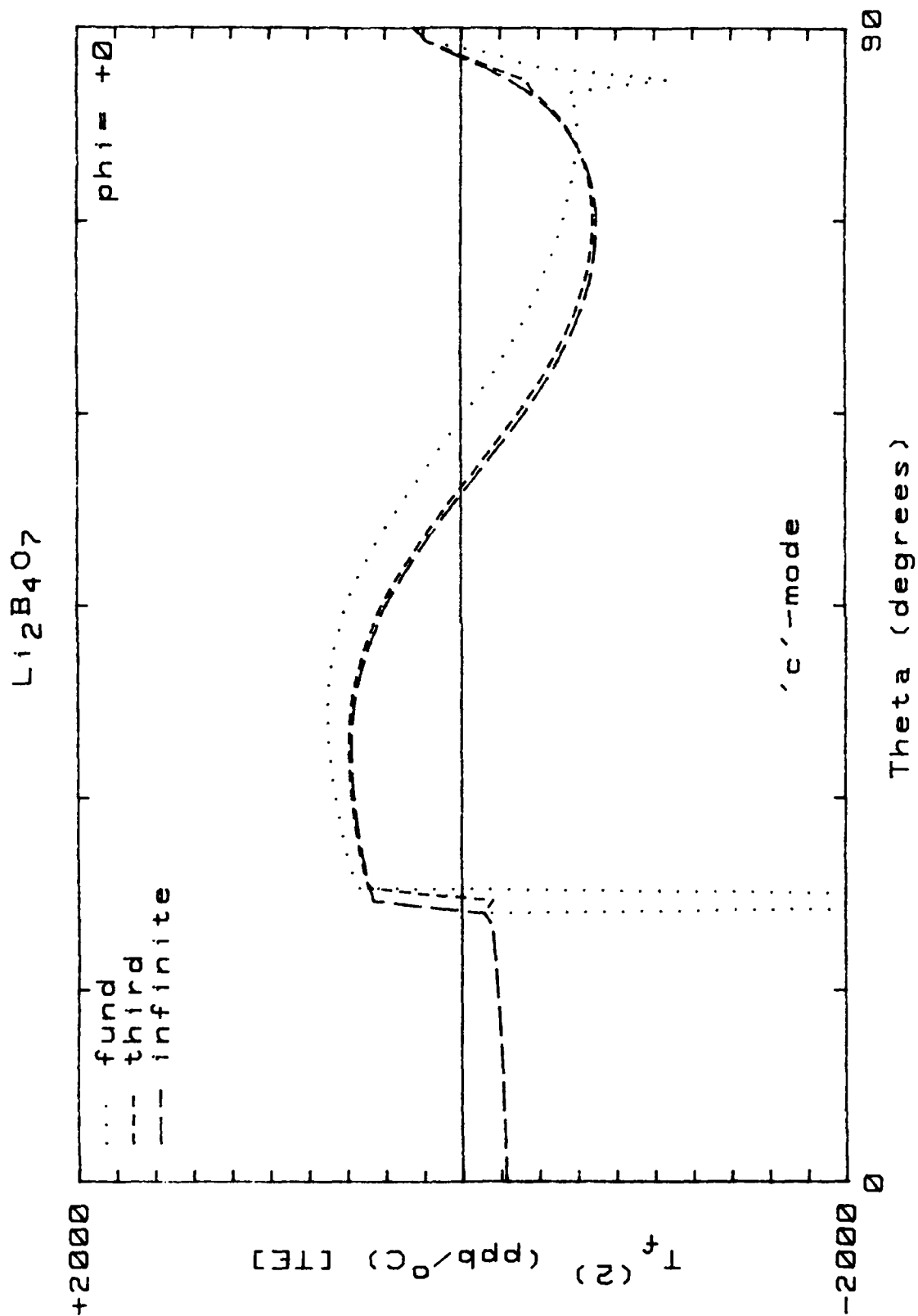


Figure 34.  $\text{TC}(2)$  for  $(yxw1)\phi=0^\circ/\theta$  cuts;  $M = 1, 3, \infty$ ; mode "c"; [TE].

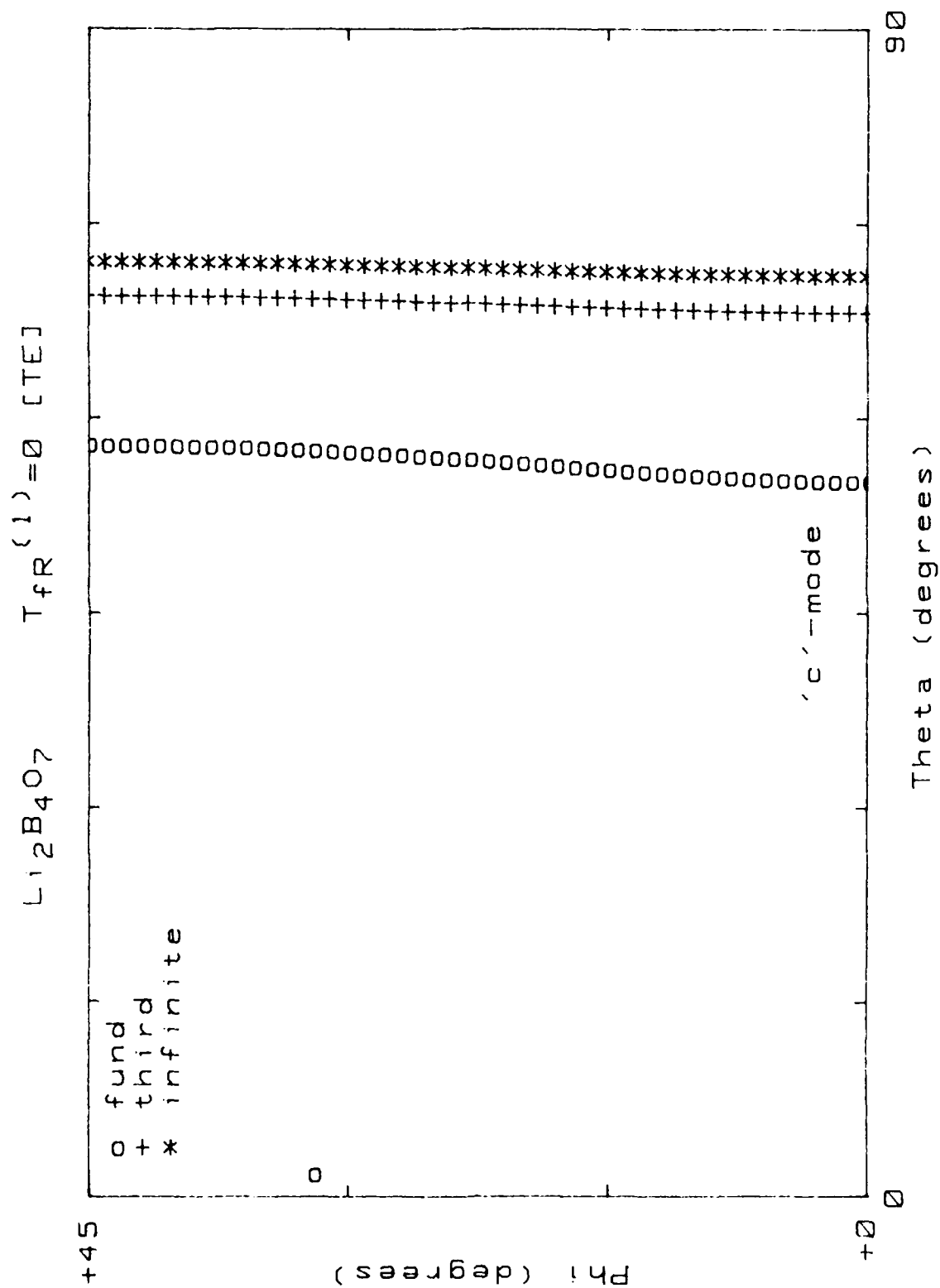


Figure 35. Locus of  $TC(1)=0$  for  $(yxw)\phi/\theta$  cuts;  $M = 1, 3, \infty$ ; mode "c"; [TE].

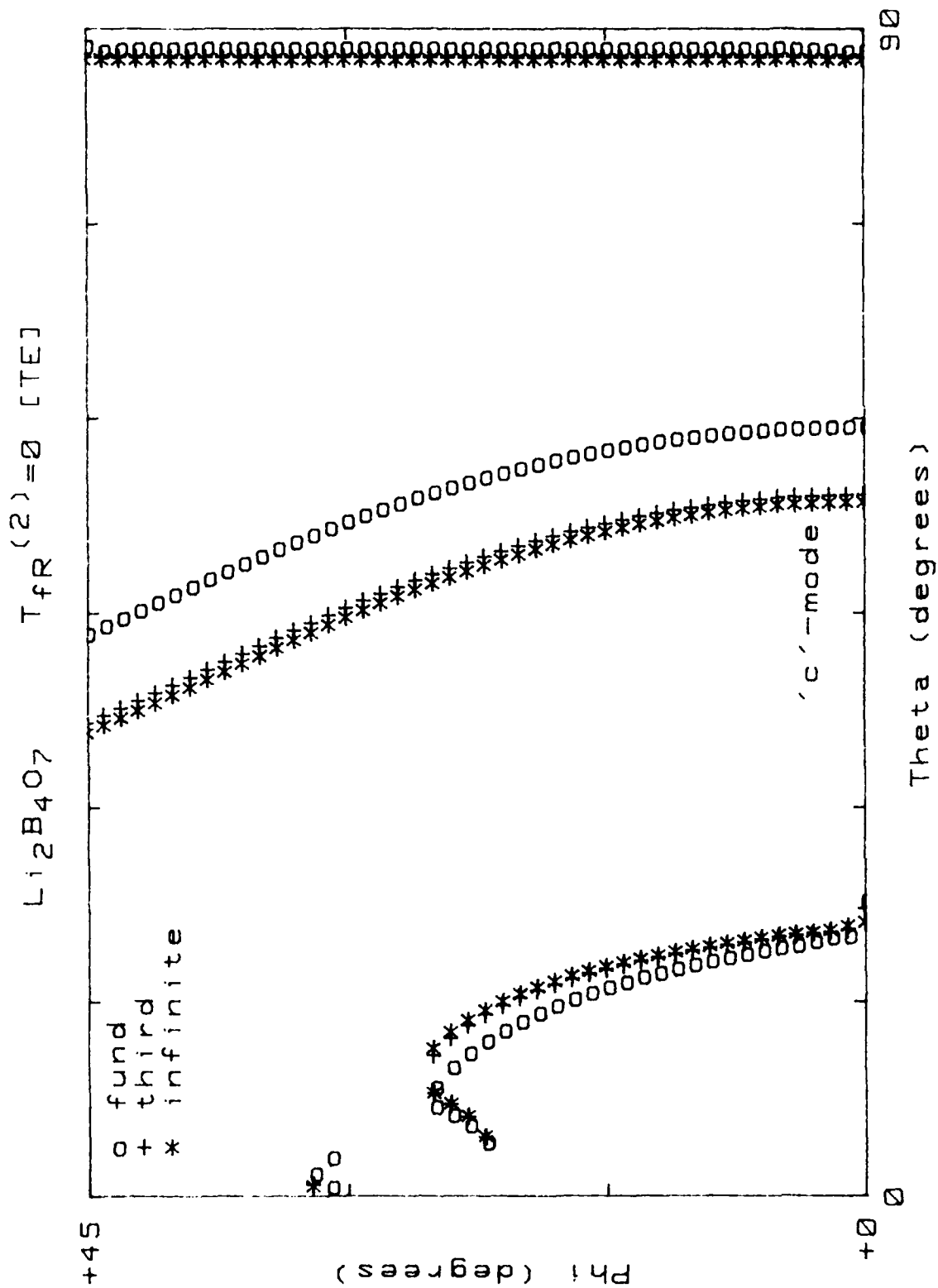


Figure 36. Locus of  $TC(2)=0$  for  $(yxw)\phi/\theta$  cuts;  $M = 1, 3, \infty$ ; mode "c"; [TE].

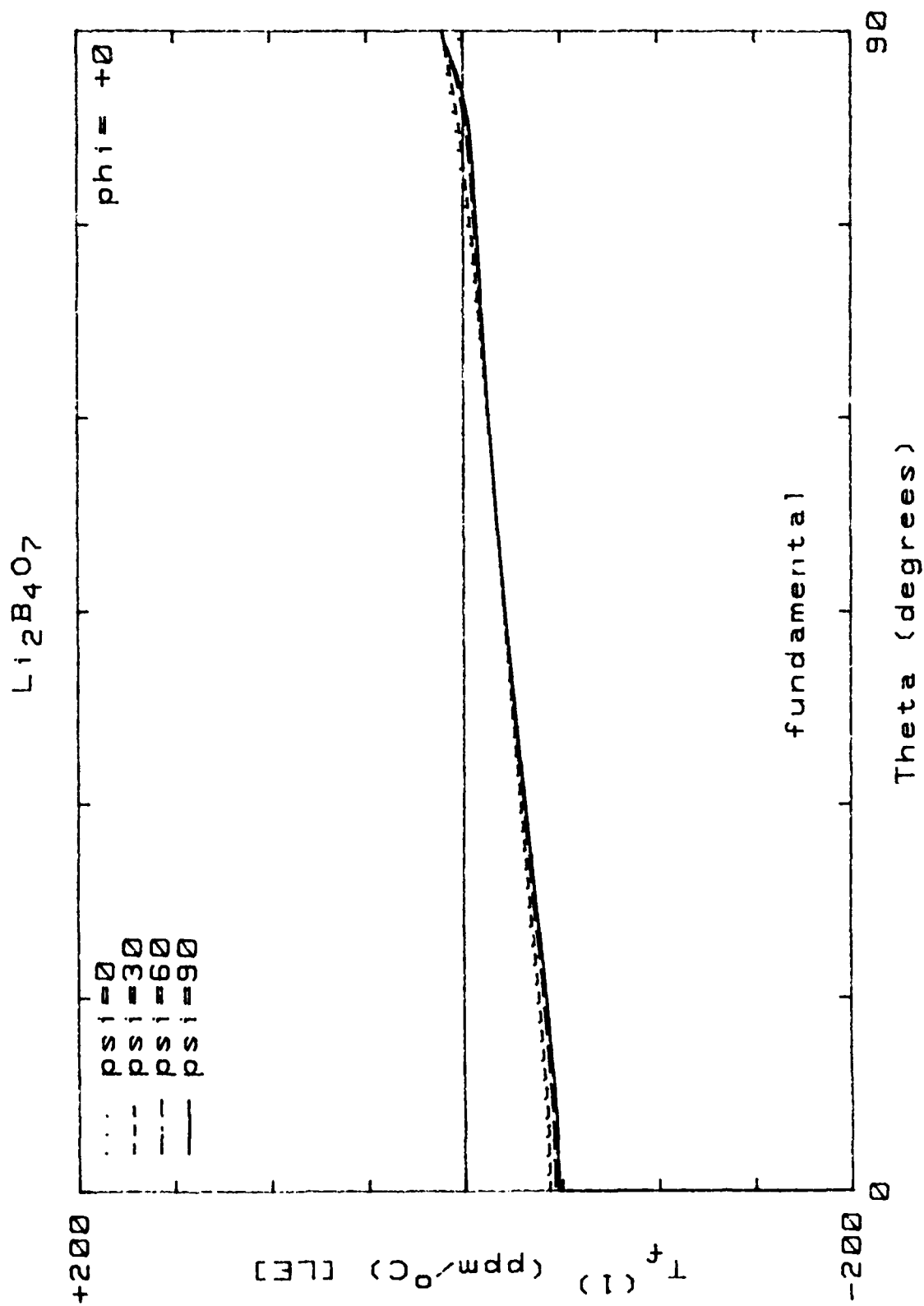


Figure 37. TC(1) for (yxw1) $\phi=0^\circ/\theta$  cuts;  $M = 1$ ; mode "a";  $\text{psi}=0^\circ(30^\circ)90^\circ$ ; [LE].

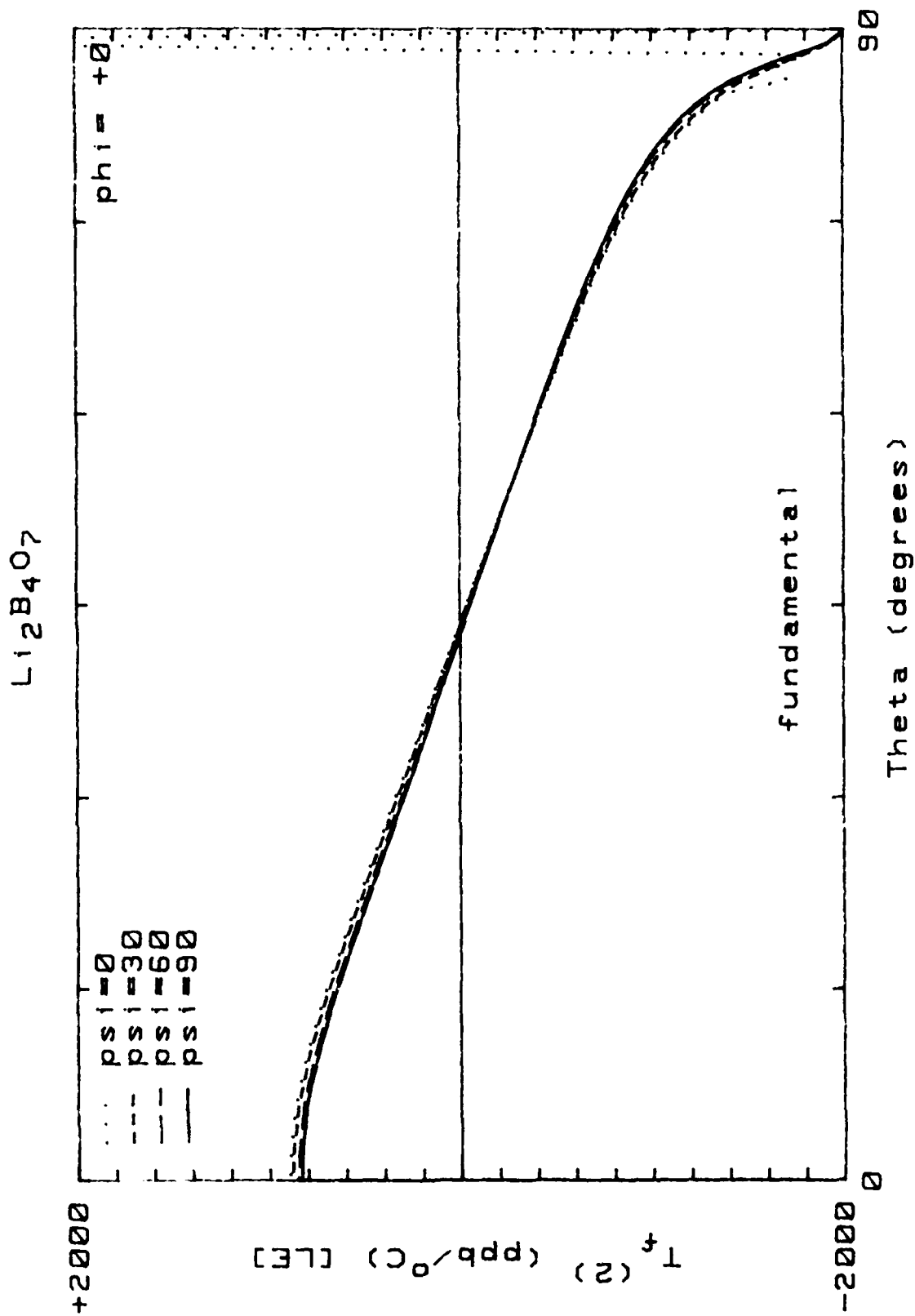


Figure 36.  $\text{TC}(2)$  for  $(\text{yxw}) \phi = 0^\circ / \theta$  cuts;  $M = 1$ ; mode "a";  $\psi = 0^\circ$  ( $30^\circ$ )  $90^\circ$ ; [LE]

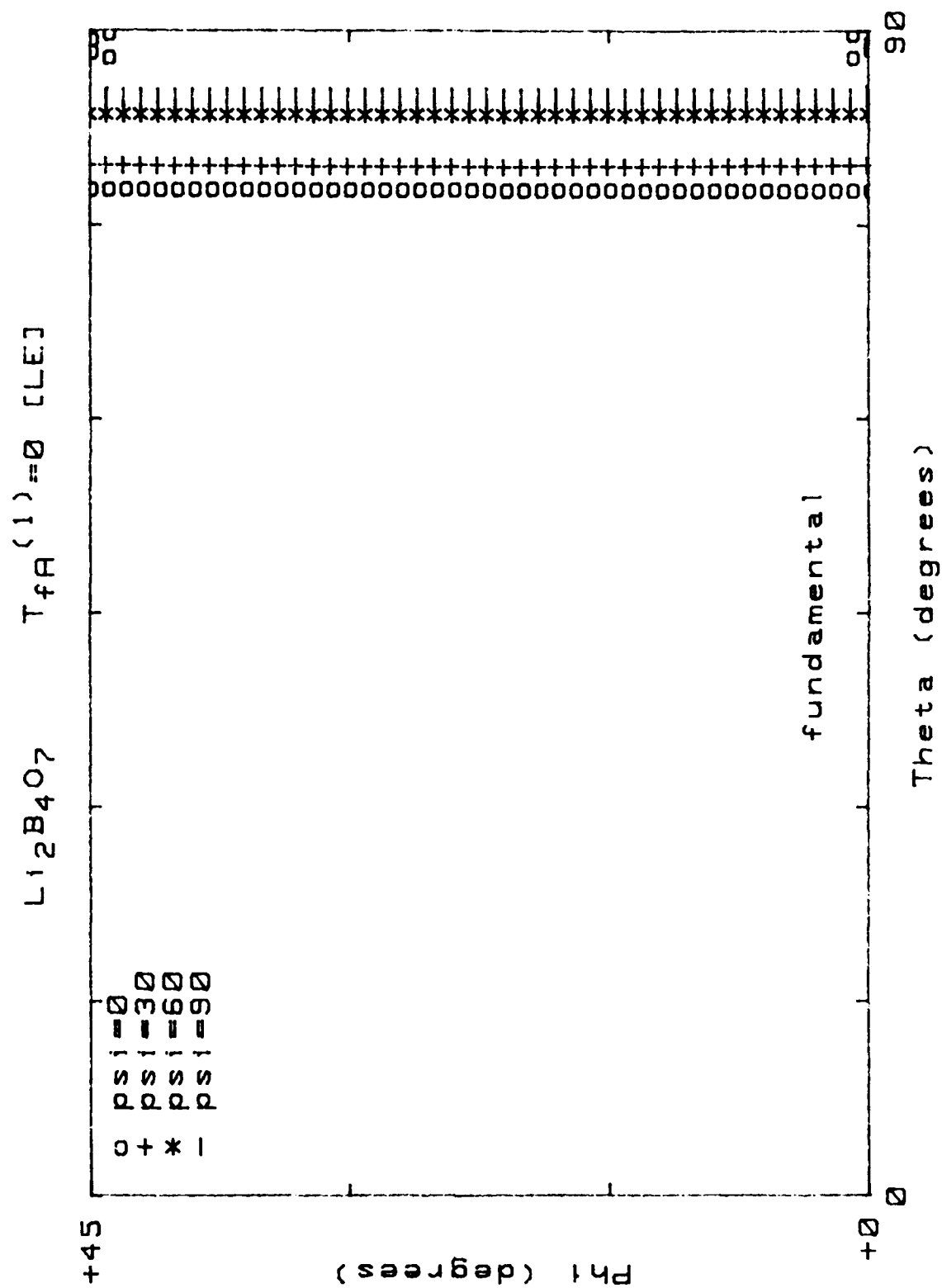


Figure 3). Locus of  $TC(1)=0$  for  $(yxw)\phi/\theta$  cuts;  $M = 1$ ; mode "a";  $\psi = 0^\circ$  ( $30^\circ$ )  $90^\circ$ ; [LE]

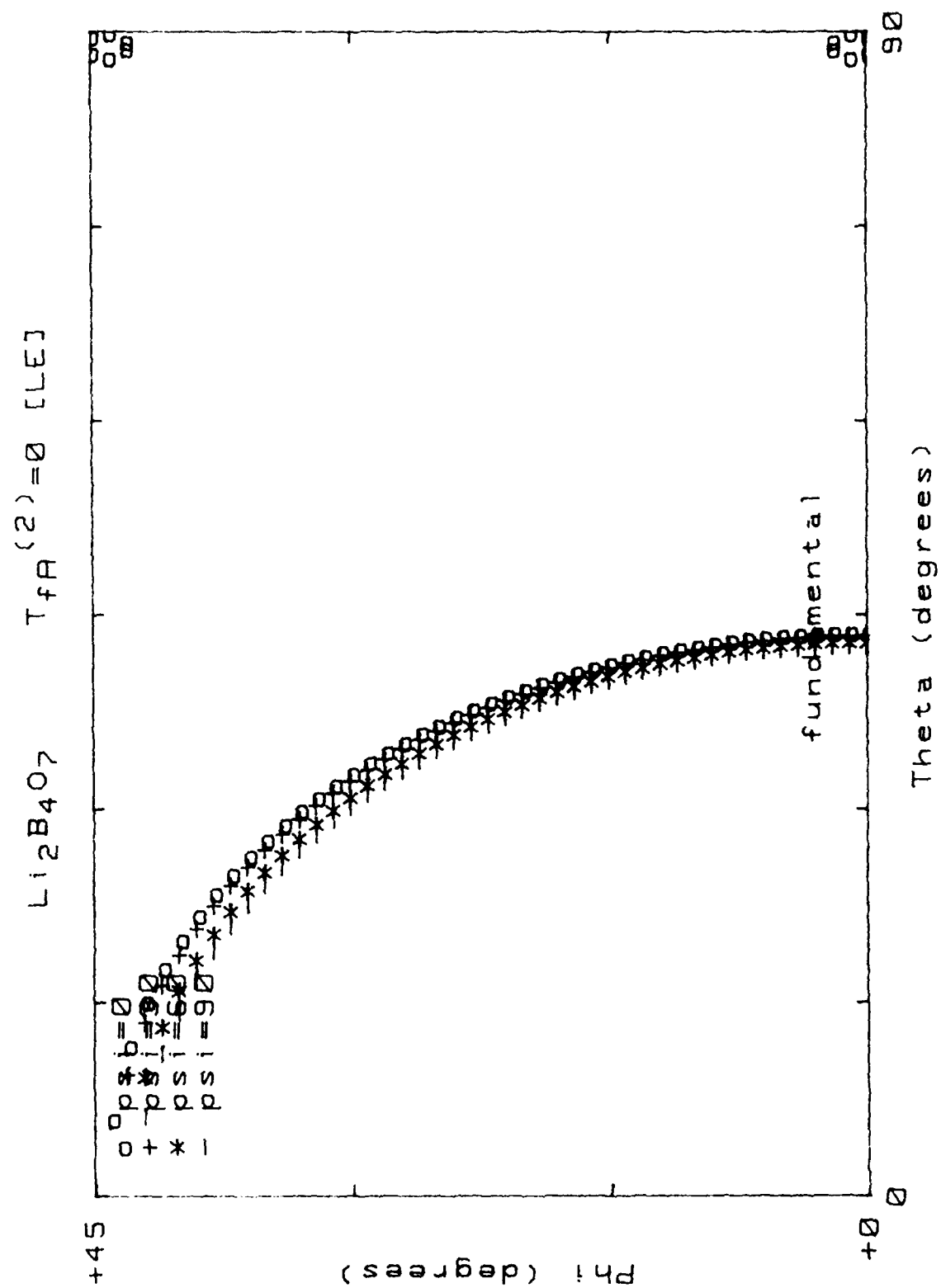


Figure 40. Locus of  $TC(2)=0$  for  $(yxw)\phi/\theta$  cuts;  $N=1$ ; mode "a";  $\psi=0^\circ$  ( $30^\circ$ )  $90^\circ$ ; [LE]

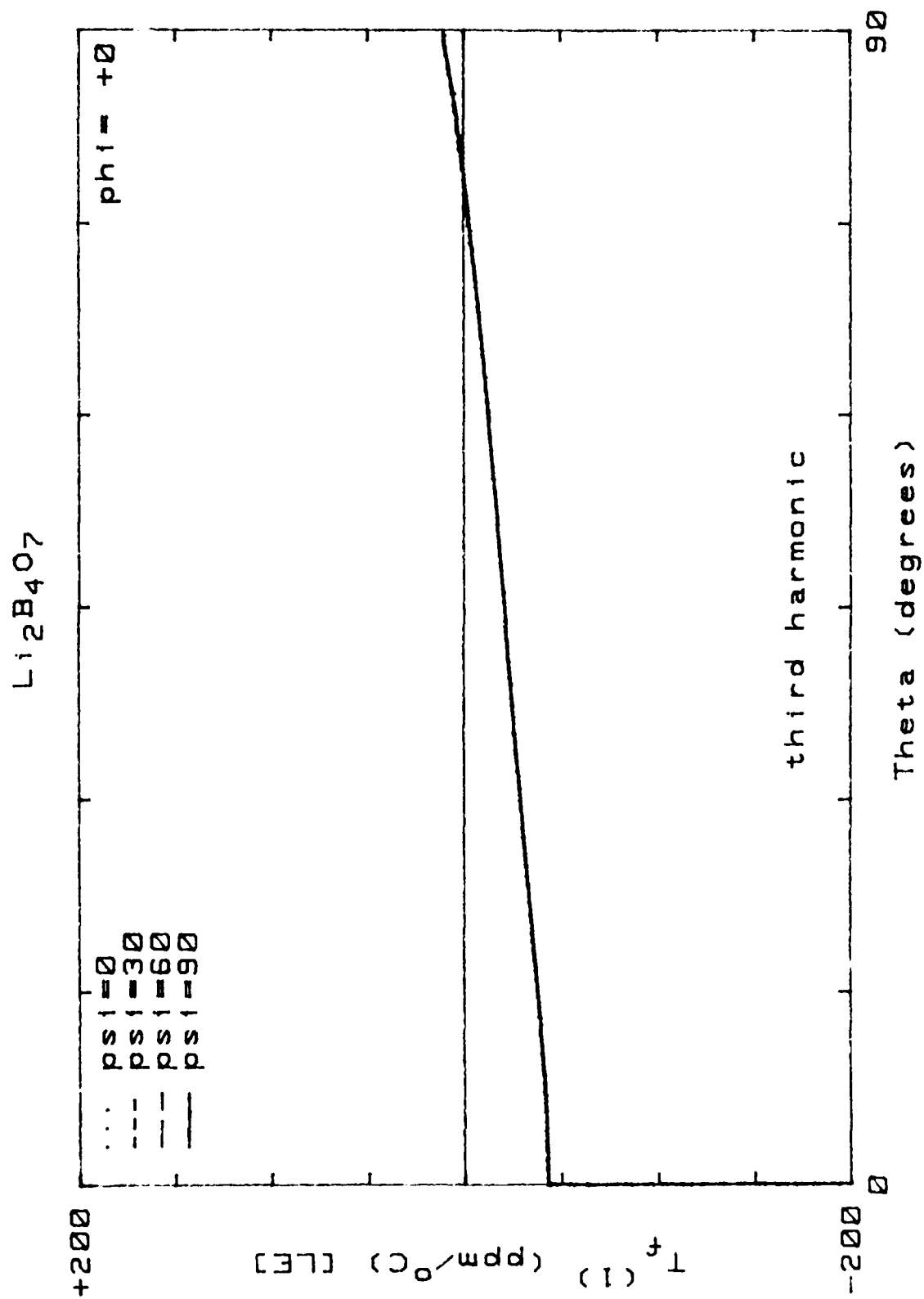


Figure 41.  $TC(1)$  for  $(yxw)\phi=0^\circ/\theta$  cuts;  $M = 3$ ; mode "a";  $\psi=0^\circ$  ( $30^\circ$ ) $90^\circ$ ; [LE]

L12B407

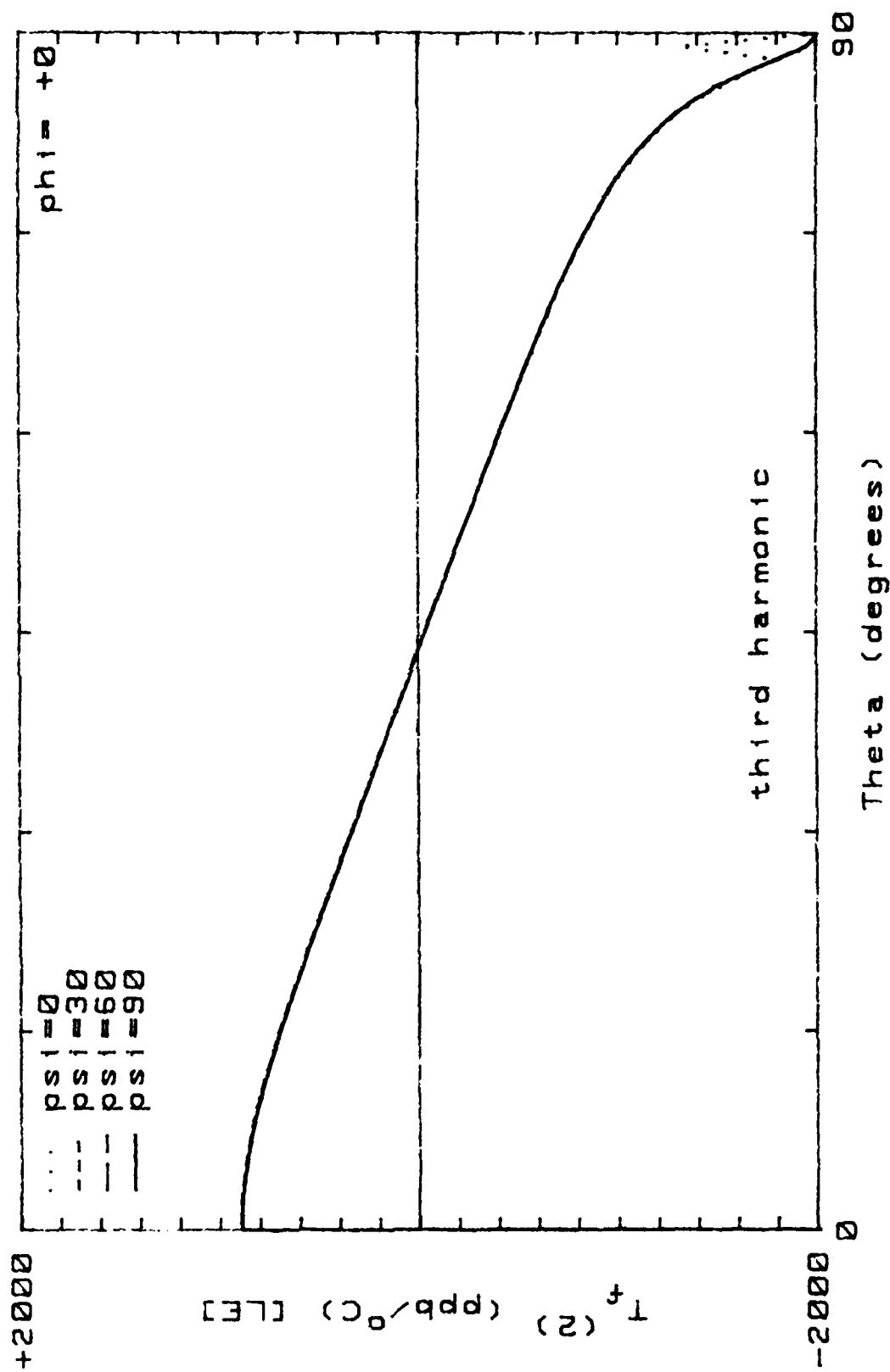


Figure 42. TC(2) for (yxw)  $\phi=0^\circ/\theta$  cuts; M = 3; mode "a"; psi=0° (30°)90°; [LE]

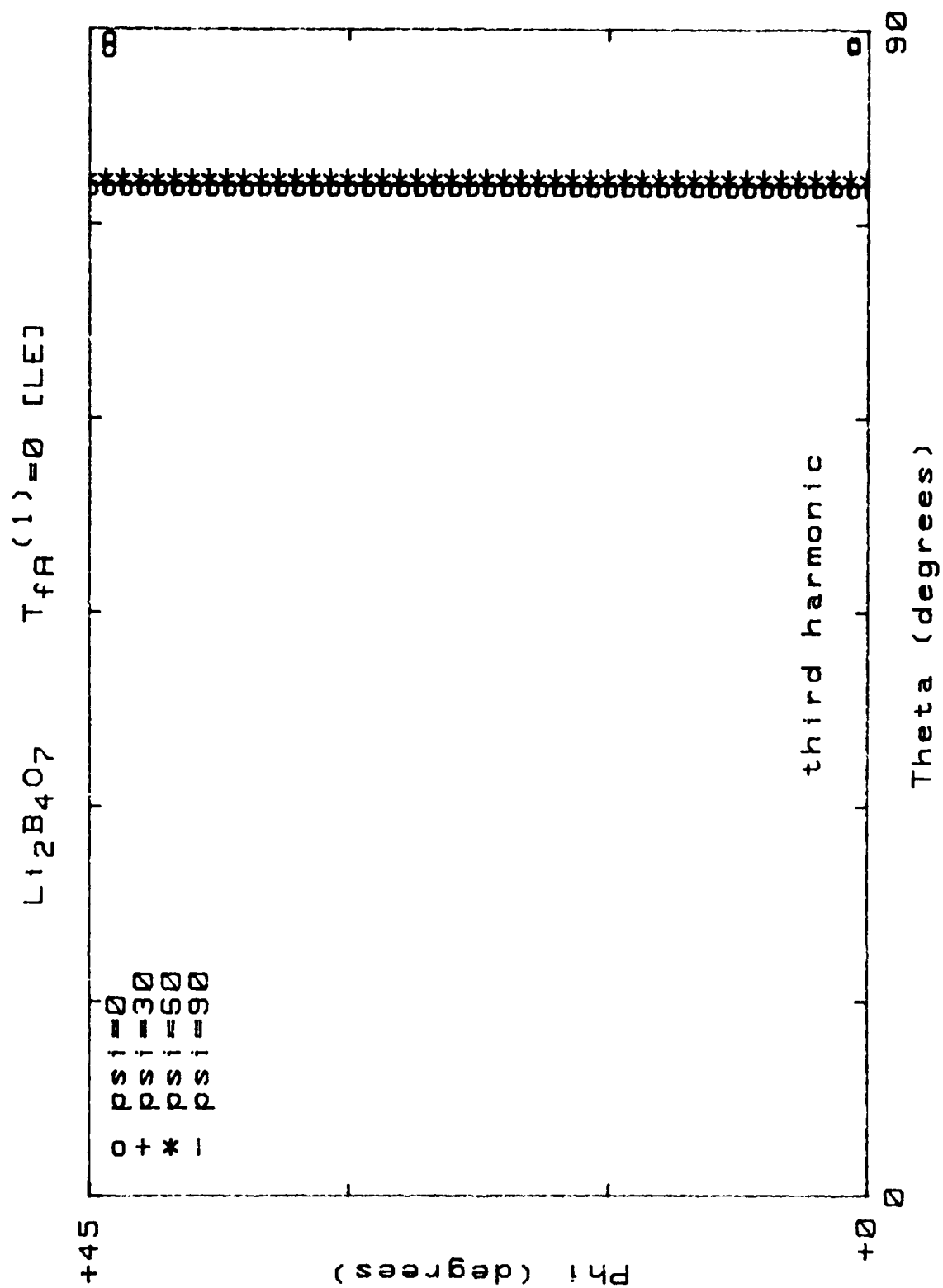


Figure 43. Locus of  $TC(1)=0$  for  $(yxw)\phi/\theta$  cuts;  $M = 3$ ; mode "a";  $\psi=0^\circ$  ( $30^\circ$ )  $90^\circ$ ; [LE]

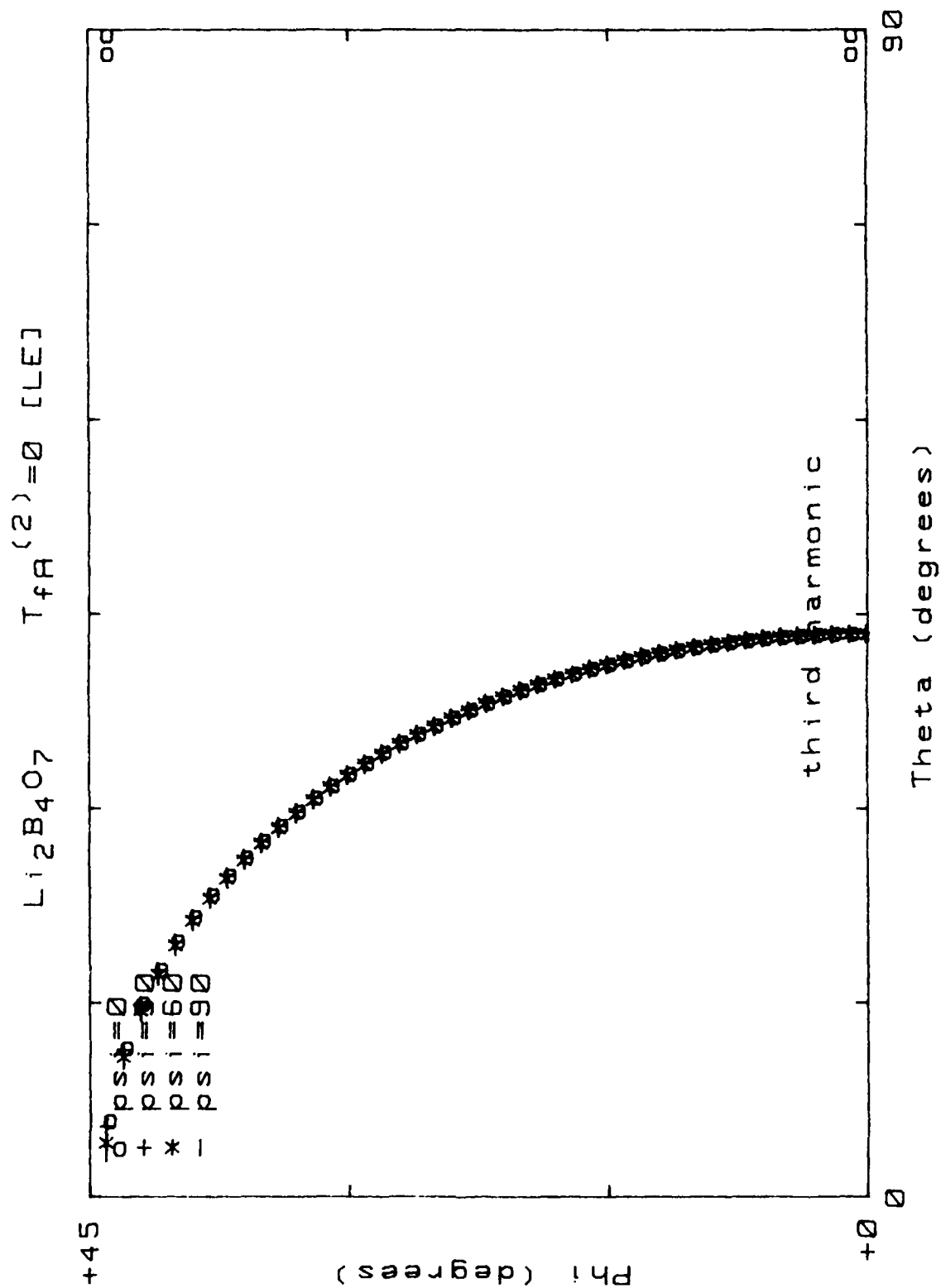


Figure 44. Locus of  $TC(2)=0$  for  $(yxw)\phi/\theta$  cuts;  $M = 3$ ; mode "a";  $\psi=0^\circ$   $(30^\circ)90^\circ$ ; [LE]

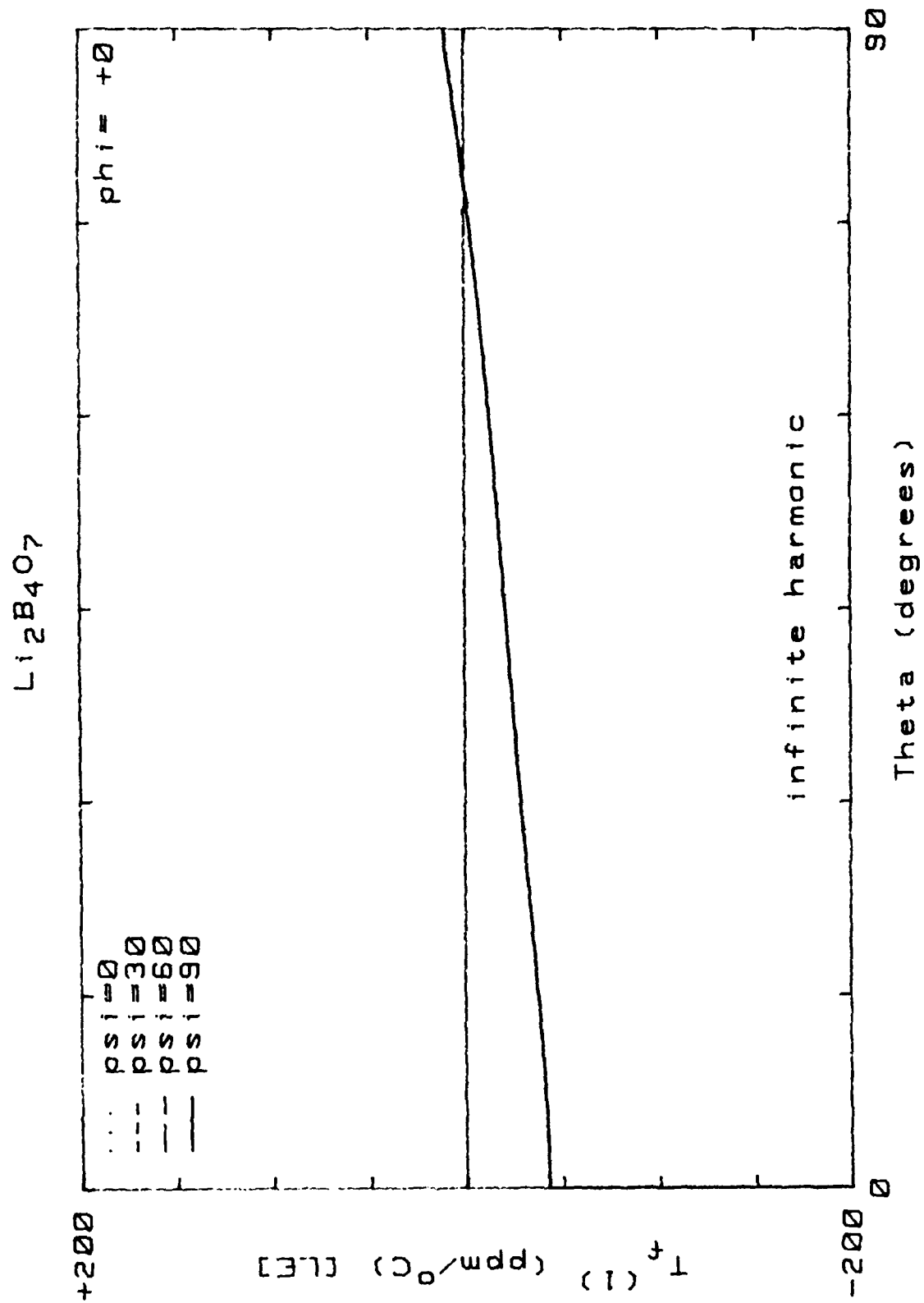


Figure 45.  $TC(1)$  for  $(yxw)\phi=0^\circ/\theta$  cuts;  $M=\infty$ ; mode "a";  $\psi=0^\circ$  ( $30^\circ$ )  $90^\circ$ ; [LE]

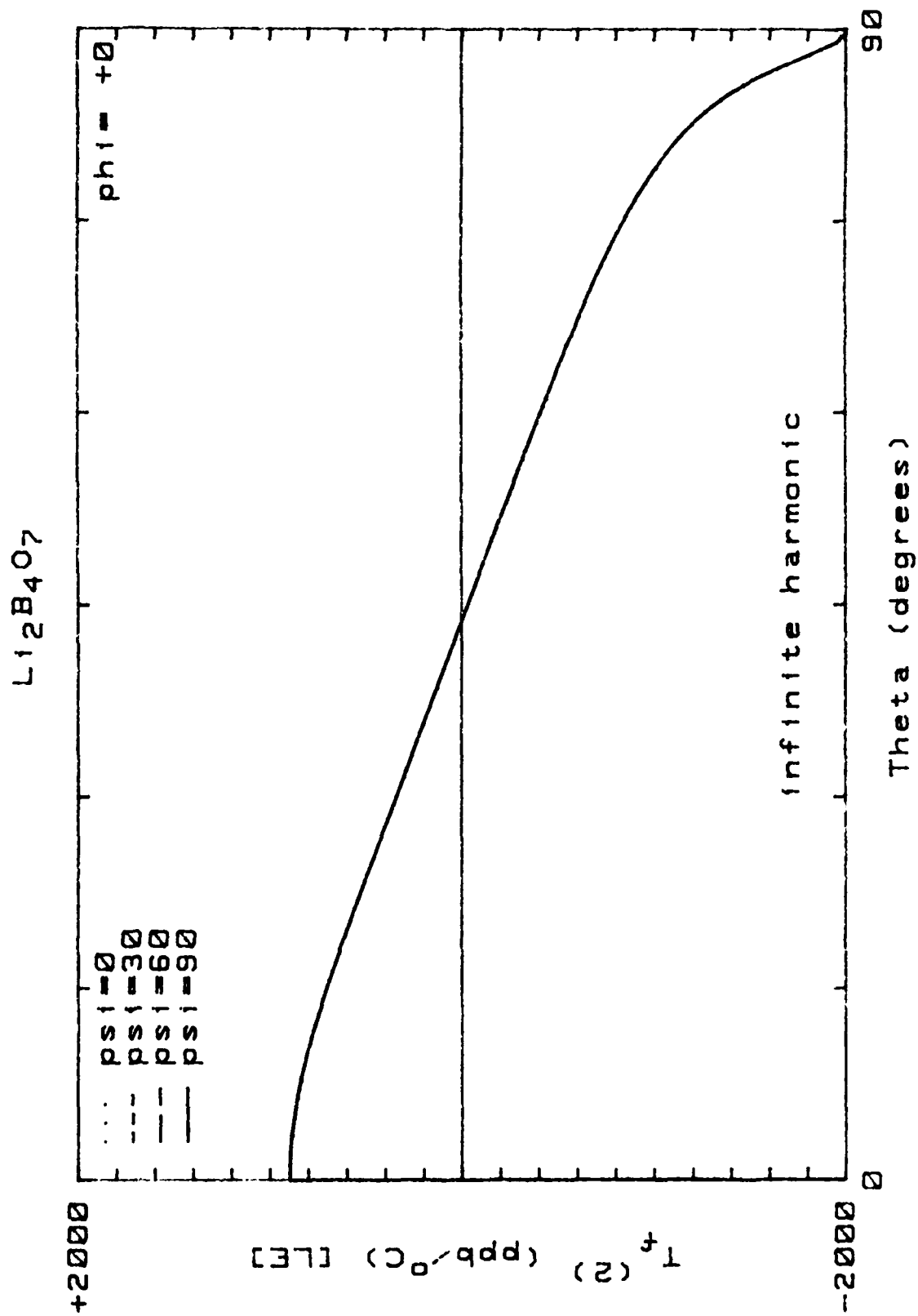


Figure 46.  $T_f(2)$  for  $(y_{xw})_{\phi=0^\circ}$  cuts;  $M = \infty$ ; mode "a";  $\psi = 0^\circ(30^\circ)90^\circ$ ; [LE]

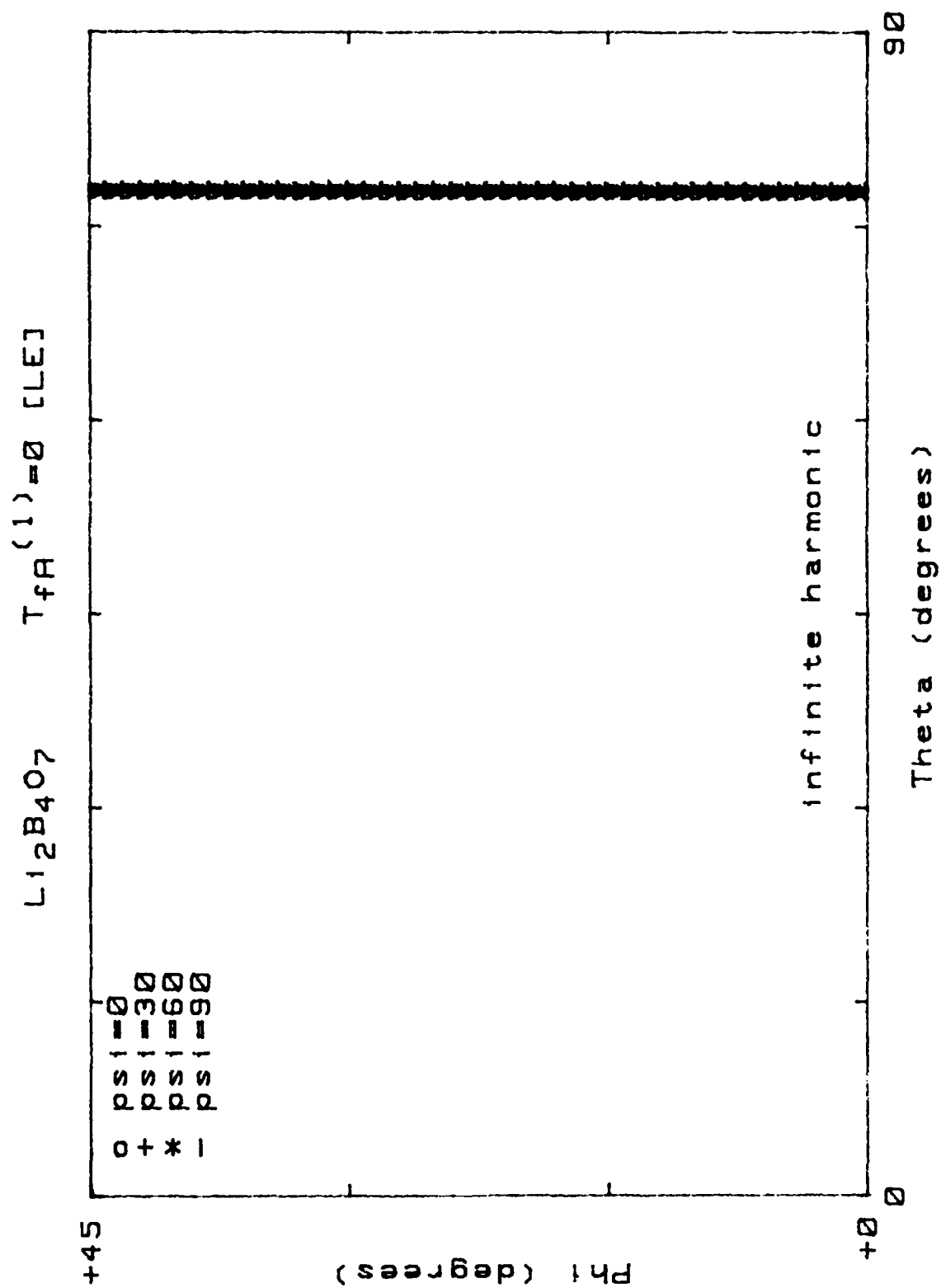


Figure 47. Locus of  $TC(1)=0$  for  $(yxw1)\phi/\theta$  cuts;  $M=\infty$ ; mode "a";  $\psi=0^\circ(30^\circ)90^\circ$ ; [LE]

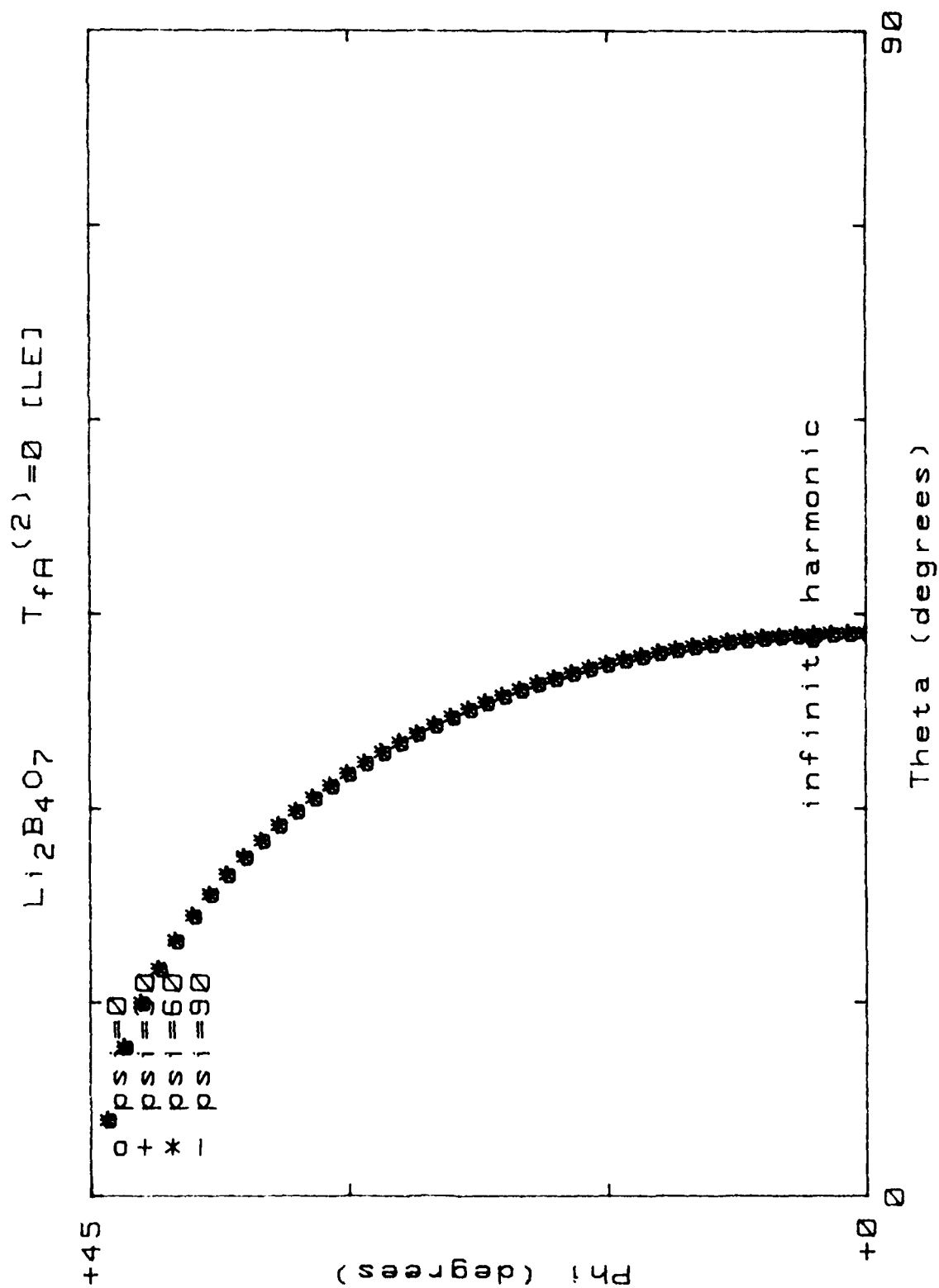


Figure 48. Locus of  $TC(2)=0$  for  $(yxwl)\phi/\theta$  cuts;  $M=\infty$ ; mode "a";  $\psi=0^\circ(30^\circ)90^\circ$ ; [LE]

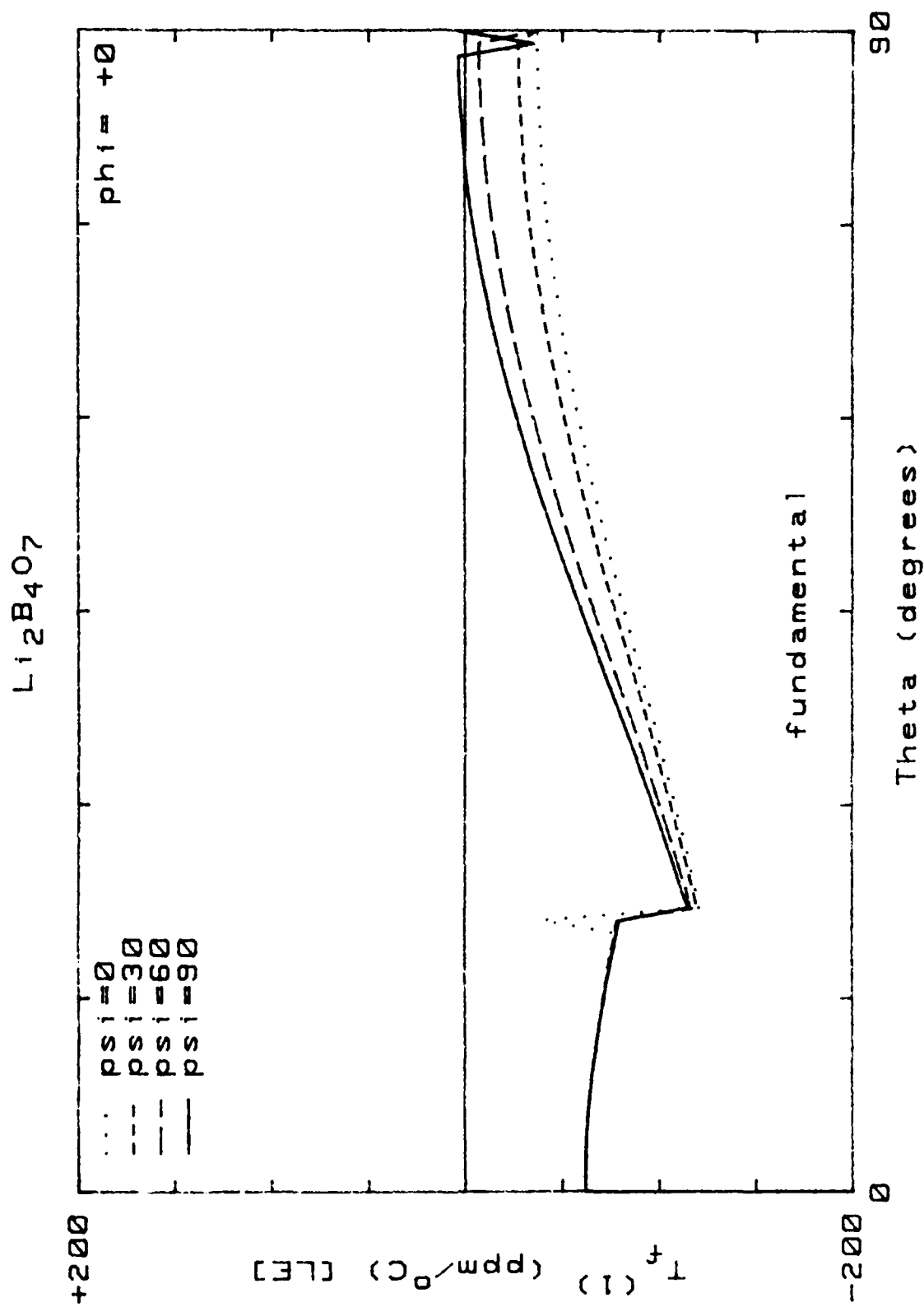


Figure 49.  $TC(1)$  for  $(yxw)\phi=0^\circ/\theta$  cuts;  $M = 1$ ; mode "b";  $\psi=0^\circ(30^\circ)90^\circ$ ; [LE]

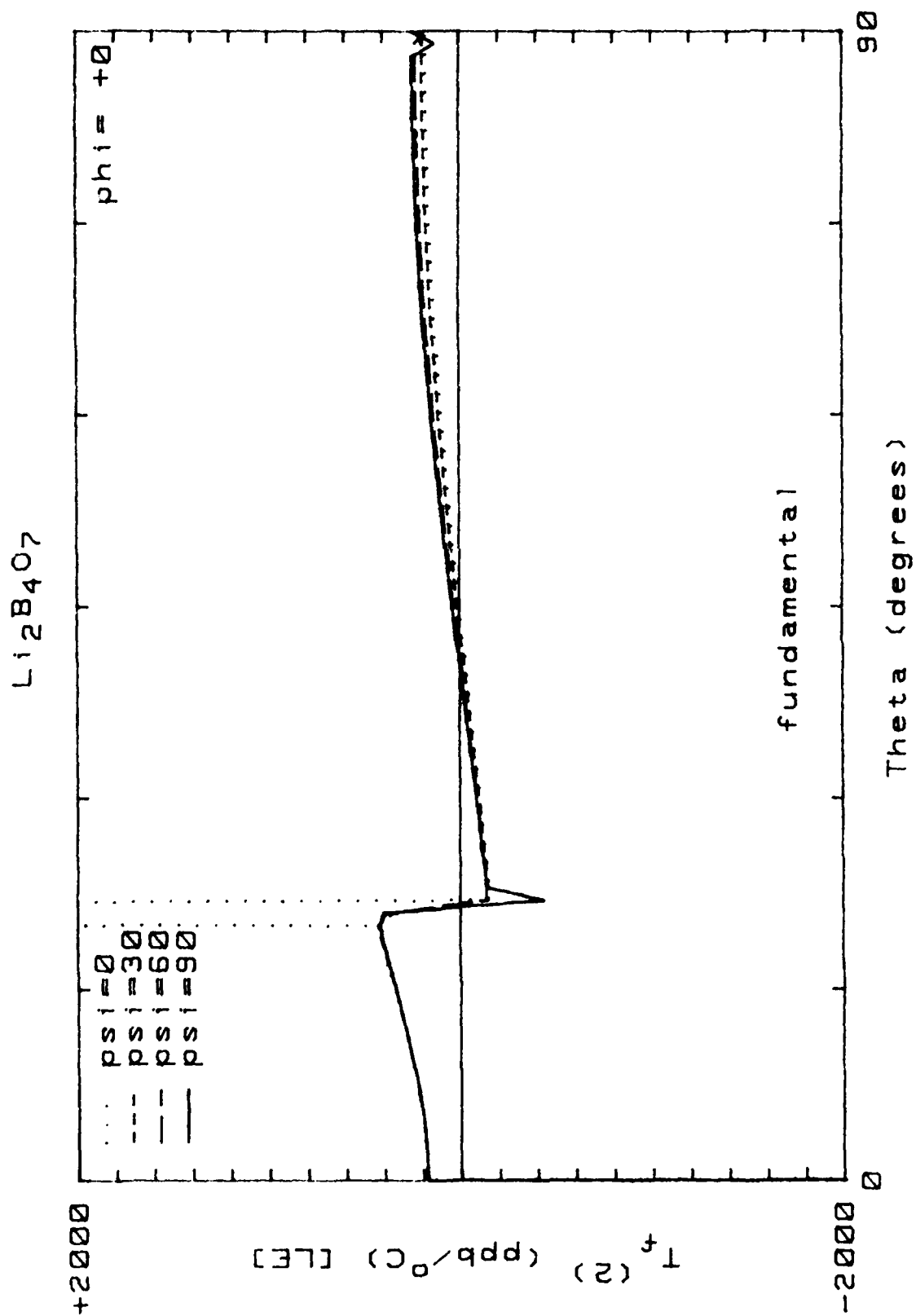


Figure 50. TC(2) for (yxw)  $\phi=0^\circ/\theta$  cuts; M = 1; mode "b"; psi =  $0^\circ(30^\circ)90^\circ$ ; [LE]

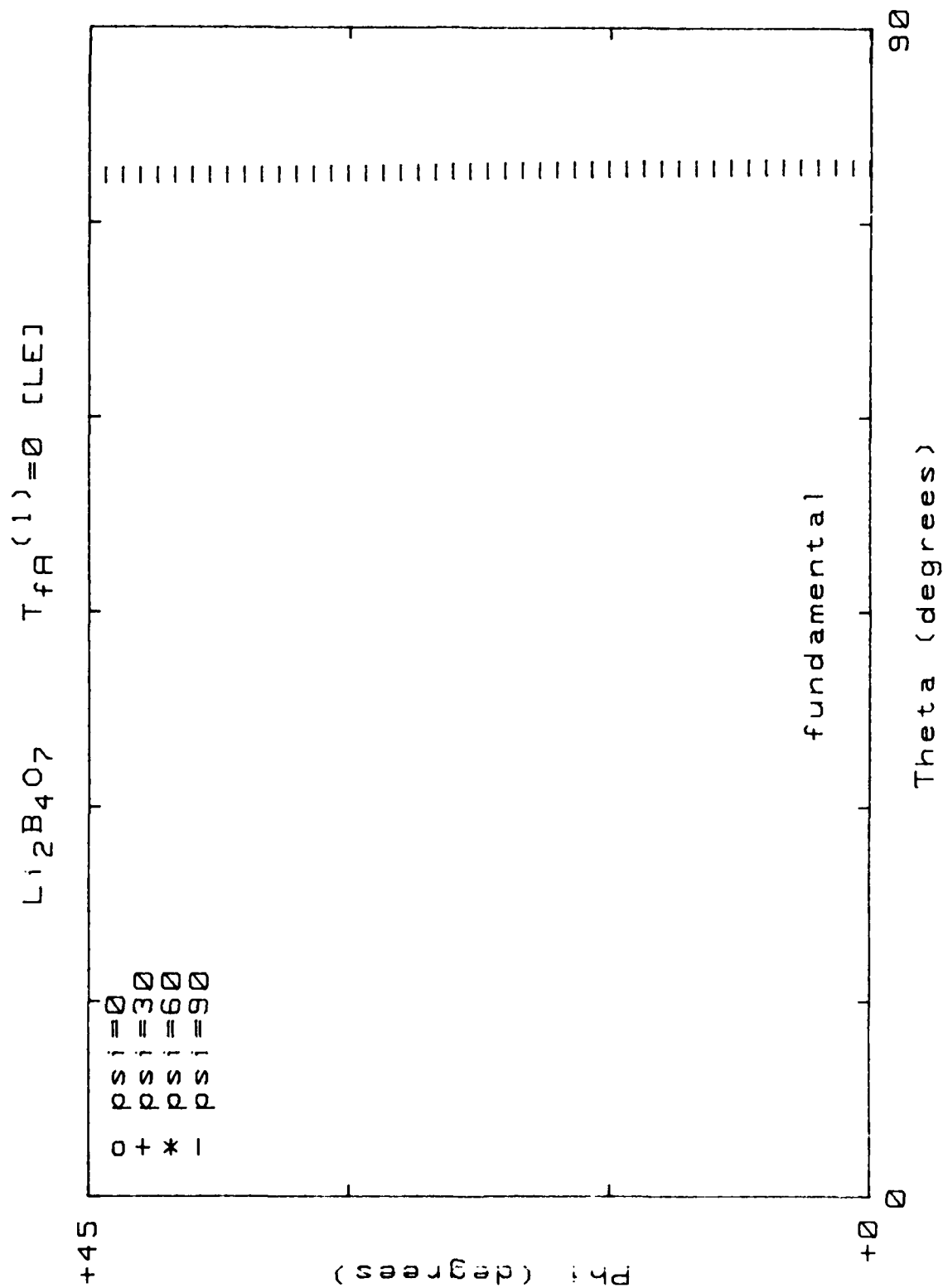


Figure 51. Locus of  $TC(1)=0$  for  $(yxw)\phi/\theta$  cuts;  $M = 1$ ; mode "b";  $\psi=0^\circ(30^\circ)90^\circ$ ; [LE]



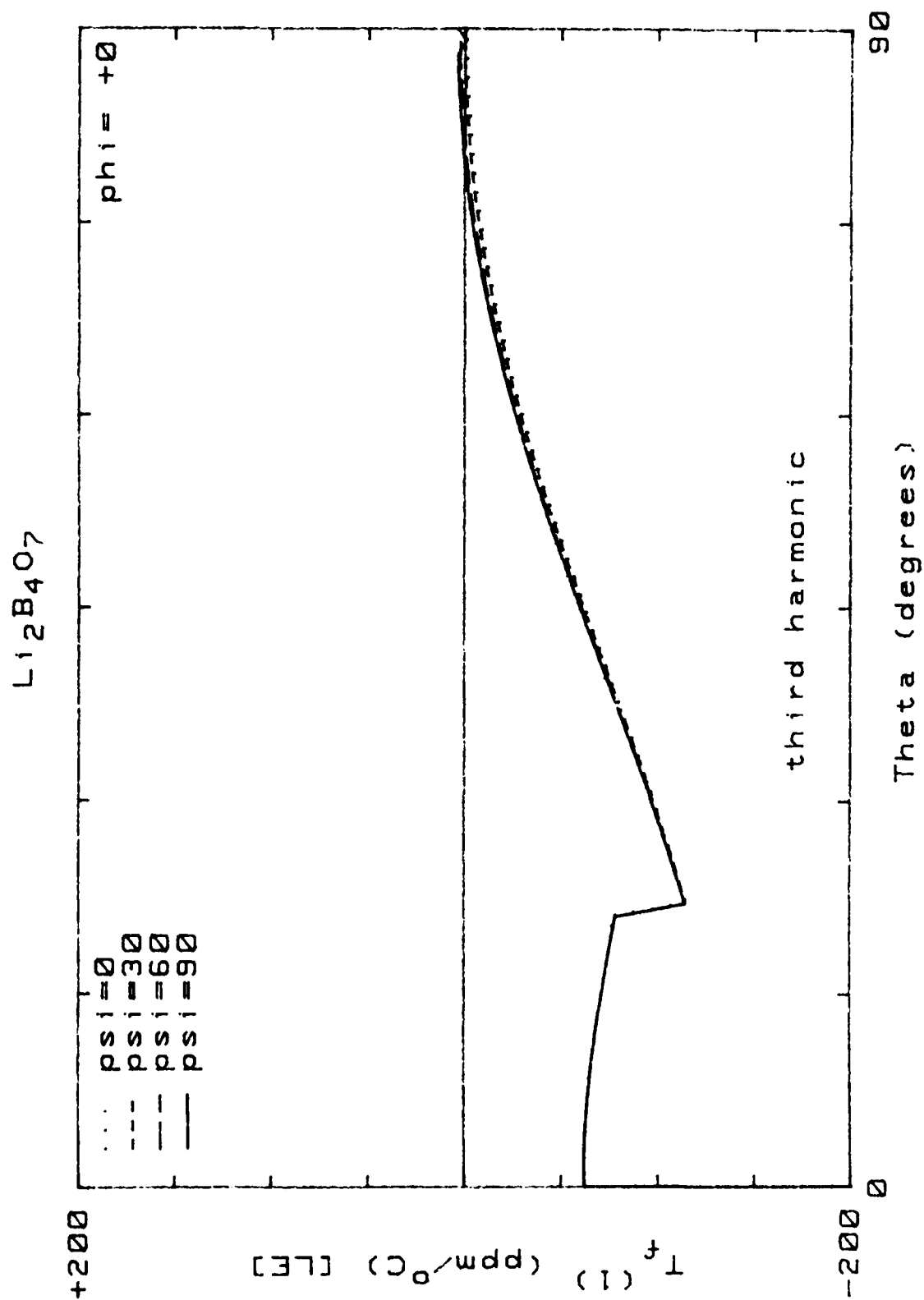


Figure 53.  $\text{TC}(1)$  for  $(\text{yxw})\phi=0^\circ/\theta$  cuts;  $M = 3$ ; mode "b";  $\text{psi}=0^\circ(30^\circ)90^\circ$ ; [LE].

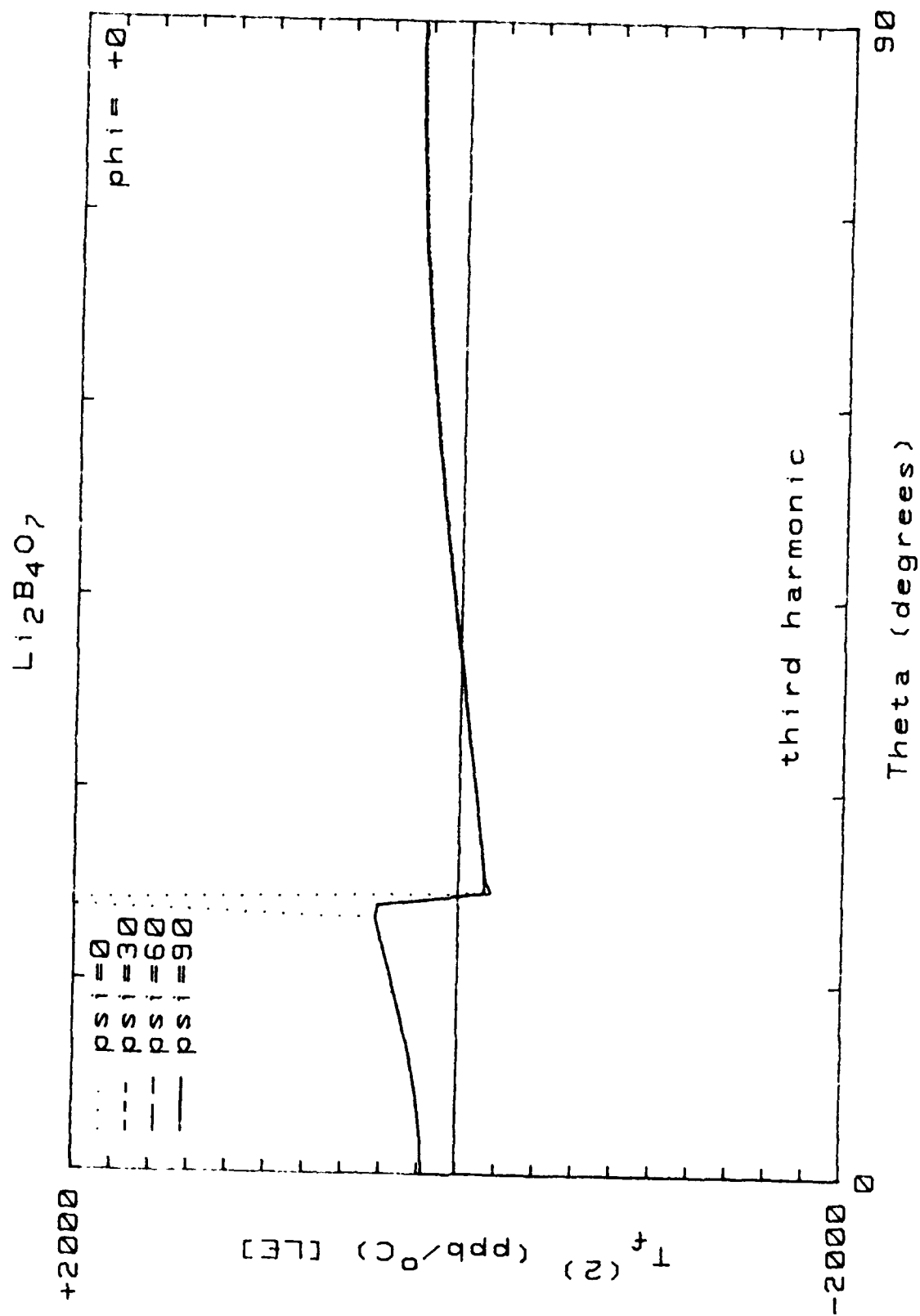


Figure 54.  $\text{TC}(2)$  for  $(yxw1)\phi=0^\circ/\theta$  cuts;  $M = 3$ ; mode "b";  $\psi=0^\circ(30^\circ)90^\circ$ ; [LE]

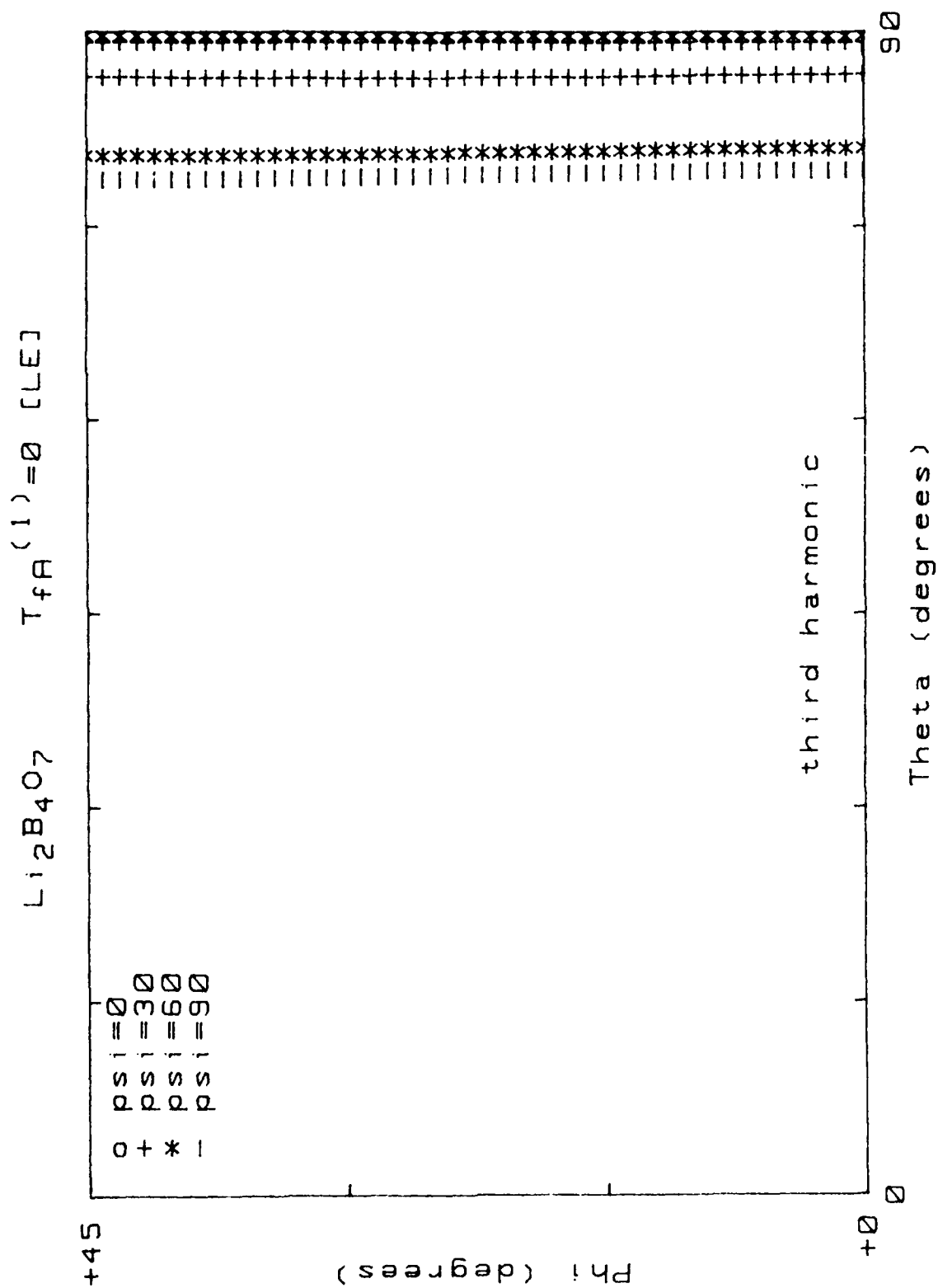


Figure 55. Locus of  $TC(1)=0$  for  $(yxw)\phi/\theta$  cuts;  $M = 3$ ; mode "b";  $\psi=0^\circ(30^\circ)90^\circ$ ; [LE].

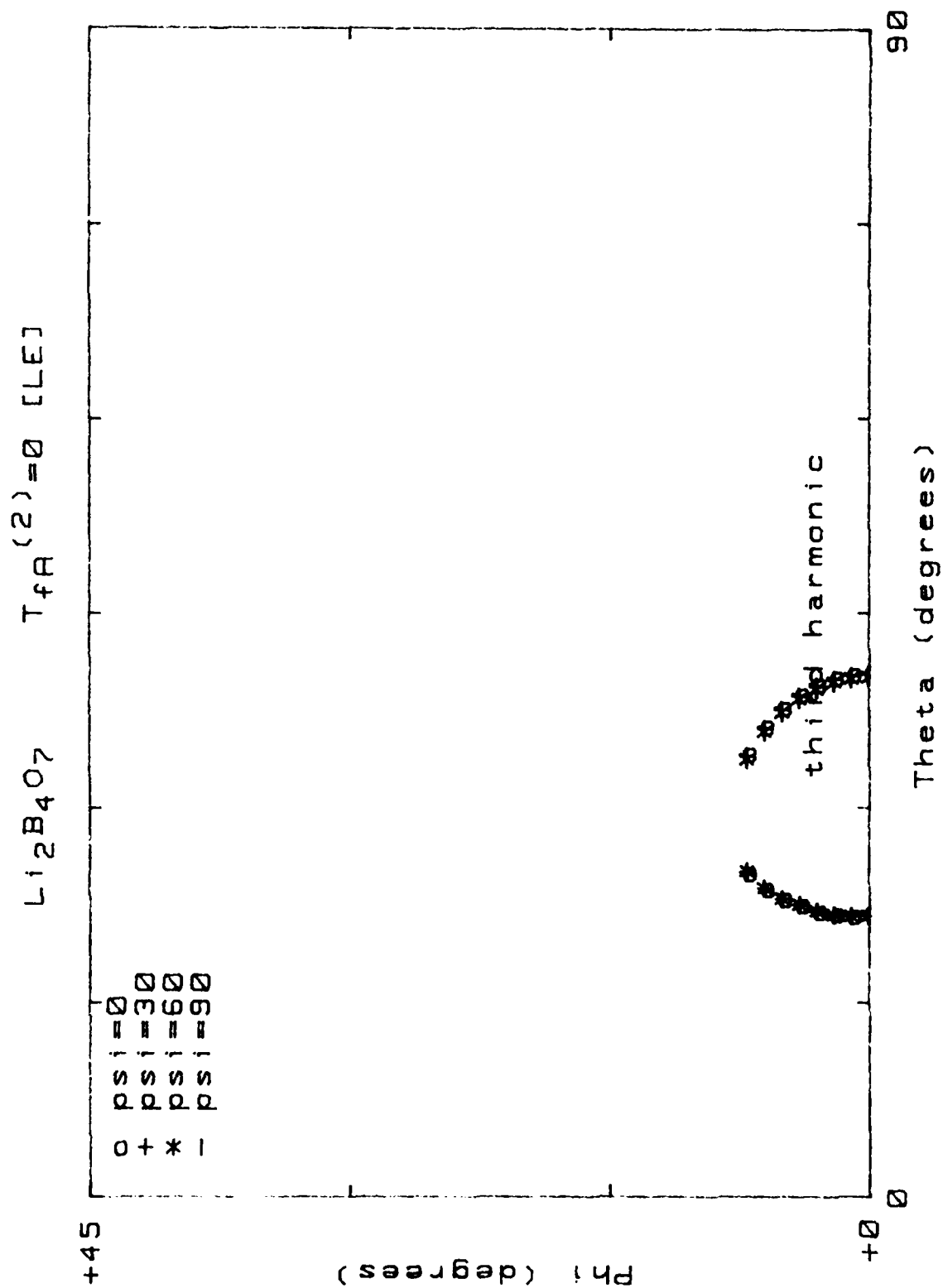


Figure 56. Locus of  $\text{TC}(2)=0$  for  $(yxw)\phi/\theta$  cuts;  $M = 3$ ; mode "b";  $\text{psi}=0^\circ(30^\circ)90^\circ$ ; [LE].

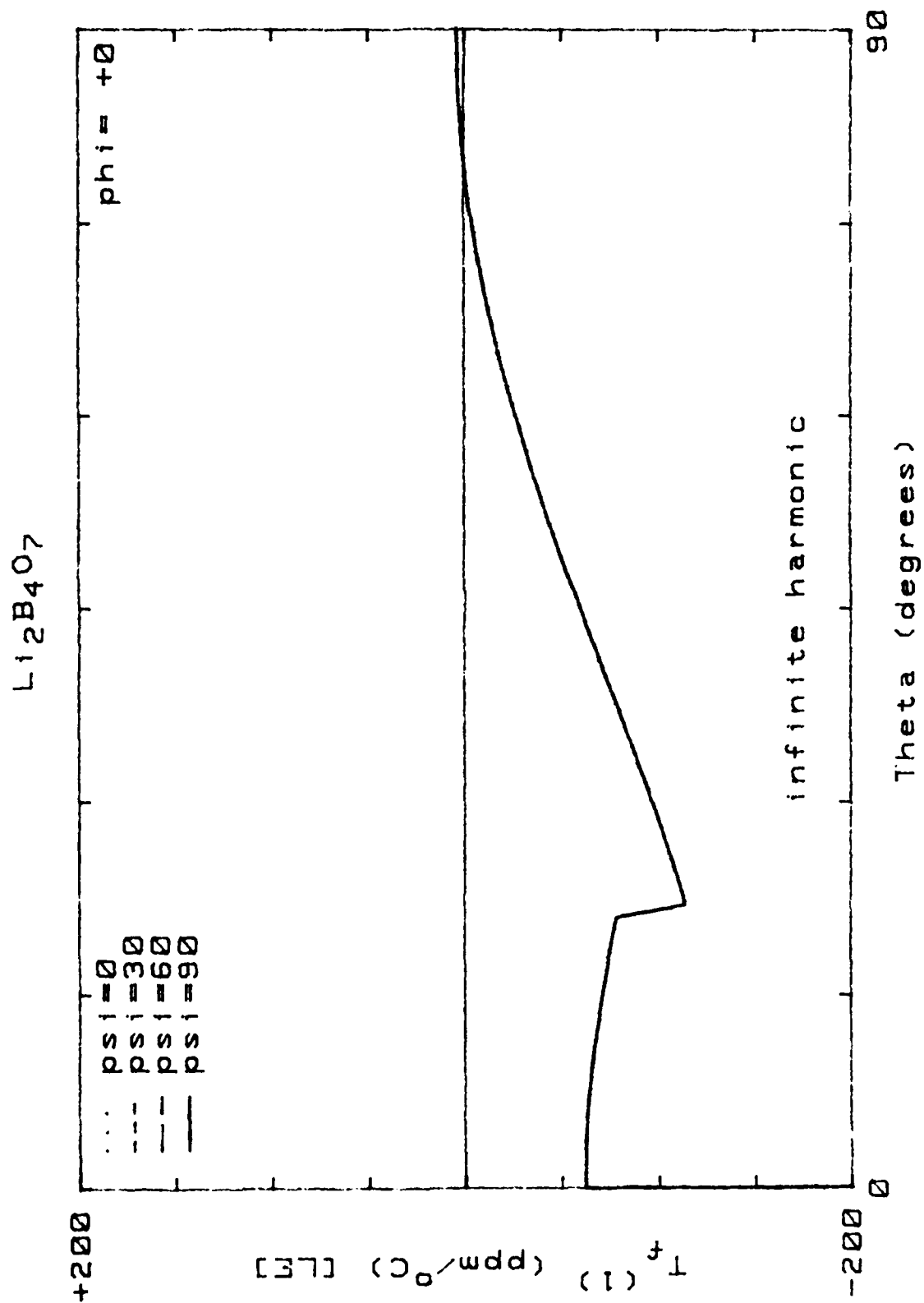


Figure 57.  $\text{TC}(1)$  for  $(\text{yxw})\phi=0^\circ/\theta$  cuts;  $M=\infty$ ; mode "b";  $\text{psi}=0^\circ(30^\circ)90^\circ$ ; [LE].

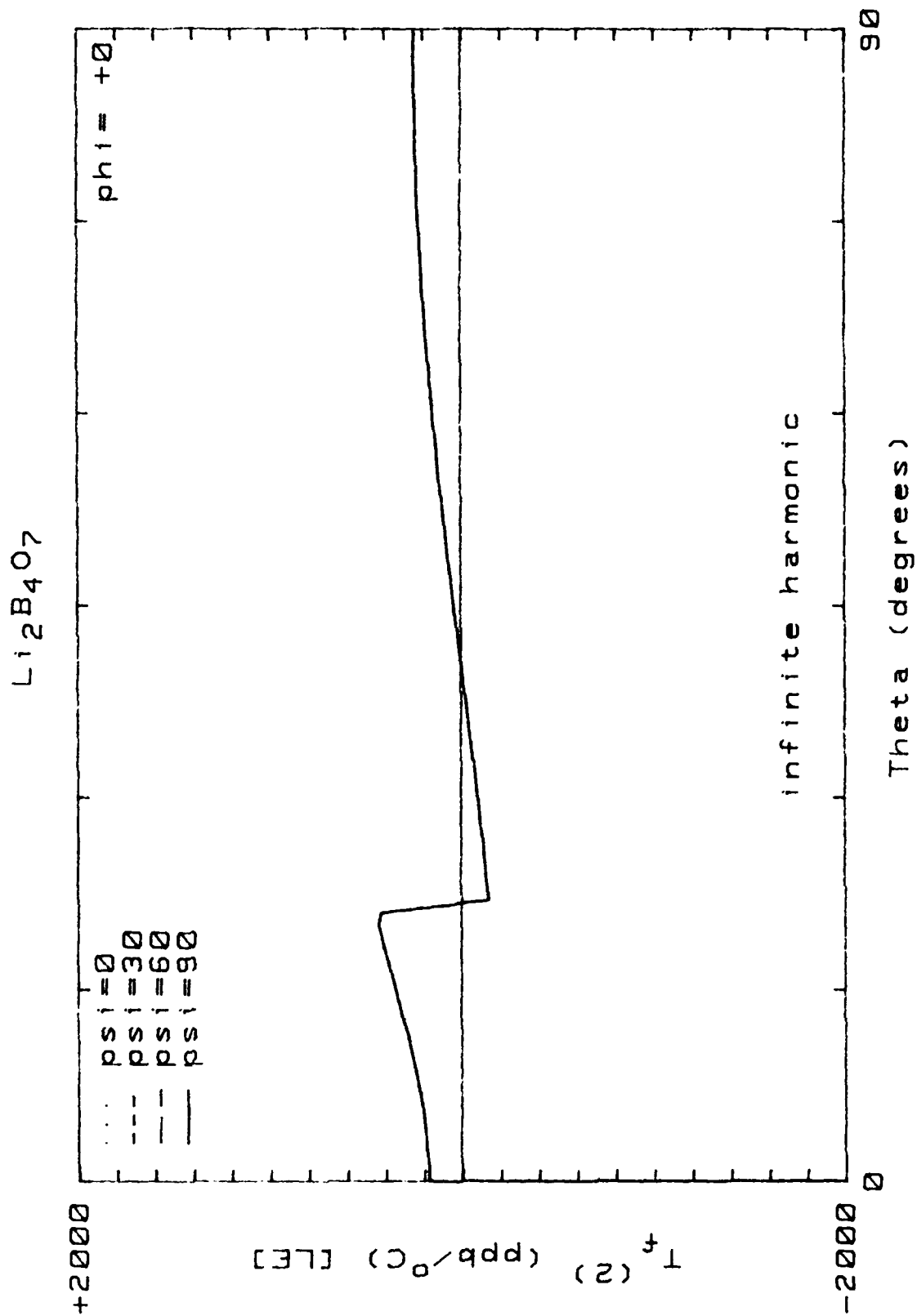


Figure 58.  $TC(2)$  for  $(yxw)\phi = 0^\circ/\theta$  cuts;  $M = \infty$ ; mode "b";  $\psi = 0^\circ(30^\circ)90^\circ$ ; [LE].

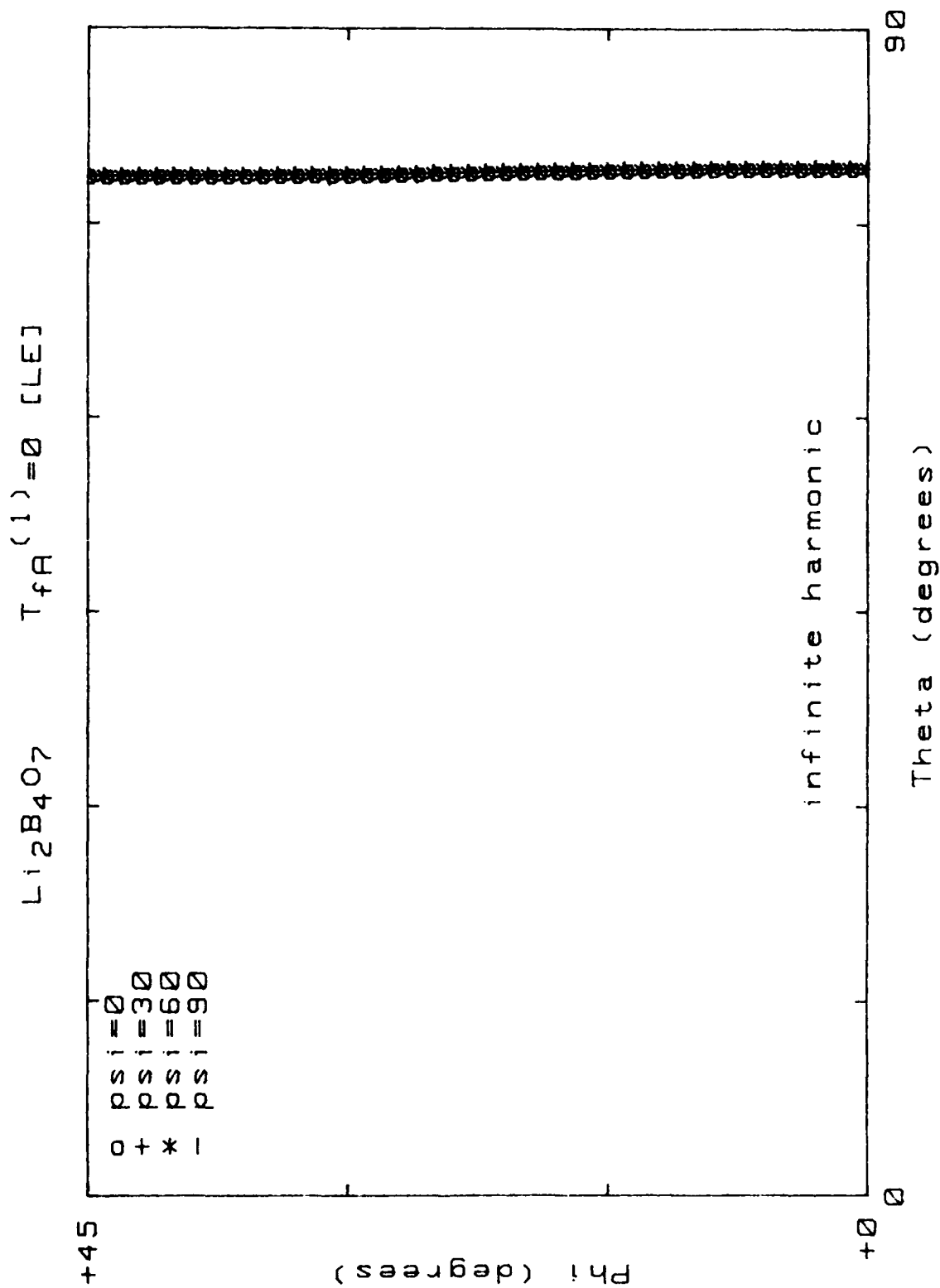


Figure 59. Locus of  $TC(1)=0$  for  $(yxw1)\phi/\theta$  cuts;  $M = \infty$ ; mode "b";  $\psi=0^\circ(30^\circ)90^\circ$ ; [LE].

Li<sub>2</sub>B<sub>4</sub>O<sub>7</sub>      T<sub>FA</sub>(2)=0 [LE]

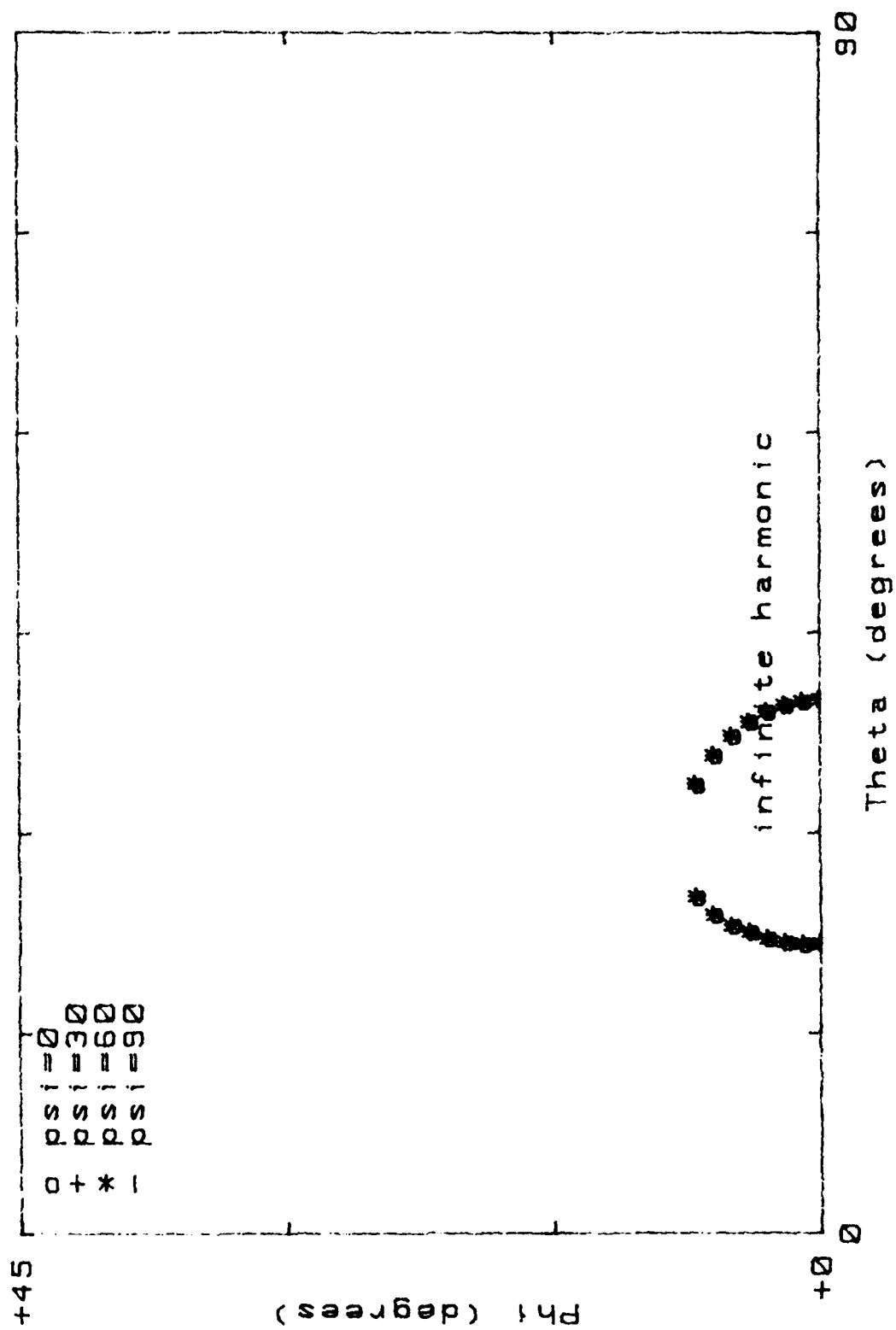


Figure 60. Locus of TC(2)=0 for (yxw1)φ/θ cuts; M = ∞; mode "b"; psi=0°(30°)90°; [LE].

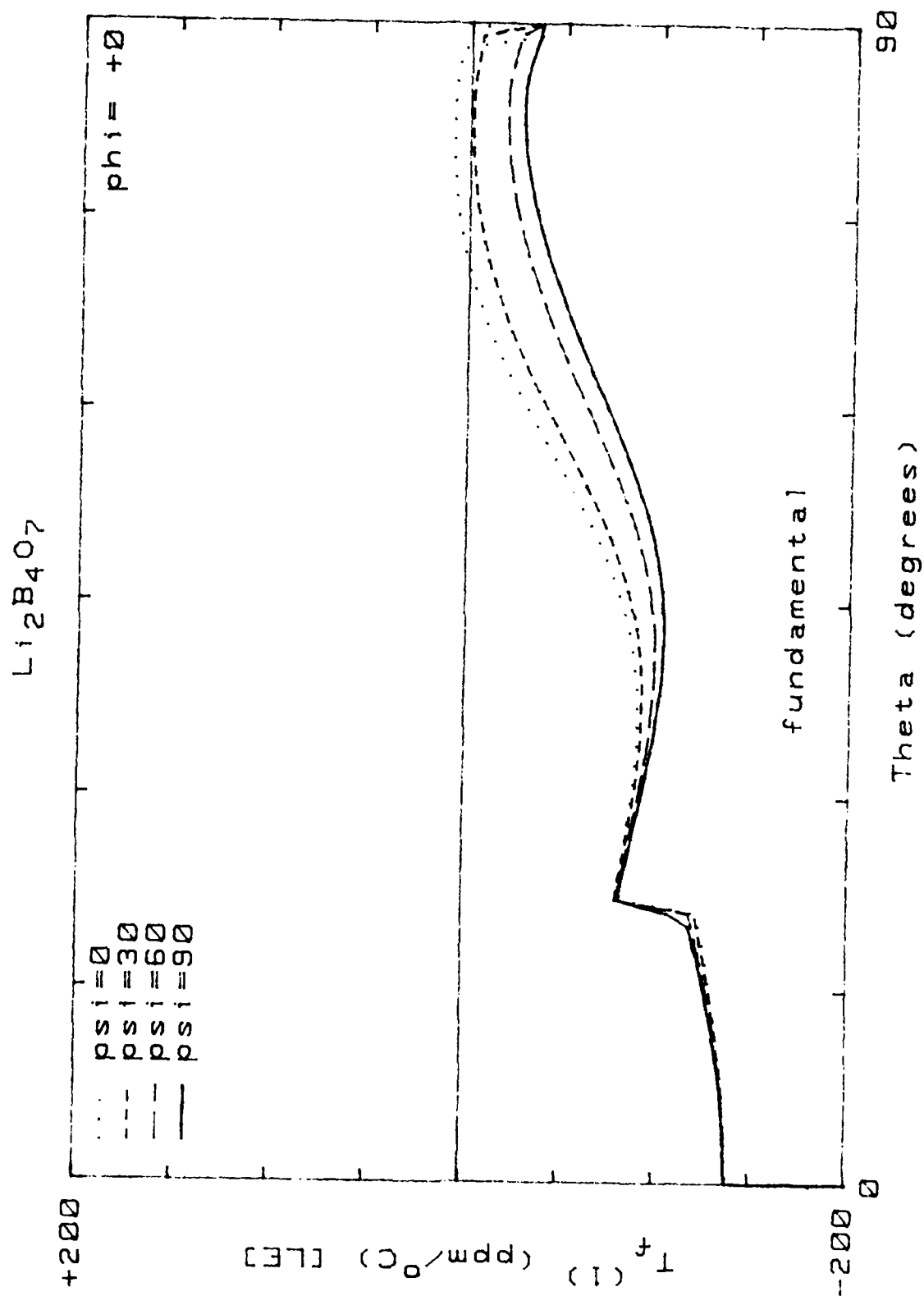


Figure 61.  $\text{TC}(1)$  for  $(yxw1)\phi = 0^\circ/\theta$  cuts;  $M = 1$ ; mode "c";  $\text{psi} = 0^\circ(30^\circ)90^\circ$ ; [LE].

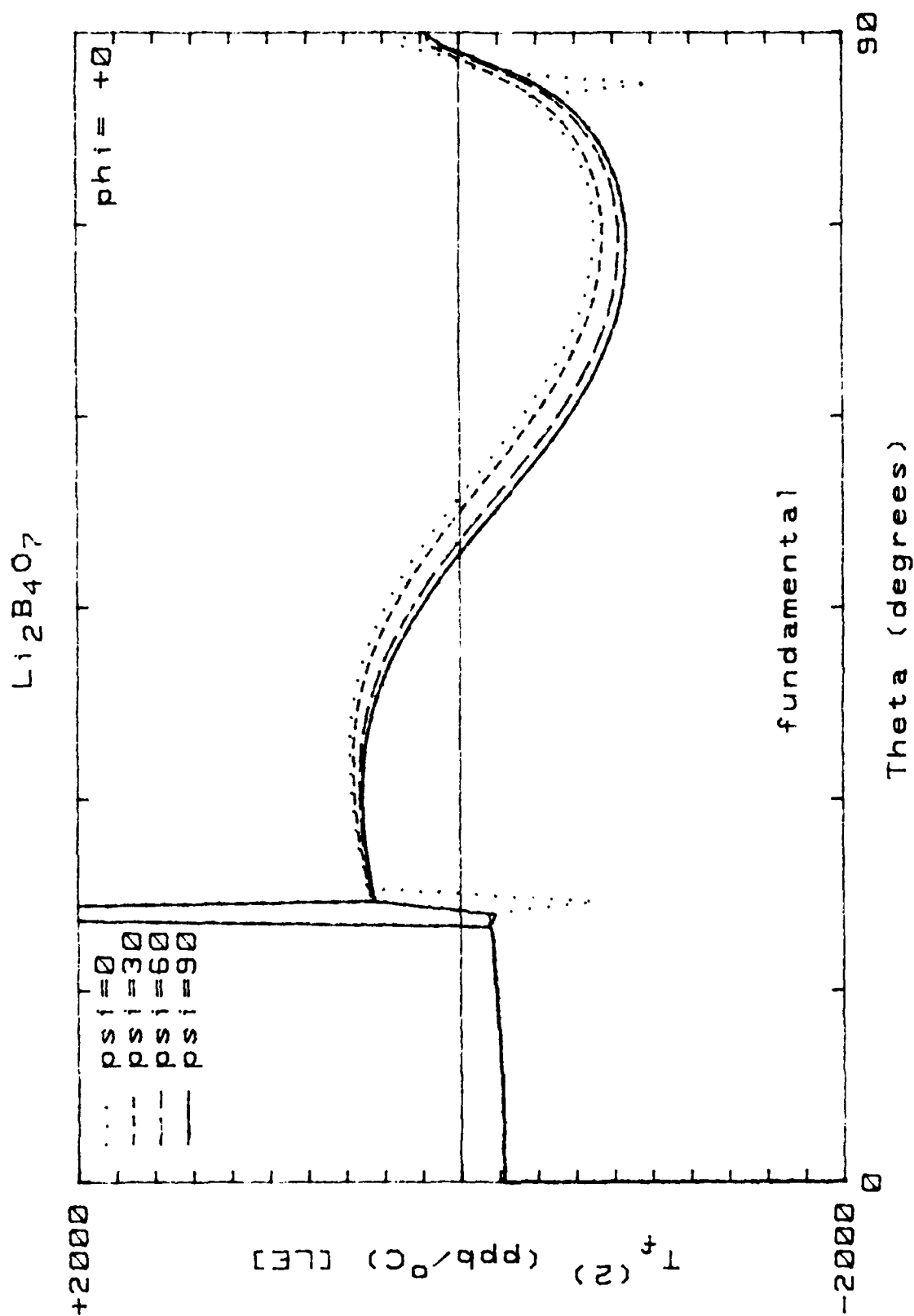


Figure 62. TC(2) for (yxw1)  $\phi = 0^\circ/\theta$  cuts;  $M = 1$ ; mode "c";  $\psi = 0^\circ(30^\circ)90^\circ$ ; [LE].

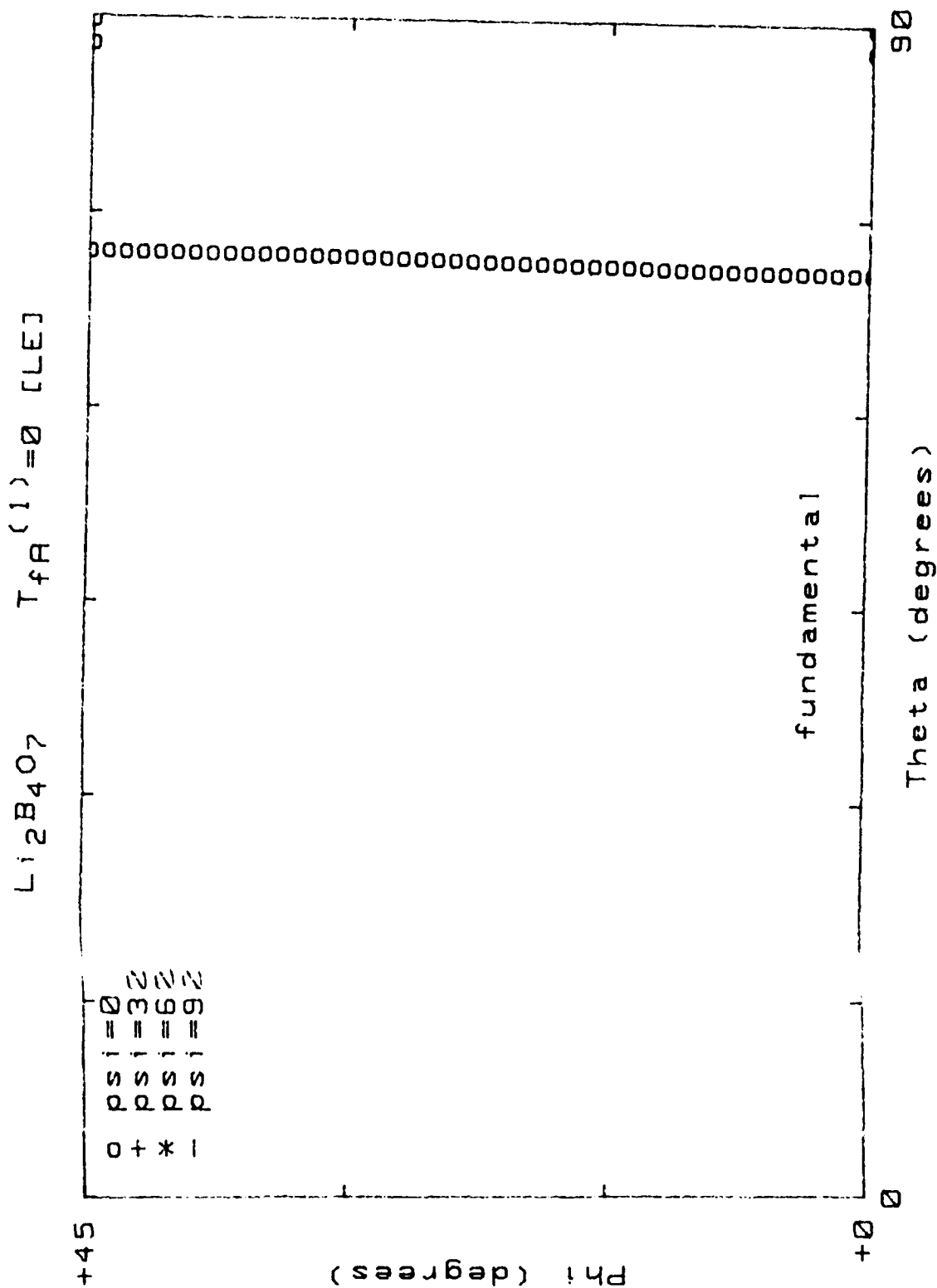


Figure 63. Locus of  $TC(1)=0$  for  $(yxw1)\phi/\theta$  cuts;  $M = 1$ ; mode "c";  $\psi=0^\circ(30^\circ)90^\circ$ ; [LE].

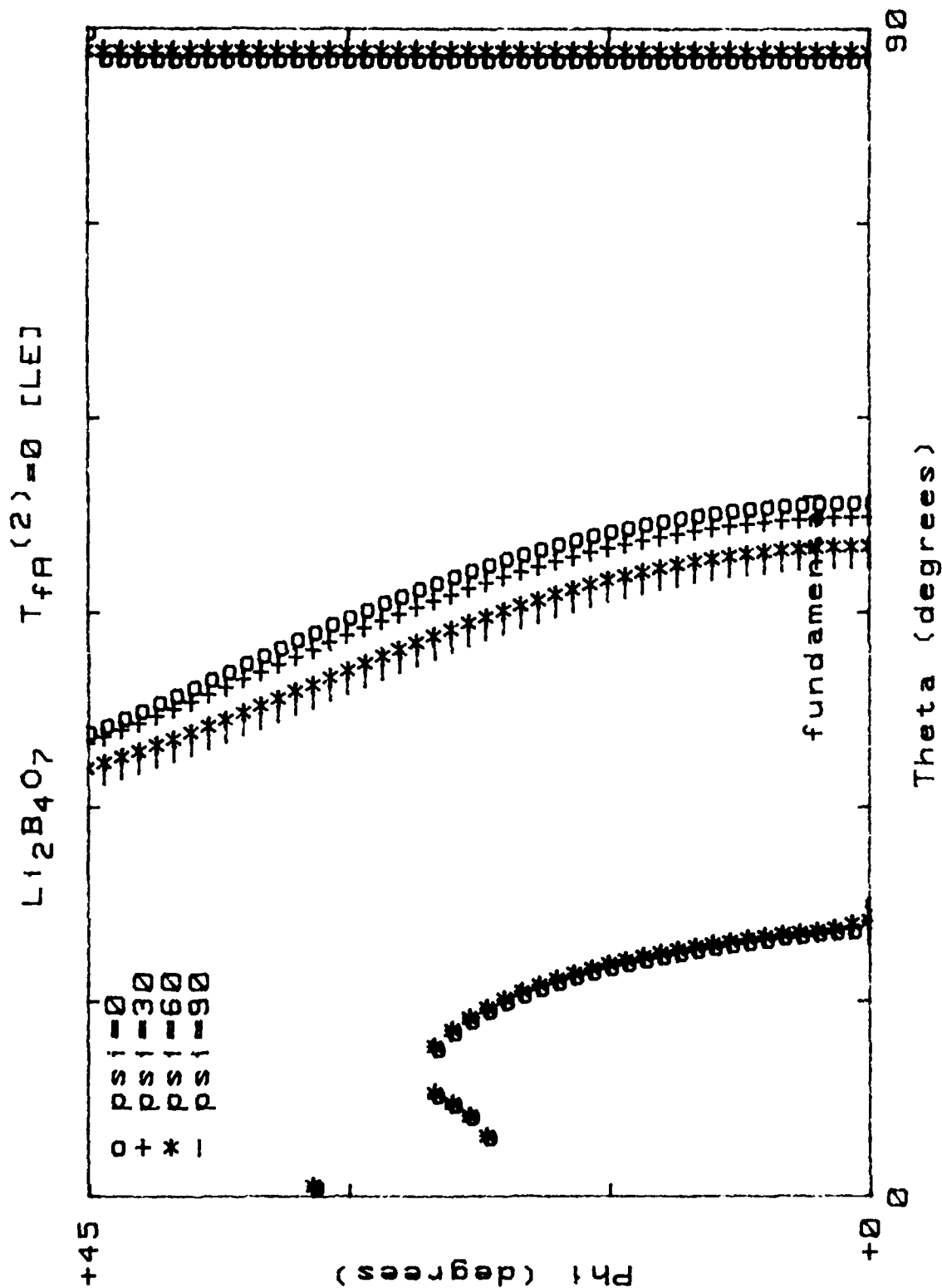


Figure 64. Locus of  $TC(2)=0$  for  $(yxw)\phi/\theta$  cuts;  $M = 1$ ; mode "c";  $\psi=0^\circ(30^\circ)90^\circ$ ; [LE].

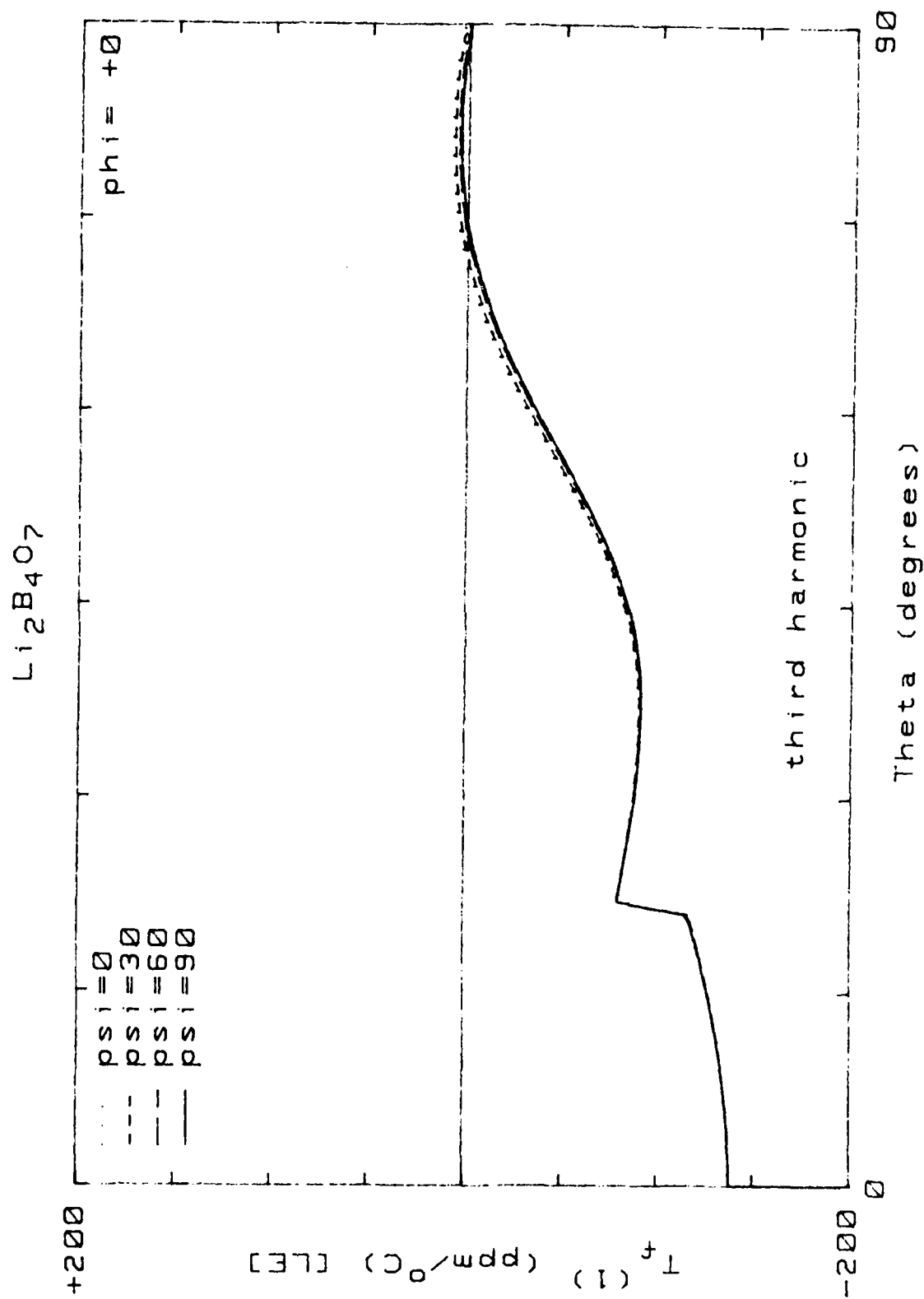


Figure 65.  $TC(1)$  for  $(yxw1)\phi = 0^\circ/\theta$  cuts;  $M = 3$ ; mode "c";  $\psi = 0^\circ(30^\circ)90^\circ$ ; [LE].

Li<sub>2</sub>B<sub>4</sub>O<sub>7</sub>

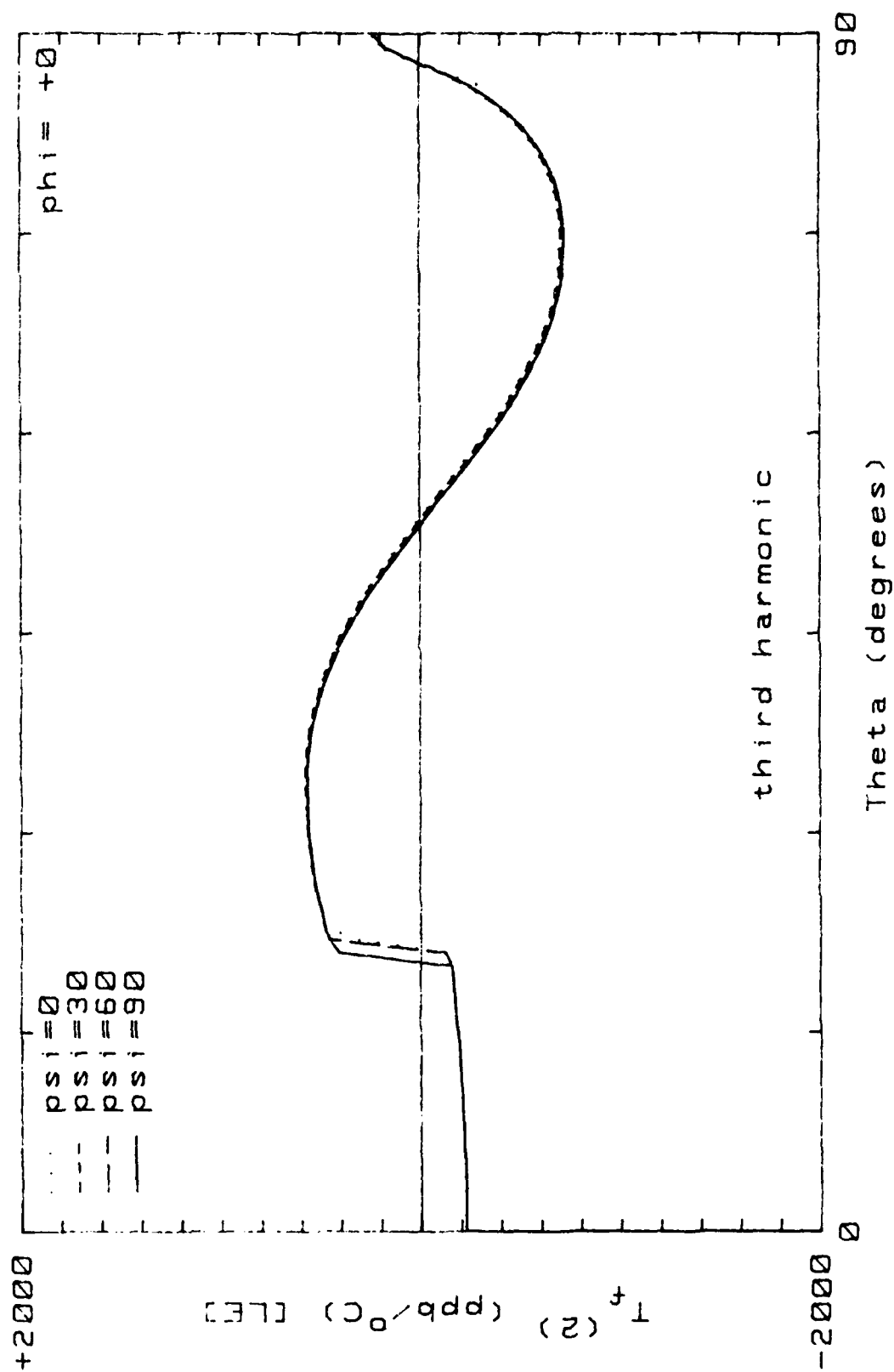


Figure 66. TC(2) for (yxw1) $\phi=0^\circ/\theta$  cuts; M = 3; mode "c"; psi=0°(30°)90°; [LE].

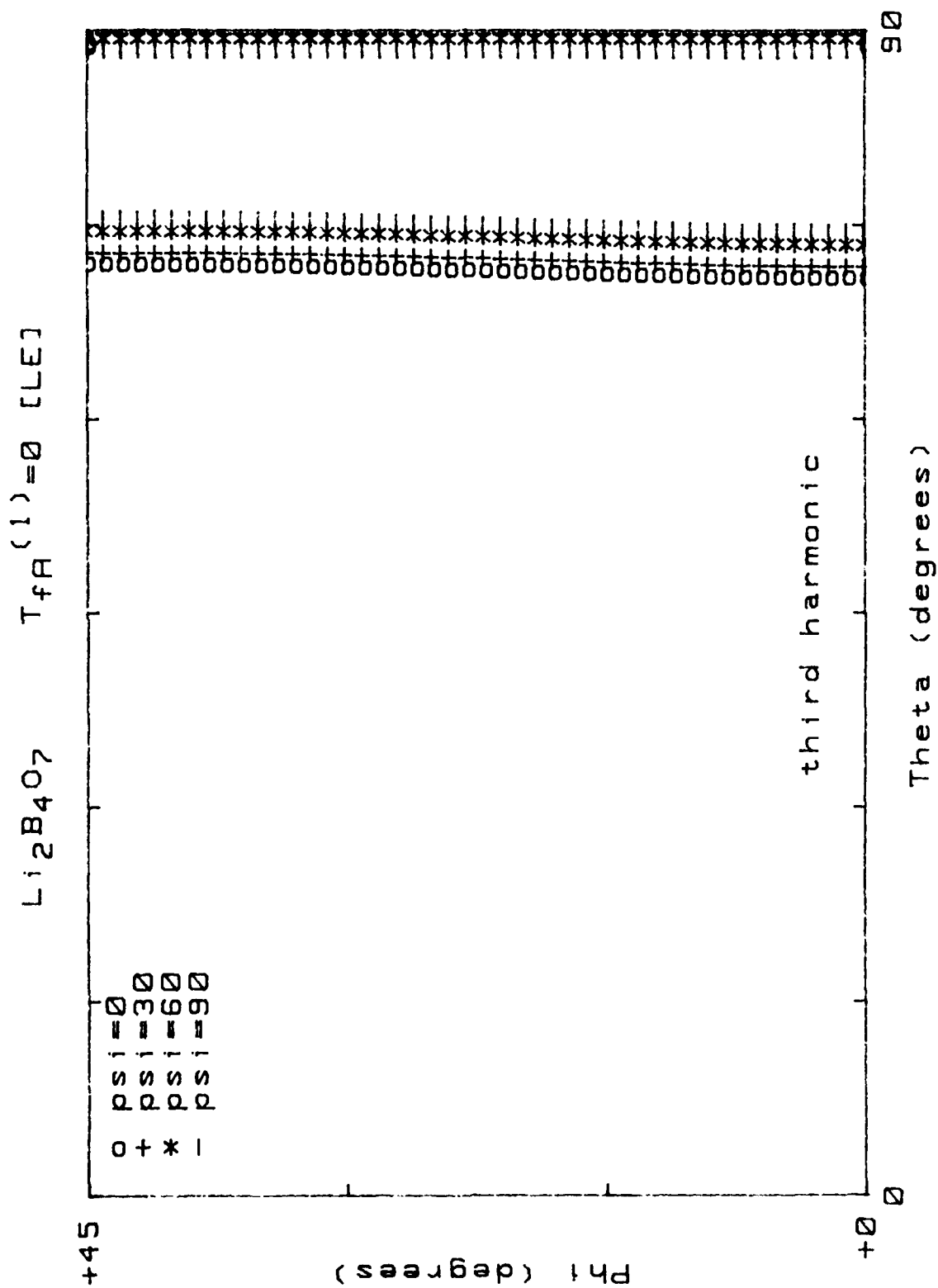


Figure 67. Locus of  $TC(1)=0$  for  $(yxw)\phi/\theta$  cuts;  $M = 3$ ; mode "c";  $\psi=0^\circ(30^\circ)90^\circ$ ; [LE].

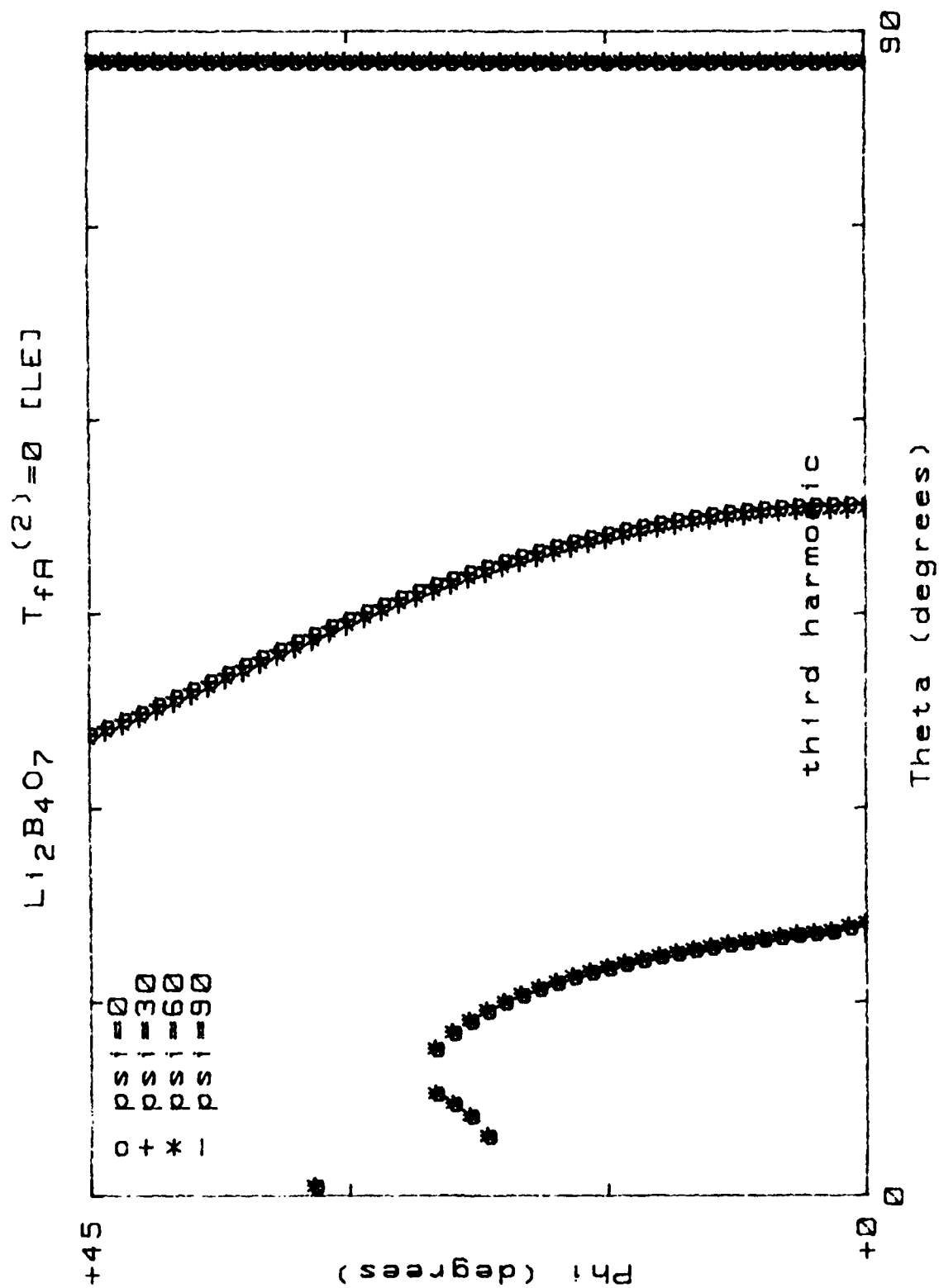


Figure 68. Locus of  $TC(2)=0$  for  $(yxw1)\phi/\theta$  cuts;  $M = 3$ ; mode "c";  $\psi=0^\circ(30^\circ)90^\circ$ ; [LE].

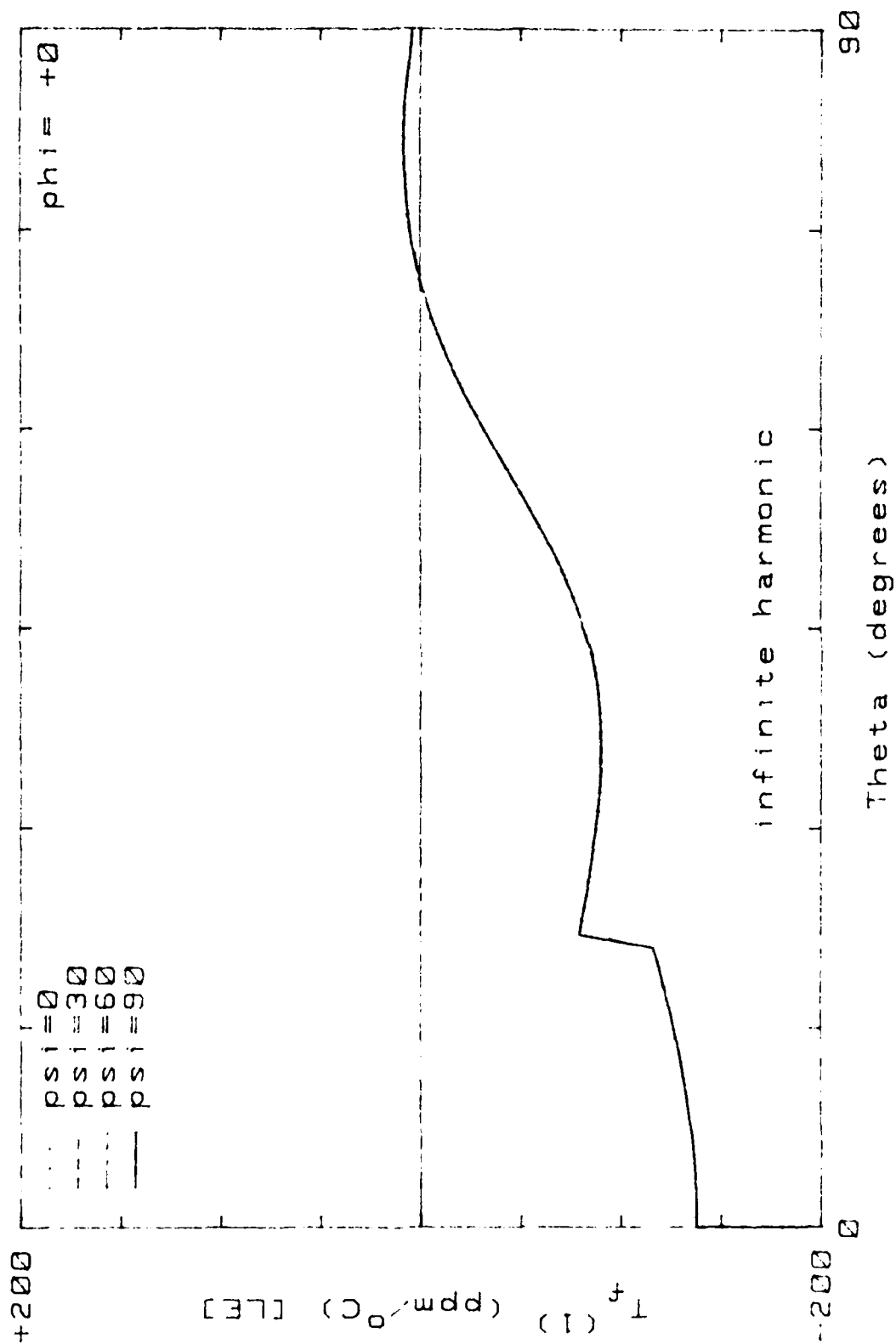
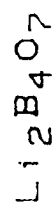


Figure 69. TC(f) for (yxw)  $\phi = 0^\circ/\theta$  cuts; M =  $\infty$ ; mode "c"; psi =  $0^\circ(30^\circ)90^\circ$ ; [LE].

$\text{Li}_2\text{B}_4\text{O}_7$

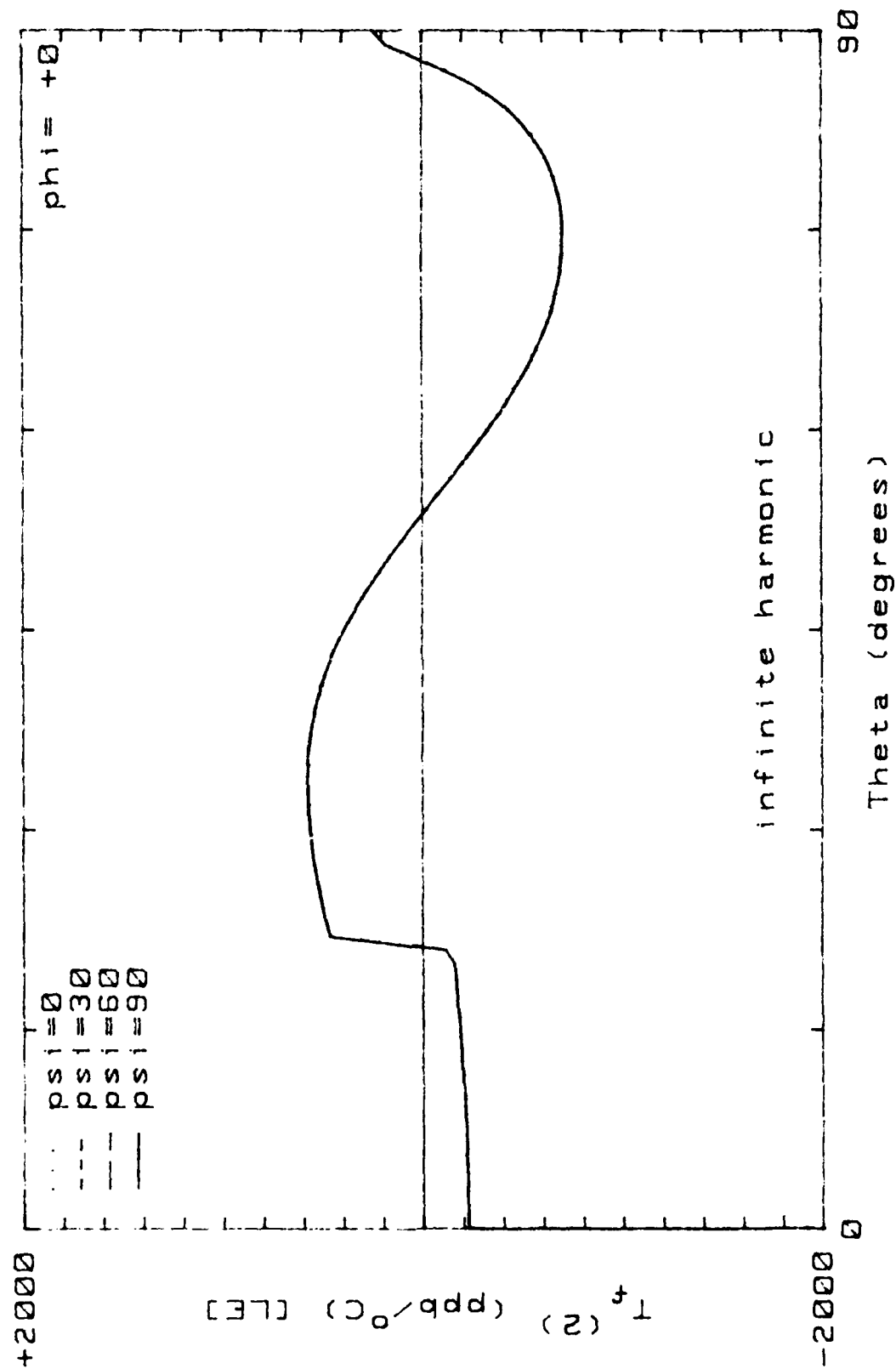


Figure 70.  $\text{TC}(2)$  for  $(yxwl)\phi = 0^\circ/\theta$  cuts;  $M = \infty$ ; mode "c";  $\psi = 0^\circ(30^\circ)90^\circ$ ; [LE].

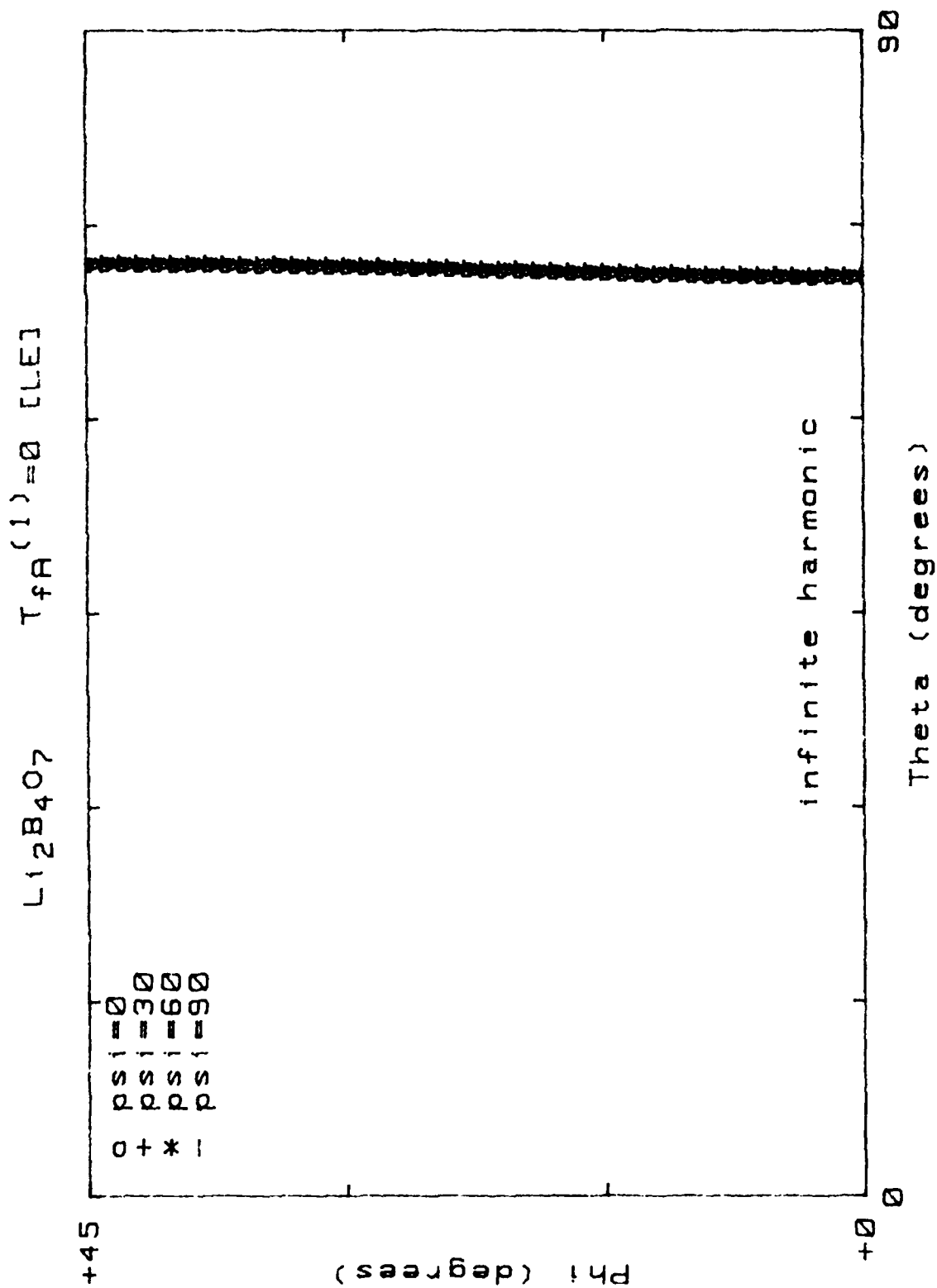


Figure 71. Locus of  $TC(1)=0$  for  $(yxw)\phi/\theta$  cuts;  $M=\infty$ ; mode "c";  $\psi=0^\circ(30^\circ)90^\circ$ ; [LE].

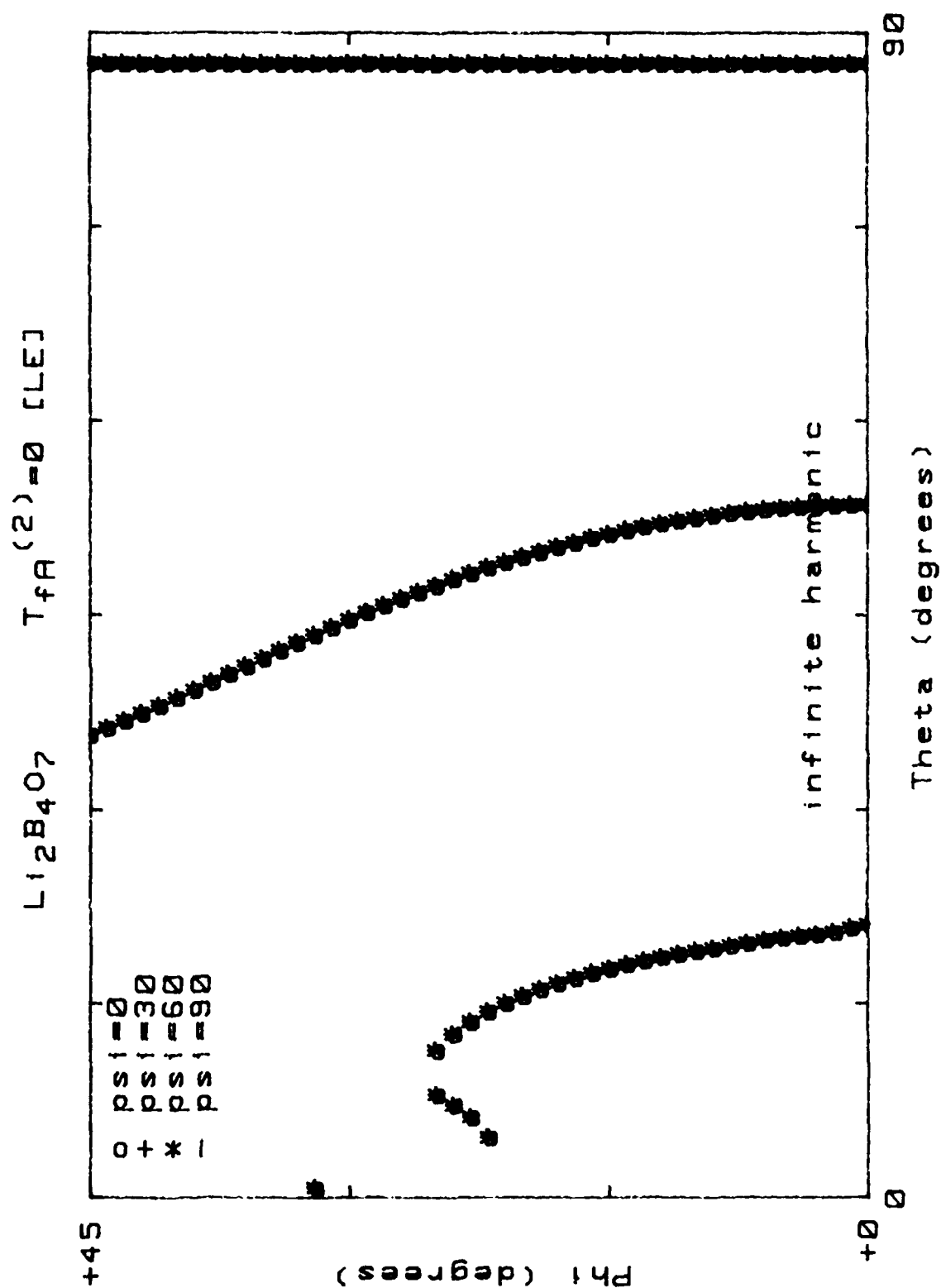


Figure 72. Locus of  $TC(2)=0$  for  $(yxw)\phi/\theta$  cuts;  $M=\infty$ ; mode "c";  $\psi=0^\circ(30^\circ)90^\circ$ ; [LE].

ELECTRONICS TECHNOLOGY AND DEVICES LABORATORY  
MANDATORY DISTRIBUTION LIST  
CONTRACT OR IN-HOUSE TECHNICAL REPORTS

15 Nov 88  
Page 1 of 2

101 Defense Technical Information Center\*  
ATTN: DTIC-FDAC  
Cameron Station (Bldg 5) (\*Note: Two copies for DTIC will  
Alexandria, VA 22304-6145 be sent from STINFO Office.)

483 Director  
US Army Material Systems Analysis Actv  
ATTN: DRXSY-MP  
001 Aberdeen Proving Ground, MD 21005

563 Commander, AMC  
ATTN: AMCDE-SC  
5001 Eisenhower Ave.  
001 Alexandria, VA 22333-0001

609 Commander, LABCOM  
ATTN: AMSLC-CG, CD, CS (In turn)  
2800 Powder Mill Road  
001 Adelphi, Md 20783-1145

612 Commander, LABCOM  
ATTN: AMSLC-CT  
2800 Powder Mill Road  
001 Adelphi, MD 20783-1145

680 Commander,  
US Army Laboratory Command  
Fort Monmouth, NJ 07703-5000  
1 - SLCET-DD  
2 - SLCET-DT (M. Howard)  
1 - SLCET-DB  
35 - Originating Office

681 Commander, CECOM  
R&D Technical Library  
Fort Monmouth, NJ 07703-5000  
1 - ASQNC-ELC-I-T (Tech Library)  
3 - ASQNC-ELC-I-T (STINFO)

705 Advisory Group on Electron Devices  
201 Varick Street, 9th Floor  
002 New York, NY 10014-4877

ELECTRONICS TECHNOLOGY AND DEVICES LABORATORY  
SUPPLEMENTAL CONTRACT DISTRIBUTION LIST  
(ELECTIVE)

15 Nov 88  
Page 2 of 2

205	Director Naval Research Laboratory ATTN: CODE 2627	603	Cdr, Atmospheric Sciences Lab LABCOM ATTN: SLCAS-SY-S
001	Washington, DC 20375-5000	001	White Sands Missile Range, NM 88002
221	Cdr, PM JTFUSION ATTN: JTF	607	Cdr, Harry Diamond Laboratories ATTN: SLCHO-CO, TD (In turn)
	1500 Planning Research Drive		2800 Powder Mill Road
001	McLean, VA 22102	001	Adelphi, MD 20783-1145
301	Rome Air Development Center ATTN: Documents Library (TILD)		
001	Griffiss AFB, NY 13441		
437	Deputy for Science & Technology Office, Asst Sec Army (R&D)		
001	Washington, DC 20310		
438	HQDA (DAMA-ARZ-D/Dr. F.D. Verderame)		
001	Washington, DC 20310		
520	Dir, Electronic Warfare/Reconnaissance Surveillance and Target Acquisition Ctr ATTN: AMSEL-EW-D		
001	Fort Monmouth, NJ 07703-5000		
523	Dir, Reconnaissance Surveillance and Target Acquisition Systems Directorate ATTN: AMSEL-EW-DR		
001	Fort Monmouth, NJ 07703-5000		
524	Cdr, Marine Corps Liaison Office ATTN: AMSEL-LN-MC		
001	Fort Monmouth, NJ 07703-5000		
564	Dir, US Army Signals Warfare Ctr ATTN: AMSEL-SW-OS		
	Vint Hill Farms Station		
001	Warrenton, VA 22186-5100		
602	Dir, Night Vision & Electro-Optics Ctr CECOM		
	ATTN: AMSEL-NV-D		
001	Fort Belvoir, VA 22060-5677		